The Canadian Journal of Chemical Engineering

formerly

CANADIAN JOURNAL OF TECHNOLOGY

CONTENTS

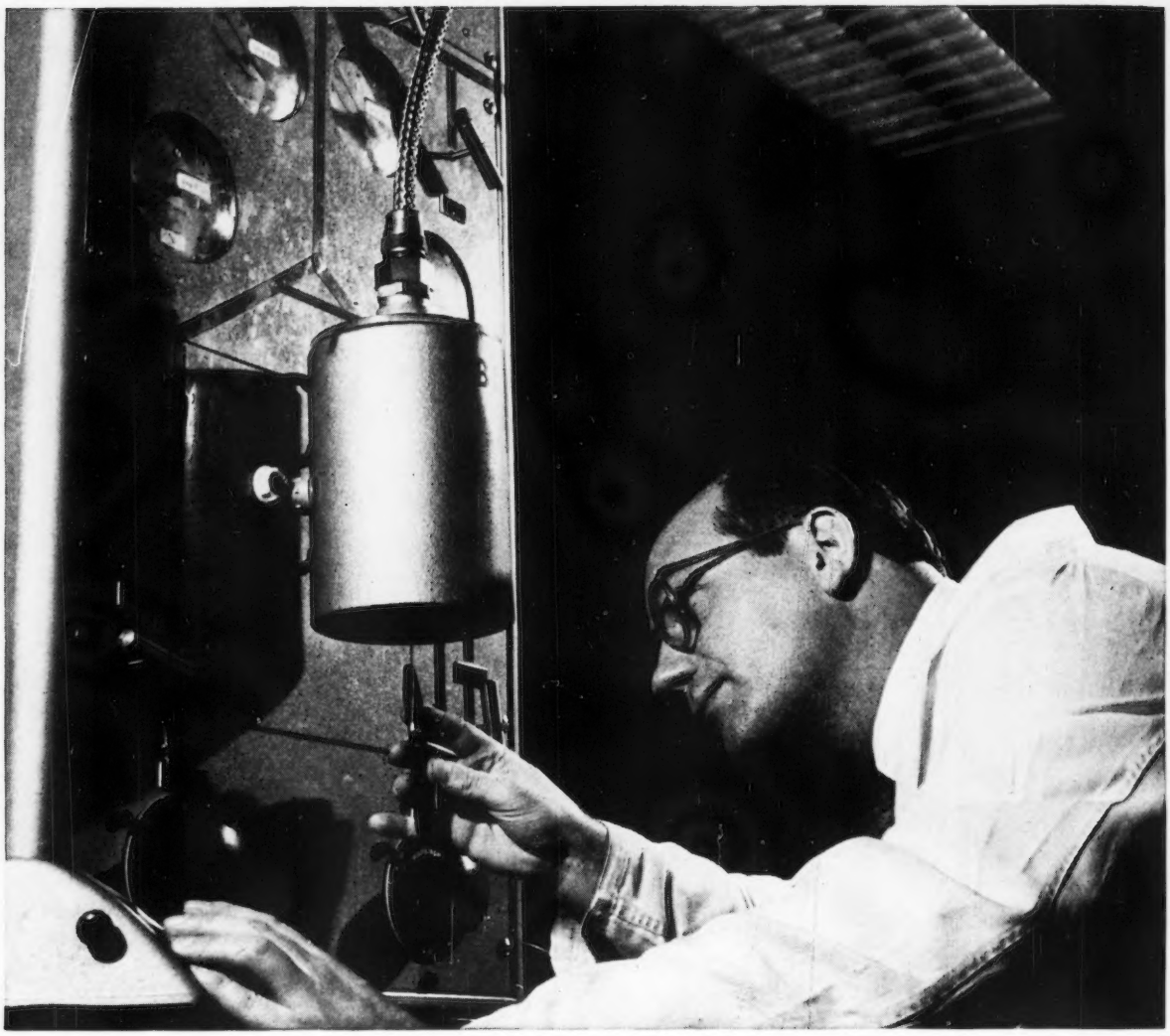

Photograph taken at C-I-L Central Research Laboratory, McMasterville, Que.

Plastics Detective

This photograph shows the High Shear Viscometer, designed and built at our Central Research Laboratory, used to investigate factors involved in complex flow behaviour of molten thermo-plastics during commercial processing.

Information on this newly developed pressure-driven capillary Viscometer has been made available to industry by C-I-L, and many industrial laboratories in the United States, England, India and Australia have built identical machines.

Such C-I-L research contributes to higher standards of performance in the plastics industry, to new and better plastics products and—through better technical service—to greater success in the application of these new materials to modern living.

C-I-L **CANADIAN INDUSTRIES LIMITED**

Serving Canadians Through Chemistry

Agricultural Chemicals • Ammunition • Coated Fabrics — Industrial Chemicals • Commercial Explosives • Paints • Plastics • Textile Fibres

VOLUME 39 1961

The Canadian Journal of Chemical Engineering

formerly

CANADIAN JOURNAL OF TECHNOLOGY

Published by
THE CHEMICAL INSTITUTE OF CANADA

48 RIDEAU ST. OTTAWA 2

Man
Editor:
Bouleva
are on

Edit
Street,

Adv
sales, T
601, 217

Plat
Journal
Ont.

The Canadian Journal of Chemical Engineering

formerly

Canadian Journal of Technology

Published by The Chemical Institute of Canada

VOLUME 39 | FEBRUARY, 1961 | NUMBER 1

Authorized as second class mail, Post Office Department, Ottawa. Printed in Canada

Manuscripts for publication should be submitted to the Editor: Dr. A. Cholette, Faculty of Science, Laval University, Boulevard de l'Entente, Quebec, Que. (Instructions to authors are on the next page).

Editorial, Production and Circulation Offices: 48 Rideau Street, Ottawa 2, Ont.

Advertising Office: C. N. McCuaig, manager of advertising sales, *The Canadian Journal of Chemical Engineering*, Room 601, 217 Bay Street, Toronto, Ont. Telephone—EMpire 3-3871.

Plates and Advertising Copy: Send to *The Canadian Journal of Chemical Engineering*, 48 Rideau Street, Ottawa 2, Ont.

Subscription Rates: In Canada—$6.00 per year and $1.25 per single copy; U.S. and U.K.—$7.00, Foreign—$7.50.

Change of Address: Advise Circulation Department in advance of change of address, providing old as well as new address. Enclose address label if possible.

The Canadian Journal of Chemical Engineering is published by The Chemical Institute of Canada every two months.

The Canadian Journal of Chemical Engineering

INSTRUCTIONS TO AUTHORS

Manuscript Requirements for Articles

1. The manuscript should be in English or French.
2. The original and two copies of the manuscript should be supplied. These are to be on 8½ x 11 inch sheets, typewritten, and double spaced. Each page should be numbered.
3. Symbols should conform to American Standards Association. An abridged set of acceptable symbols is found in the third edition of Perry's Chemical Engineers' Handbook. Greek letters and subscripts and superscripts should be carefully made.
4. Abstracts of not more than 200 words in English indicating the scope of the work and the principal findings should accompany all technical papers.
5. References should be listed in the order in which they occur in the paper, after the text, using the form shown here: "Othmer, D. F., Jacobs, Jr., J. J., and Levy, J. F., Ind. Eng. Chem. **34**, 286 (1942). Abbreviations of journal names should conform to the "List of Periodicals Abstracted by Chemical Abstracts". Abbreviations of the common journals are to be found in Perry's Handbook also. All references should be carefully checked with the original article.
6. Tables should be numbered in Arabic numerals. They should have brief descriptive titles and should be appended to the paper. Column headings should be brief. Tables should contain a minimum of descriptive material.
7. All figures should be numbered from 1 up, in Arabic numerals. Drawings should be carefully made with India ink on white drawing paper or tracing linen. All lines should be of sufficient thickness to reproduce well, especially if the figure is to be reduced. Letters and numerals should be carefully and neatly made, with a stencil. Generally speaking, originals should not be more than twice the size of the desired reproduction; final engravings being 3¼ in. or 7 in. wide depending on whether one column or two is used.
8. Photographs should be made on glossy paper with strong contrasts. Photographs or groups of photographs should not be larger than three times the size of the desired reproduction.
9. All tables and figures should be referred to in the text.

Submission of Manuscripts

1. The three copies of the manuscript, including figures and tables, should be sent directly to:
   DR. A. CHOLETTE, editor,
   The Canadian Journal of Chemical Engineering,
   Faculty of Science, Laval University,
   Boulevard de l'Entente,
   Quebec, Que.
2. The authors addresses and titles should be submitted with the manuscript.
3. The author may suggest names of reviewers for his article, but the selection of the reviewers will be the responsibility of the editor. Each paper or article is to be reviewed by two chemical engineers familiar with the topic. Reviewers will remain anonymous.
4. All correspondence regarding reviews should be directed to the editor.

Reprints

1. At least 50 free "tear sheets" of each paper will be supplied.
2. Additional reprints may be purchased at cost. An estimated cost of reprints, with an attached order form, will be sent to the author with the galley proofs.
3. Orders for reprints must be made before the paper has appeared in the Journal.

Communications, Letters and Notes to the Editor

Short papers, as described below, will be considered for publication in this Journal. Their total length should not exceed 600 words, or its equivalent.

Communications

A communication is a prompt preliminary report of observations made which are judged to be sufficiently important to warrant expedited publication. It usually calls for a more expanded paper in which the original matter is republished with more details.

Letters

A letter consists of comments or remarks submitted by readers or authors in connection with previously published material. It may deal with various forms of discussion arising out of a publication or it may simply report and correct inadvertent errors.

Notes

A note is a short paper which describes a piece of work not sufficiently important or complete to make it worth a full article. It may refer to a study or piece of research which, while it is not finished and may not be finished, offers interesting aspects or facts. As in the case of an article a note is a final publication.

* * *

The R. S. Jane Memorial Lecture Award

Terms of Reference

1. The R. S. Jane Memorial Lecture Award was established to commemorate the memory of the late Dr. Robert Stephen Jane who has made an outstanding contribution to the chemical profession and the chemical industry in Canada.

2. The Award shall be presented to a resident of Canada for exceptional achievement in a field of chemical engineering or industrial chemistry.

3. The Award shall be presented at the Annual Conference of The Chemical Institute of Canada. The recipient of the Award shall be required to present a lecture at the Annual Meeting of the Canadian Chemical Engineering Conference of The Chemical Institute of Canada in the year in which the Award is made. The subject of the lecture shall be the outstanding work of the lecturer in the field of chemical engineering or industrial chemistry. The lecture will be published in *The Canadian Journal of Chemical Engineering.*

4. The candidate chosen for this honor shall be known as "The R. S. Jane Memorial Lecturer". He will receive a cash award of $300, and travelling expenses.

5. It is intended that the Award shall be granted annually. However, in order to maintain the standard of the Award, the Selection Committee may omit the Award in any year in which a suitable recipient is not available.

6. The recipient may become eligible for the Award in a subsequent year, provided that he has again made new significant contributions to chemical engineering or industrial chemistry in Canada.

7. Nominations for the Award shall be made in writing to the Secretary of The Chemical Institute of Canada, 48 Rideau St., Ottawa 2, Ont., by not less than five (5) professional members of the Institute, by January 1 of each year. All accepted nominations remain in good standing for a period of three years.

8. The Director of Scientific Affairs shall refer all nominations to the Selection Committee which shall consist of:

The Chairman of the Chemical Engineering Division

The Editor of *The Canadian Journal of Chemical Engineering*

A representative of the Trustees of The R. S. Jane Memorial Lecture, to be selected by the Trustees

A representative from the Chemical Engineering Division to be appointed by the Director of Scientific Affairs; the latter is a non-voting member of this committee.

The Award Committee shall determine, prior to March 1, the candidate who is to receive the Award.

Dr. E. R. Rowzee, F.C.I.C., president and managing director, Polymer Corp. Limited, Sarnia, Ont. is the first recipient of this Award.

CHEMICAL ENGINEERING AWARDS

Commencing last fall, the Chemical Engineering Division of the C.I.C. established two awards – the first for the best paper published in *The Canadian Journal of Chemical Engineering* during the year immediately preceding the Fall Conference, and the second for the best oral presentation of a technical paper at the C.I.C. Annual Conference (Chemical Engineering Session) and at the Fall Conference of the Chemical Engineering Division. The awards will take the form of an engraved certificate and silver tankard with the proper inscription.

The first award for best paper was won by L. B. Torobin and W. H. Gauvin of McGill University and the Pulp and Paper Research Institute, Montreal, for their series of papers on "Fundamental Aspects of Solids-Gas Flow".

The first oral award winner was J. M. Smith, Northwestern University, Evanston, Ill. for his presentation of "Heat Transfer to a Surface Reacting Fluid in Turbulent Flow". His co-author was Ronald I. Rothenberg, and the paper was published in the December 1960 issue of *The Canadian Journal of Chemical Engineering.*

CHEMICAL ENGINEERING DIVISION EXECUTIVE FOR 1961

Chairman: W. M. Campbell, Atomic Energy of Canada Limited, Chalk River, Ont.

Vice-Chairman: J. W. Hodgins, McMaster University, Hamilton, Ont.

Secretary-Treasurer: W. J. M. Douglas, McGill University, Montreal, Que.

Immediate Past Chairman: W. H. Gauvin, McGill University, Montreal, Que.

Executive Members: D. B. Robinson, University of Alberta, Edmonton, Alta.
D. S. Scott, University of British Columbia, Vancouver, B. C.
John Klassen, Du Pont of Canada Limited, Sarnia, Ont.
J. H. Kemper, Dominion Tar & Chemical Co. Limited, Montreal, Que.
H. K. Rae, Atomic Energy of Canada Limited, Chalk River, Ont.
David Craig, Ontario Paper Co. Limited, Thorold, Ont.
A. I. Johnson, University of Toronto, Toronto, Ont.

THE R. S. JANE MEMORIAL LECTURE

E. RALPH ROWZEE,

President and Managing Director,
Polymer Corp. Limited,
Sarnia, Ont.

Rubber, Research and Human Resources

I am honored to be the 1960 R. S. Jane Memorial lecturer; particularly since this is the inaugural lecture of this fitting memorial. As the first recipient of the award, I am aware of a heavy responsibility; namely, that of presenting an address in which Dr. Jane might take pride. I sincerely hope that I may discharge this responsibility creditably, and that I may conform to the high standards which Dr. Jane always set for himself.

I knew Dr. Jane for many years, and held him in high regard as a friend and fellow chemist. I appreciated his quiet, unassuming manner, and I respected his views and judgment. In particular, I should like to emphasize his contribution to our profession, to our industry, and to Canada. His contribution to the C.I.C. is testimony of the faith he had in the chemist, the chemical engineer, and the chemical industry.

Dr. Jane had a sincere interest in people and their progress. The status enjoyed by the company which he served is a reflection of his ability and leadership. His thinking was always broad, imaginative and dynamic. His efforts extended beyond his company and his profession. He served his community and his country. I should like, therefore, to feel that he would accept this address as a contribution and a challenge to the industry he worked for and the people he worked with.

The terms of reference for this lecture stipulate that the subject shall be related to the work of the lecturer in the field of chemical engineering or industrial chemistry. There is little doubt therefore, that I am to make some reference to synthetic rubber but, if I may, I should like to interpret this memorial as I believe Dr. Jane would wish it, as an opportunity to use the history of the past only as a challenge to the future.

This Lecture was presented to the C.I.C. Canadian Chemical Engineering Conference, Quebec, Que., Nov. 7-9, 1960.

The title of the lecture is "Rubber, Research and Human Resources". I should like to start out, strangely enough, with natural rubber. It is not a technical paper, but rather a statement of my experience in the rubber industry and certain conclusions which I have drawn regarding technical education and research.

A Brief History of Rubber

The story of rubber is an interesting one, repeatedly emphasizing the action of the economic laws of supply and demand, and the fact that where unnatural controls are imposed, a way will be found to circumvent them.

The tale has often been told of how Sir Henry Wickham, in 1876, smuggled seedlings of the rubber tree out of Brazil to Kew Gardens, from where they were transplanted to Ceylon and the Straits Settlement. Here they formed the basis for the far eastern plantations.

The real stimulus which led to the large scale development of these plantations, however, was the market pool operated by Brazilian growers and speculators which ran prices of natural rubber to over $1.00 a pound in 1906 and to $3.00 a pound in 1910. While the speculators reaped the harvest, they sounded the doom of Brazilian rubber. The industry moved to the far east and British interests dominated the field.

In the 1920's, arbitrary price controls by the British, through the Stevenson Act, restricted output and affected supply. The result of this control was to raise the price, encouraging heavy plantings by other interests (primarily the Dutch). It also led to some serious thought about synthetic rubber. The immediate result was that independent planters became active, and more and more rubber came on the market. The British domination of the field declined, and the price dropped as supply increased.

With the depression of the 1930's, huge surpluses existed and rubber prices dropped to a low of 2⅝¢ a pound. An agreement reached in 1934 imposed restrictions on an international scale, and prices gradually recovered to the 20-25¢ level. In the last quarter of 1941, just before Pearl Harbor, all rubber possible was being shipped out of the East. This is a significant item since it provided notice of the urgent need for rubber that stimulated the wartime synthetic rubber program in North America.

Synthetic Rubber

Synthetic polymers with certain rubber-like properties had been known for almost a century, starting with the work of Tilden in the 1860's. During World War I, natural rubber was cut off from Germany by the British Blockade and the German scientists succeeded in developing rubber-like polymers based on dimethyl butadiene which they used for truck tires and gun carriages. The material was not a good rubber and, with the armistice, production lapsed until the Nazi regime came to power with ambitions for world domination. Realizing that rubber would again be cut off at the beginning of a war, the full support of the government was given to the scientists to evolve a rubber-like polymer which would serve as a substitute for natural rubber.

Among the many chemical advances made by I. G. Farben chemists during this period, were the discoveries of emulsion polymerization, copolymerization, and a series of polymers based on butadiene. A sodium catalyzed butadiene rubber was developed. Factories were designed for copolymers of butadiene and styrene (Buna S) and just before the war, were brought into production.

The Standard Oil Company acquired the rights to many of the Farben patents through an arrangement with I. G. Farben, which provided for exchange information in areas of mutual interest; thus, knowledge of buna polymers came to America.

In America, with plenty of rubber available, there was little incentive for the development of synthetic rubber during the early 30's. The matter received attention, however, and research quietly went forward. In 1922 Thiokol was accidentally discovered by an American chemist, J. C. Patrick. Thiokol was oil resistant, but had other less desirable characteristics, and although used for a few special applications, never became an important product. In the late 1920's, DuPont acquired the rights to a promising material discovered by Father Nieuland of Notre Dame University. This material, later called neoprene, excelled in certain characteristics where natural rubber was weak, but it was some years before neoprene was produced commercially.

It was at this time, 1931, that I graduated from M.I.T., as a chemical engineer, and went to work in the Research Division of the Goodyear Tire and Rubber Company, in Akron. Goodyear had done some research work from time to time on synthetic rubber, but it had always been interrupted by more urgent things. In 1933, P. W. Litchfield, one of the outstanding leaders in the rubber industry, and then President of Goodyear, called for a full time major assignment on synthetic rubber. Asked about the possibility of conflict with German patents, Litchfield is reported to have said: "Damn the patents! We'll cross that bridge when we come to it. Our job now is to find out everything we can about synthetic and go on from there."

From Test Tube to Test Tire

In 1935, I was assigned the job of devising means, and then producing, in lots of approximately ten pounds each, a variety of the most promising synthetic rubbers based on butadiene. Test tube quantities previoulsy produced by Goodyear chemists had been insufficient for compounding evaluation. Within a short time, the assignment was expanded to the production of several hundred pounds of a particular rubber so that test tires could be produced. Today, we produce synthetic rubber in such quantities that it is difficult to visualize the time and work involved in producing a few pounds of rubber in 1936, let alone several hundred pounds.

Some of the problems faced in those days were: long reactions often requiring weeks to complete; reactions were stopped short of completion because by accident it was discovered that at 70% conversion of monomers a tough rubber-like material was produced whereas at 90% conversion, the material had few rubber-like properties. Reasons for this were only hazily understood by the organic chemist but were later explained by the physical chemist; there were no facilities to recover unreacted monomers; equipment had to be improvised for coagulating, washing and drying the product.

Other problems presented major assignments in themselves. Of the principal monomers, only styrene could be purchased. Butadiene, acrylonitrile and methylacrylonitrile had to be produced from intermediate materials in the laboratory, using very crude and laborious techniques.

Many years after the event, an engineer of the Pfaudler Company at Elyria, Ohio, recalled my first visit to his plant to discuss a reactor for synthetic rubber. It seems that I represented one of two Akron rubber companies who approached him within a few days of one another. Each presented a sketch of a five gallon glass-lined pressure vessel which Pfaudler was to manufacture as quickly as possible. He said that he was amazed to find the sketches so similar. Those five gallon reactors produced by Pfaudler in 1936 were the first of what later became a standard item in the laboratory of every copolymer plant. From these developed the large, glass-lined reactors which are found in copolymer plants today.

This basic development period was followed by a period of scaling up through a pilot plant, and the construction of two plants; one that Goodyear built for the United States Government which was six months away from completion at the time of Pearl Harbor, and one that Goodyear operated privately. In retrospect, it stands out clearly that most of the things that had to be done in this early development stage, made use of my chemical engineering education.

A Date with History

Shortly after Pearl Harbor, the synthetic rubber program was adopted and urged on with high priority. In spite of the plentiful supply of natural rubber available a few years earlier, North America suddenly became a "have not" continent in the matter of supply of this important commodity. These words "have not" were used by the Rubber Study Committee chaired by Bernard Baruch in 1942 to stress the urgency of the situation with which we were faced. The Committee, in its report, emphasized that large scale production of synthetic rubber was essential by the end of 1943. Victory or defeat was in the balance.

The Canadian Government decided early in 1942, to participate in this program as one of its major contributions to the war effort. It undertook to build a plant in Sarnia to produce both GR-S and Butyl rubbers, as well as butadiene, isobutylene, and styrene, the major chemicals required in the processes. I was assigned to the copolymer part of the project, on loan from Goodyear. This was the start of my association with Polymer, and with Canadians, and the beginning of my becoming a Canadian.

The synthetic rubber program has been called one of the major chemical engineering achievements of all time. Certainly, it was not without its problems that now provide interesting, pleasant reminiscence. Of major significance was the coordination of pooled processes, and ideas of many companies, into a so-called standard plant. The development of the standard plant is an excellent example of good chemical engineering design. It is more remarkable because of the limited operating experience that had been gained before Pearl Harbor.

How good was the design? There have been many pieces of equipment that, for one reason or another, operators and management would have liked to replace, but in spite of a real effort to find better equipment, relatively few changes have

been made. Most basic equipment ordered for new plants today, is very similar to the equipment installed in existing plants almost twenty years ago.

This does not imply, of course, that changes have not taken place. On the contrary, many improvements have been made, but these have been primarily process changes, and changes in auxiliary equipment. The conversion of the copolymer reaction from a batch to a continuous process was highly important since it increased the capacity of the plant substantially. New controls and instrumentation have improved uniformity and other quality characteristics; new types of rubber have been introduced to supply the specialized needs of industry. These are but a few of the changes, and in all of them can be seen the work of the chemical engineer.

Polymer has pioneered many new types of rubber, and has made many noteworthy industrial chemical and chemical engineering achievements which give the Company important technical advantages, some of which have not yet been disclosed. The application of Dow, type B, dehydrogenation catalyst is an example of the constructive work done in this field by the technical staff of the Company.

Further indication of the application of chemical engineering work has been the increase in capacity achieved by bottleneck removal programs and process improvements.

The Construction Period

I should like to refer briefly to the construction period. The first rubber was produced on September 29, 1943, well ahead of the deadline established by the Baruch Committee in its report, to which I referred earlier. That we were able to do so is a tribute to all who participated; engineers, contractors, suppliers, administrators and workers of all kinds. It is true, there was a great incentive, but the feat was accomplished in the face of great odds and we, in Canada, can be justly proud of our participation.

Many people considered the synthetic rubber plants to be expendable items in a wartime emergency, and that recovery of the natural rubber areas would make these plants worthless or at least idle — and so it could have been. The challenge, however, was there to make an industry for peace-time. To meet this challenge, it was essential to find a market for the capacity of the Polymer plant; a capacity that could supply much more than the Canadian requirements for rubber.

Development of Markets

The places to turn, of course, were the major rubber consuming areas of the world. A proposal to develop these export markets was accepted, though most advice said that Europe would never buy synthetic rubber. Starting in Europe, top Polymer representatives dealt with trade commissioners, governments and rubber consumers. Their efforts were rewarded and, eventually, orders started to flow. Today, the western world consumes almost 4,000,000 tons of rubber annually, compared with 1,000,000 tons 20 years ago and almost half of this present consumption is synthetic. Polymer exports 65-70% of its output, and its products flow to more than 60 countries of the world. This is an annual export of product valued in excess of $50 million, and is an important factor in Canada's economy.

This has required concentrated effort in marketing and technical service. It has required a consistency of approach to supply and price. It has required diversification of production and a strong research effort. Starting in 1946, competent agents were appointed in major countries, and this group has made a significant contribution to the respect in which the name POLYMER is held.

In this highly competitive industry, Polymer operates in a manner similar to that of any private company. It pays taxes and dividends, and absorbs all of the normal costs of business. It contributes its full share to the life and welfare of the community in which it operates. In the last fifteen years, using the same basic facilities, production has been increased from 50,000 to 150,000 tons per year.

Perhaps it is not too much to say that this is an amazing record. In 1941, Canada was a most unlikely location for a synthetic rubber plant, and one would have been considered out of his mind if he had predicted that within fifteen years Canada would be a significant factor in the world rubber supply.

I believe the story of Polymer points out the possibilities of enterprise against heavy odds. It highlights the contribution of the chemist and the chemical engineer to meet the challenge in such an industry. It provides an example of converting a "have not" situation to a "have" with great benefit to the country. It can be said that the circumstances were unusual, but ideal conditions are most unlikely to exist for any venture.

Canada is a growing nation. Estimates of a population of over 26 million by 1980 have been given in comprehensive studies of Canada's future. At the present time, Canada has a wealth of natural raw materials, but because of our relatively small population, it is considered too small a market for the mass production conversion of out natural resources to consumer goods. This is, I am sure, sound economics if we consider the limits of the Canadian market but — do we need to look at it as such? Are there not products that we can produce for a much larger market, and should we not look to wider fields to sell products which could be, but have not yet been, produced in Canada?

Our prospects for a prosperous Canada, with a population of 26 million, are dependent on the opportunities we can provide for employment, not only in our present industries, but also in new industries and services which should begin to take shape in the next ten years. This growth will bring a Canadian market better able to sustain many of the consumer goods industries, but there is a bridge to cross before this is achieved. To cross it will require the utmost in initiative and enterprise by all Canadians; management and labour — financier and investor — manufacturer and consumer — educator and industry — government and the people. The challenge is great if we are to prosper in a generally buoyant world economy.

Important Factors

I do not have any panacea to assure success in this growth. I know that it will mean hard work, understanding and cooperation among all segments of our people. I should like to consider two factors that we shall need in the next decade, which I believe will make a special contribution to the development of Canada. These important factors are:

One — our trained people, and

Two — industrial research.

I think that it will be evident to you that these two fields are of particular interest to me because of my industrial association and background.

First, let us discuss our trained people!

Since our economy is based on the second highest average labor cost in the world, technology is of great importance. In order to compete with goods manufactured by lower cost labor, we must concentrate on discovering, ahead of other countries, know-how in as many appropriate fields as possible. We must also strive for the highest productivity level we can achieve by automation, by work simplification, and by just plain hard work.

Canada already owes much to the chemist and the chemical engineer. Even more will depend on these people in the future. You are present at this meeting because of your interest in technical development. You have all graduated from university; most of you from Canadian universities, and many of you recently. I should like you to consider with me some aspects of this educational system.

We have, in Canada, an excellent educational system at all levels. There will always be arguments about speeding the progress of the above average student through elementary and secondary schools. There is the problem of facilities to meet

the increasing enrollment of students. Industry has recognized the need of the universities for expansion to turn out more trained people and, along with other groups, has contributed generously to the building program of our universities.

What About Our Courses?

What has been happening to the curricula of our engineering courses during the last several years? I believe that the technical training has in many cases been diluted by what I will call secondary factors. There has been a tendency for employers to demand, and for the universities to adopt, courses which provide such generalized training that the individual graduating from these courses lacks depth in technical training to fill the engineering or chemical requirements of industry. Much of this change has been introduced with the objective of graduating managers. There are many people who believe this is possible. I do not disagree with the desirability of producing managers from an educational system but, I believe that we are years away from perfecting the techniques to accomplish this. Of prime importance in such a development is the selection of the right candidate. In the meantime, these generalized courses tend to develop impatience in the graduate to become an executive over night. You and I know that a graduate cannot become an effective supervisor, let alone an executive, until he has met the tests that only experience can give him.

We are all to blame for this development. The universities have been under heavy pressure from industry and business generally, to provide such training. I suggest that a good scientific training, specializing in the field of the individual's particular ability, is of prime importance to the engineer and the chemist. For those especially talented as leaders or managers, further training at the graduate level in university, or within industry, will better equip them to meet the challenge than will the generalized type of undergraduate course. Some authorities are now pointing out that additional training at graduate level would be most effective after some years of experience in industry.

These remarks have been directed particularly toward undergraduate courses in chemistry and chemical engineering. We must not, however, lose sight of the humanities. I am well aware of the time factor, but I believe that the graduating student who has had an introduction to the humanities should be better adjusted to meet the challenge of his profession. I would make it clear that I believe emphasis must first be placed on the technical aspects of the course, but that the student should not be permitted to lose sight of the importance of the humanities, particularly with the continually broadening sphere of activity and employment available to the chemical engineer and science graduate.

Compensation

Another important development which is taking place relates to compensation. Today there is a trend to pay the qualified graduate employee performing top flight technical work in accord with salaries paid for supervisional and managerial types of work. This, I believe, properly takes away some of the anxiety of the young graduate who seeks the utmost in financial reward through early advancement to managerial posts, and provides a better perspective as to the true importance of the scientist. There is a delicate balance to be achieved in this matter of compensation, and I believe that the scale is now tipping to achieve this balance more appropriately than has been the case in past years.

When we speak of productivity, we are too apt to think only of the output of our wage earners. Excellent articles have been written to present the argument that productivity is a measure of the total output achieved from total input. It is important that we should not lose sight of the fact that management, engineering, research, purchasing, traffic, accounting, and marketing along with production, in fact, all costs of business are a part of the input contributing to the productivity of the business. It is therefore essential that we utilize all personnel effectively to achieve the utmost in productivity.

I mention this because there has been a tendency to use chemists and chemical engineers in the capacity of technicians, which is hardly in keeping with the objectives of using people most effectively. I believe it is a mistake to have a chemist or chemical engineer doing routine work that could be done regularly by a less qualified individual. Even if the chemist, or chemical engineer, is prepared to accept such assignments, it is a misuse of the training developed in our educational system. It is therefore desirable to stress the proper utilization of our trained people by industry and business.

Today the chemist or chemical engineer is being used in Management and Marketing, in Economic Evaluation and in Technical Services, and in Research and certain special functions; he is being used wherever his particular talents indicate that there is an activity through which he can make a significant contribution to his organization. This represents a great change from the situation which prevailed when I entered industry and that which I found on coming to Canada almost 20 years ago, when I was told by a number of people that the chemical engineer was neither fish nor fowl, that he was neither chemist nor engineer, and therefore of little value.

The Use of Trained People

There is one other aspect of the use of our trained people to which I would refer. We have, over the years, tended to confine the chemist to the laboratory and the chemical engineer to the plant. This probably results from looking at the chemical engineer as the applied chemist and the plant problems as applied problems. Much might be gained by assigning the chemist to the plant and the chemical engineer to the laboratory, not necessarily to try to interchange the two individuals, but rather to bring a fresh perspective to the problems of the plant and the problems of the laboratory. Improvements in processes and process design might result from the fresh approach of the chemist — and improvements in laboratory equipment might be developed by the engineer in the laboratory. Moreover, having both chemist and engineer working together cooperatively and objectively provides a combination of talent that might recognize new concepts and important departures from our standard processes that will contribute to the industrial growth we seek.

The Case for Research

Research is the second factor that I should like to have you consider. You are all as well aware as I am of the importance of research to technological development. Considerable research has been carried on in Canada in the universities, hospitals, research institutes, in industry, and especially in the National Research Council. Industrial research, with which I am particularly concerned, has stimulated interest in specific fields of research and this has led, in turn, to the stimulation of basic research in related fields within the universities. As an example, I believe that research carried on by Polymer Corporation has stimulated interest in polymerization generally, which in turn has had a bearing on the formation of the High Polymer Forum and the Polymer Research Institute. This is a healthy kind of development.

Industrial research in any company, of course, is justified on the basis that it will provide a return to that company. There is, unquestionably, a risk involved. The stakes are great, and the payout can be most attractive. Polymer has benefited from the research carried on by its staff, both in the technical and process fields, and in the respect which is accorded its research and technical people. Polymer has also benefited from the research being carried on at the N.R.C. in the universities, and from the work of the High Polymer Forum.

I should like to stress, however, that with Canada's economy tied closely to that of technological development, research on an ascending scale is important, not only in the interests of

extracting raw materials, but also in converting our raw materials to finished consumer goods.

The case for industrial research has been advanced before. I should like to review some of the arguments supporting this case:

1. Research is required to develop know-how and world-wide patent positions.

New discoveries that lead to a knowledge and experience in any field in advance of other countries and, that can be upheld by a strong patent position, have far reaching effects. They stimulate further research in the same and related areas. In addition to the financial reward, the resulting prestige adds strength to negotiations with others and leads to exchanges with others doing important work in the same basic fields.

2. Research is required to develop new equipment, new machines and new techniques.

I have mentioned the importance of productivity in the field of competitive marketing. We must not be satisfied to continue doing things the same way, with the same tools, but must continually seek for better ways and means. Our ingenuity in developing machines and techniques may contribute greatly to the productivity factor. This is primarily a job for industrial research.

3. Research is required to develop secondary and consumer goods manufacturing in Canada.

This development is closely related to the size of the market. So long as we accept the idea that the market we can develop in Canada and other areas is not large enough for an operation in Canada, we can expect to be dependent on other countries and, therefore, provide employment opportunities in those other countries rather than in Canada. Industrial Research is one of the many factors that can contribute to the development of secondary and consumer goods manufacturing.

4. Research is required to encourage the interest of young people in scientific careers and, through enhanced stature, encourage our talented, technically trained people to remain in Canada.

I have emphasized the excellent educational system in Canada, and that science and engineering graduates from this system will play an important role in Canada's future. As industrial research assumes a broader and more important role, the stature of those engaged in it will be greatly enhanced. This is an important factor in attracting young people of ability, and of the right temperament, into research work.

These arguments are of interest to the Canadian owned firm. Are they of equal interest to the company whose Canadian plant is a subsidiary of a foreign controlled corporation which conducts centrally operated research facilities in its home territory? This is, of course, a difficult situation. Every owner must weigh the pros and cons, and determine the best course of action for his own interest. I suggest that he should be continually aware of the contribution which research in Canada can make to this country with material benefits to himself when planned and conducted on the basis of a long term approach.

Several important Canadian companies whose control lies outside of Canada have taken this approach, I believe to their advantage.

I have mentioned that Dr. Jane was not restricted in his thinking. This was particularly true of his views on research. I recall discussing with him ways and means of stimulating research in Canada. He was prepared to explore every avenue which might have a chance of success. He advanced the idea that several companies might pool their research activities for the benefit of all, and of Canada. It is not my intention to discuss a thought of this kind. However, I would bring to your attention the need for an imaginative approach to Canadian needs and the means of fulfilling them; an approach that may generate the growth in Canada of industries we now have, and of new ones that may appear as uncertain of success as Polymer did in the early 1940's.

I believe Dr. Jane, in all his many activities, was thinking and working for a better Canada. He worked for the development and growth of industry and society. I hope that my remarks may be accepted in the same spirit, and that they would be acceptable to him.

★ ★ ★

A
the he
depth
below
mecha
to occ
simple

Opt
bench-
by me
studied
diamet
ured w
ment p
phase

Conv
ti
mixing
chambe
either b
two liqu

The
cocurre
gested
develop
betwee
operatio
liquid a
flowing
the hea
heavy li
would
breakin
currentl
light ph
were to
rium co

In
velocity

.....

1*Manusc*
2*Researc*
3*British*
4*Associat*
of Briti
Contribu
versity o
presented
13-15, 1

A Spouted Mixer-Settler[1]

T. R. JOHNSTON[2], C. W. ROBINSON[3] and N. EPSTEIN[4]

A new type of mixer-settler is described wherein the heavy liquid phase is spouted upward through a depth of light liquid phase and allowed to settle below the light phase. The method does not require mechanical agitation, allows both mixing and settling to occur continuously in the same chamber, and is simple in design.

Optimum conditions have been determined for bench-scale extraction of benzoic acid from toluene by means of a water spout. Independent variables studied were water rate, toluene rate, spout pipe diameter and wall effect. Dependent variables measured were spout height, spout spread, initial entrainment points and stage efficiency. Murphree spouted-phase efficiencies up to 96% were obtained.

Conventional single-stage mixer-settlers, when they are continuous flow devices, almost invariably require that the mixing and the settling be performed in separate units or chambers[1,2,3]. This is because the mixing is brought about either by mechanical agitation or by parallel "line" flow of the two liquids being contacted[3].

The present device was originally conceived as a two-pass cocurrent-countercurrent liquid-liquid contactor. It was suggested by and named after the fluid-solid contacting operation developed by Mathur and Gishler[4], though the resemblance between fluo-solid "spouting" and the present liquid-liquid operation is superficial. The intention was to inject the denser liquid at high velocity vertically upward through a cocurrently flowing column of the lighter liquid, the interface of which with the heavier liquid was to be located immediately below the heavy liquid inlet. It was hoped that the spout of dense liquid would rise through a very large height of light liquid before breaking into droplets, which would then descend countercurrently through the annular region of the upward moving light phase. In this way two long passes of the heavy phase were to perform the equivalent of several mass transfer equilibrium contacts.

In fact, however, the liquid-liquid spout heights at high velocity were considerably smaller than, for example, those obtained by spouting liquid into air (Figure 1a), spouting velocities were limited by entrainment considerations, and in the case of confined column spouting (Figure 1c), a turbulently mixed dispersion zone was set up in the region of the spout and below it, rather than orderly cocurrent-countercurrent contacting of the two phases. As a result the equivalent of a single equilibrium contact was never exceeded. For this reason the method was studied with the altered viewpoint of optimizing its performance as a single-stage single-chamber continuous flow mixer-settler.

[1]*Manuscript received August 13; accepted October 12, 1960.*
[2]*Research Centre, Du Pont of Canada Limited, Kingston, Ont.*
[3]*British American Oil Co. Limited, Port Moody, B.C.*
[4]*Associate Professor, Department of Chemical Engineering, The University of British Columbia, Vancouver, B.C.*
Contribution from the Department of Chemical Engineering, The University of British Columbia, Vancouver, B.C. Based in part on a paper presented to the 43rd Annual Conference, C.I.C., Ottawa, Ont., June 13-15, 1960.

Spouting Behavior

That liquid-liquid spouting is feasible was first demonstrated by injecting water into both gasoline and toluene via a centrally located vertical 5 mm. tube in a 2.3-in. i.d. glass column with a contracting conical bottom, geometrically similar to a fluo-solid spouting column. It was quickly realized, however, that the conical bottom fulfilled no useful function in the liquid contacting operation and was actually detrimental to the settling and separation of the denser phase. The cone was therefore eliminated in the subsequent column experiments, and instead, a tapered expanding section was used for decelerating the outlet water.

Figure 2 is a schematic diagram of the apparatus used for studying the characteristics of a water spout in toluene in a 4-in. i.d. Pyrex column under both continuous-flow and semi-batch (zero toluene flow) conditions, and in an inverted 13-gal. glass carboy under semi-batch conditions alone. Except for the copper breather tube in the carboy, which caused slight discoloration of the toluene with time, especially in the presence of dissolved benzoic acid, and some ace Saran sampling leads, all lines were type 316 or type 304 stainless steel. A standard tapered 6-in. to 4-in. Pyrex reducer at the water outlet was used to minimize bottom entrainment of toluene by water in the column, while a 6-in. toluene outlet section was employed to diminish any overhead losses of water. The narrow 3-in. diameter neck at the bottom of the 16-in. diameter carboy, on the other hand, served to enhance bottom entrainment of toluene, thereby limiting the carboy to a water capacity of 1.2 U.S. gal./min.

Interface control, initially effected by a barometric loop from the water outlet, was later accomplished by manipulating the outlet water valve. Where a well-defined toluene-water interface was formed, as in the carboy runs and at the beginning of a column run, this interface was kept slightly below the top of the spout pipe so as to prevent its disturbance by the high velocity water leaving the pipe. For the continuous flow runs, toluene was introduced at the initial interface level via two 1/4-in. schedule - 40 pipes adjacent to the spout pipe. Inter-

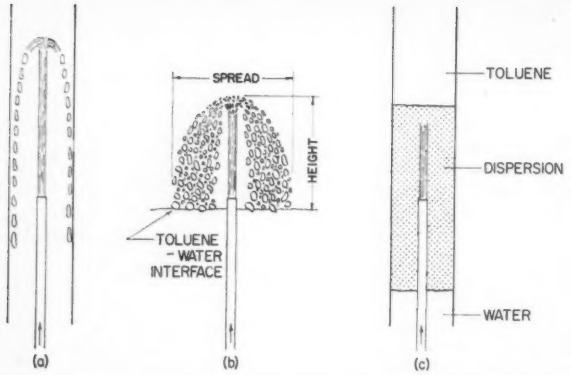

Figure 1—Diagrammatic representation of water spouting into (a) air, (b) unconfined toluene, (c) confined toluene.

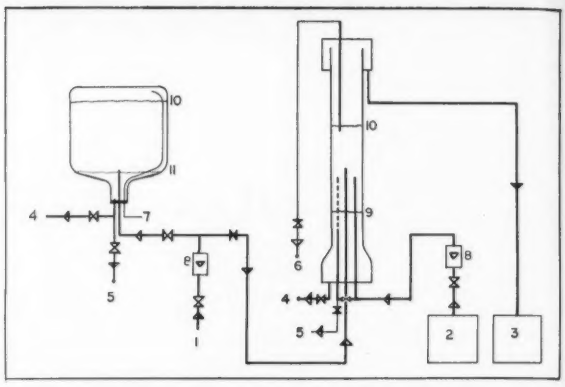

Figure 2—Schematic flow diagram of apparatus. Dotted line disconnected and toluene-phase supply shut off during semi-batch run. 1. Tapwater supply line; 2. Toluene-phase feed tank with pump; 3. Toluene-phase receiver; 4. Water-phase drain lines; 5. Water-phase sampling lines; 6. Toluene-phase sampling line; 7. Breather pipe; 8. Rotameters; 9. Dispersion-water interface; 10. Air-toluene interface; 11. Toluene-water interface.

facial scum was eliminated between runs, as was any discolored toluene in the carboy.

Figure 3 shows spout height as a function of water rate, at zero toluene flow in the 4-in. column, for a 1/4-in. o.d. and 1/8-in., 1/4-in., 3/8-in. and 1/2-in. schedule - 40 spout pipes. For each pipe, with the possible exception of the largest, spout height rises in approximately linear fashion at first and then tapers off with water rate. At a given volumetric water rate, spout height increases with decreasing inside diameter of the spout pipe, as would be expected from the accompanying increase in entering velocity of the spout. At low water rates spouting is poor — there is no fountain-formation at the peak of the ascending water column, which breaks up into large globules rather than dispersing into small drops. This region of "globulation" is followed by one of good spouting, in which a well-formed fountain at the summit of the spout breaks into well-dispersed droplets. Finally a limitation to the region of stable spouting is reached when some of the water droplets formed are so small as to be entrained upward by the slightest upward flow of toluene. It should be noted that the water flow range in which good stable spouting occurs, as indicated by the region between the dotted lines, increases with spout pipe size at first and then decreases sharply.

The effect of upward toluene flow rate on spout height for a 1/8-in. schedule - 40 spout pipe is shown in Figure 4, for two constant water rates. The small influence of toluene rate can be explained by the fact that the average linear velocity of the toluene is only 1/220th that of the entering water spout velocity, for equal volumetric rates of toluene and water. This explanation could also account for the larger effect of toluene rate at the lower water rate, where the linear velocity of toluene relative to the water spout is greater by a factor of two than at the higher water rate, for a given volumetric rate of toluene.

The glass carboy was used to observe under semi-batch conditions the characteristics of an unconfined spout, diagrammatically illustrated by Figure 1b. Here the water spout breaks into a shower of discrete droplets which flare out as they descend into the relatively quiescent toluene medium. The photographs of Figure 5 give some impression of how globule-formation is superceded by good spouting at water rates exceeding 0.5 U.S. gal./min., and how the resulting fountain continues to spread out radially with increasing water rate, at the same time as its vertical growth is arrested. These trends are also shown in Figure 6, where radial spread and vertical height of the unconfined spout are plotted as a function of water rate.

Figure 6 also indicates that spout heights in the 4-in. column were somewhat lower than corresponding spout heights in the carboy, for the higher water rates. This effect is believed to be caused by the greater strength and proximity to the spout of the downflow currents, created by the water drops falling within the confined annular space of the column, than the corresponding currents in the carboy, where the water drops are

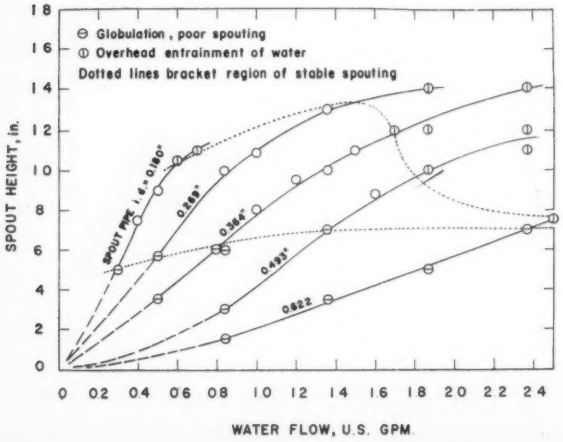

Figure 3—Water spout heights in static toluene within 4-in. column.

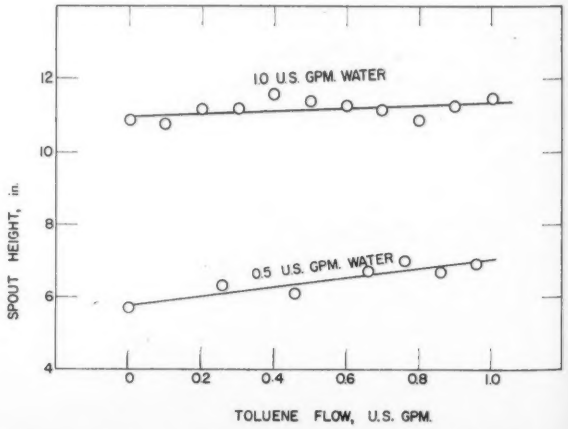

Figure 4—Effect of toluene rate on water spout heights in 4-in. column, using ⅛-in. schedule-40 spout pipe.

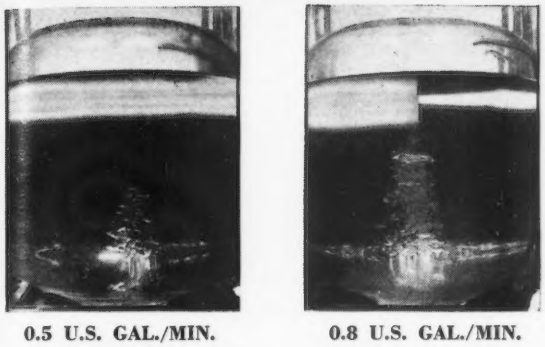

0.5 U.S. GAL./MIN. 0.8 U.S. GAL./MIN.

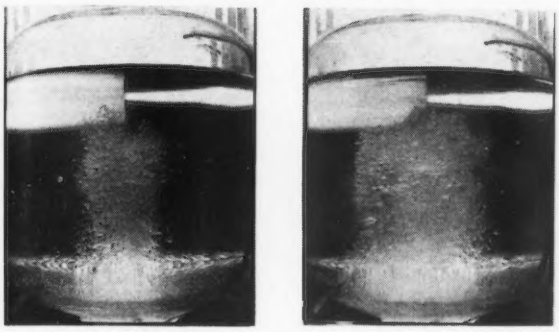

1.0 U.S. GAL./MIN. 1.2 U.S. GAL./MIN.

Figure 5—Photographs of unconfined spout. Rates are for water spouting into static toluene via ⅛-in. schedule-40 spout pipe.

free to spread out. These downflow currents of toluene or dispersion exert a retarding shear on the ascending water spout, and by sweeping with them the smallest water droplets, could also account for the observed fact that overhead entrainment of water droplets occurred at slightly lower water rates in the carboy than in the column.

The dotted lines of Figure 6 represent heights of spout predicted by the following frictionless form of the mechanical energy balance, based on the space-average velocity leaving the spout pipe and derived by assuming zero water velocity at the peak of the spout:

$$H = \frac{\rho_s}{\rho_s - \rho} \cdot \frac{U^2_{avg}}{2\alpha g} \quad \ldots\ldots\ldots\ldots\ldots\ldots (1)$$

For water spouting into air, Equation (1), using values of the kinetic-energy factor α computed by Kays[5] and reproduced by McCabe and Smith[6], gives reasonably good prediction of spout heights, though the predicted values are slightly on the low side. Had H been based on the axial velocity leaving the spout pipe, equivalent to taking α in Equation (1) as equal to $(U_{avg}/U_{max})^2$, then the predicted values would have been high to a similar degree. For water spouting into toluene, on the other hand, the theoretical spout heights given by Equation (1) are far above the observed values. This large discrepancy is believed to be caused by the energy consumed in creating the considerable new droplet surface at the head of the spout, especially at the higher velocities, an effect which is almost absent during the upflow of water into air.

It is the large inlet velocity at the base of the spout, coupled with the large surface created at the summit, which makes for the possibility of good mass transfer between the spouted liquid and the surrounding liquid.

Mass Transfer

For studying mass transfer by liquid-liquid spouting, the system water-benzoic acid-toluene was chosen. This system,

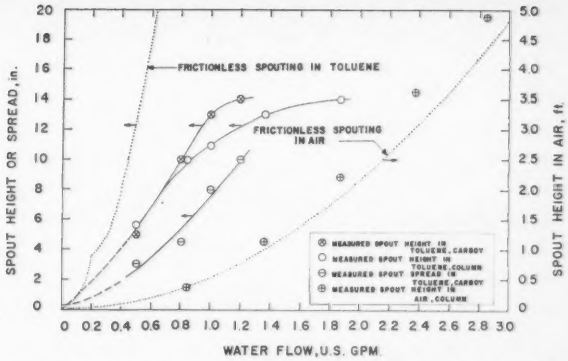

Figure 6—Water spouting characteristics in static media for ⅛-in. schedule-40 spout pipe.

the equilibrium data for which are readily available[7] and show little effect of benzoic acid concentration on the immiscibility of water and toluene, has been used by many other investigators[7,8,9] as a standard for evaluating liquid-liquid extractors.

The direction of extraction was from toluene to the water spout, which entered free of benzoic acid. Four continuous flow runs were performed in the column, with the toluene phase entering at a point slightly below the top of the spout pipe. Ten semi-batch runs were made, two of which were done in the carboy. Periodic sampling of inlet toluene, and outlet toluene and water streams, presented no problem in the continuous runs, but in the semi-batch runs, special lines had to be provided for simultaneous sampling of both changing phases, as shown in Figure 2. The toluene phase in the carboy runs was sampled before the start of a run and by quickly flushing out the carboy at the end of a run.

Water streams were analyzed for benzoic acid by alkaline titration to phenolphthalein end point. Benzoic acid analysis of toluene streams was effected either by titration with excess aqueous sodium hydroxide followed by back-titration with hydrochloric acid, after Mayfield and Church[8], or by direct titration with alcoholic sodium hydroxide, after Appel and Elgin[9].

The index used for evaluating and comparing mass transfer efficiency was the Murphree extract efficiency E_{ME}, as illustrated in Figure 7. For the continuous runs, the Murphree raffinate efficiency E_{MR} and the more fundamental fractional stage efficiency E could also be evaluated, but E_{MR} was far more sensitive to experimental error and to fluctuations from steady state than the other two efficiencies, which were practically equal to each other in all cases. For the semi-batch runs, only E_{ME} could be evaluated, using the simplified formula for the present case of a solute-free inlet water stream:

$$E_{ME} = \frac{C_{w2}}{C^*_{w2}} \quad \ldots\ldots\ldots\ldots\ldots\ldots (2)$$

Since, to the extent that it deviated from E at all, E_{ME} was always slightly smaller than E for the given operating system, the reported results are not slanted in favor of the equipment.

The equilibrium line at 59.9°F. in Figure 7 is that of Row, Koffolt and Withrow[7], who also provided equilibrium data at four other temperatures. To interpolate these data for other temperatures a factor α_t was defined by

$$(Cw^*)_t = \alpha_t (Cw^*)_{59.9°F.} \quad \ldots\ldots\ldots\ldots\ldots\ldots (3)$$

where both values of C_w^* apply to the same value of C_T. An analysis of all the equilibrium data provided by Row et al. indicated that α_t was independent of C_T[10] and therefore a function of temperature only. This function is plotted in Figure 8. To arrive at C_w^* for a given value of C_T at a fixed temperature t, it is necessary only to read off C_w^* at 59.9°F. from the equilibrium line of Figure 7, and multiply it by α_t at temperature t from Figure 8.

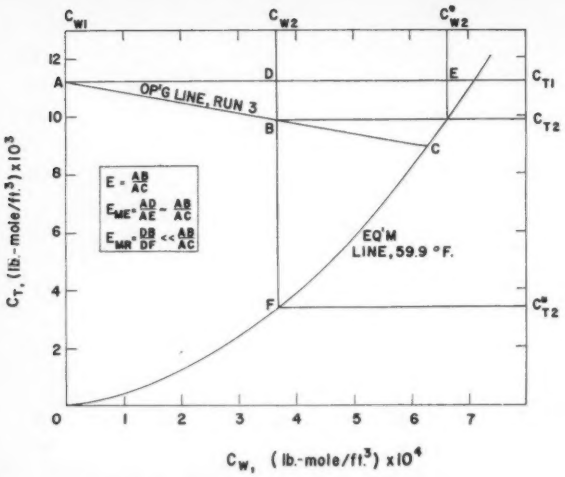

Figure 7 — Equilibrium line, operating line, and stage efficiencies for continuous run.

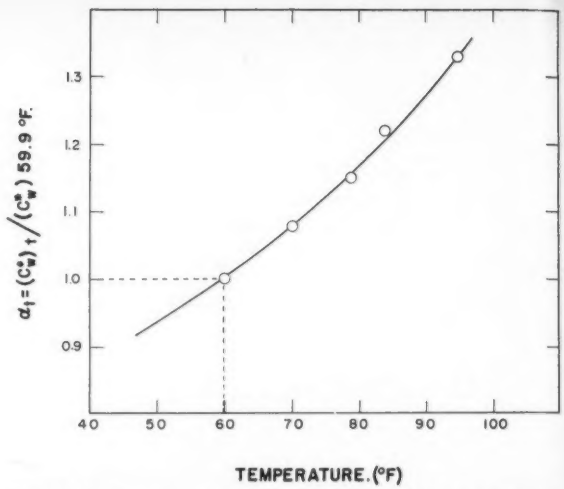

Figure 8—Temperature correction factor for equilibrium data.

A compilation of all the mass transfer results is given in Table 1. Although runs 1, 2, 7 and 10 were performed at the water rate at which overhead entrainment of water droplets by toluene starts, no water droplets were actually carried out of the column by continuously flowing toluene, due to the quiescent expanded section at the top.

For the continuous runs, the first column of outlet toluene concentrations in Table 1 are average measured values, while the second column are values calculated by material balance from a knowledge of the steadier concentrations of the other three streams and of the relative flow rates of the two phases. The values of Murphree extract efficiency based on these two figures are in satisfactory agreement and were therefore averaged.

For the two carboy runs, the first values of C_{T2} and E_{ME} listed are based on samplings at the beginning of a 5-minute run and are unambiguously reliable. The second or bracketed values, however, were based on samples of the mixed toluene phase at the end of a run, and were calculated on the assumption that all of the toluene within the carboy participated in the mass transfer of benzoic acid to the water. In both cases the bracketed values are lower than the initial values. The final data were

TABLE 1
SUMMARY OF MASS TRANSFER RUNS
$C_{W1} = 0$

Run No.	Enclosure	Spout pipe i.d. inches	Water rate U.S.gal./min.	Toluene rate U.S.gal./min.	Temp. °F.	C_{W2}	C_{T1}	C_{T2}	C_{T2} (calc'd)	C_{W2}*	E_{ME} %	
						lb.-moles/cu. ft. × 10^3						
1	column	0.269	1.5	0.5	64	0.653	12.21	10.92		0.717	91.1	92.7
									10.25	0.693	94.2	
2	column	0.622	2.5	0.5	60	0.191	12.20	11.68		0.721	26.5	26.8
									11.24	0.707	27.0	
3	column	0.269	1.0	0,26	60	0.367	11.19	9.91		0.661	55.5	55.7
									9.78	0.656	55.9	
4	column	0.269	1.0	0.56	60	0.345	11.19	10.04		0.666	51.8	51.1
									10.57	0.684	50.4	
5	carboy	0.269	1.0	0	59	0.300	10.63	10.63		0.709	42.3	
						0.279		(10.20)		(0.675)	(41.3)	
									9.80	0.661	42.2	
6	carboy	0.180	0.5	0	74	0.314	9.10	9.10		0.704	44.6	
						0.250		(8.96)		(0.699)	(35.8)	
									5.93	0.557	44.9	
7	column	0.180	0.6	0	53	0.387	8.33	8.33		0.572	67.6	
						0.314		6.87		0.518	60.6	
8	column	0.269	1.0	0	55	0.378	8.82	8.82		0.625	60.5	
9	column	0.269	1.0	0	48	0.383	8.30	8.30		0.555	69.0	
						0.357		7.93		0.540	66.1	
						0.327		7.08		0.508	64.4	
10	column	0.269	1.5	0	55	0.488	8.50	6.01		0.507	96.2	
11	column	0.269	1.2	0	52	0.325	3.51	3.45		0.350	92.9	
12	column	0.269	0.8	0	58	0.198	8.82	8.82		0.618	32.0	
						0.165		8.53		0.606	27.2	
						0.137		8.02		0.593	23.1	
13	column	0.364	1.5	0	56	0.485	23.7	23.7		0.982	49.4	
						0.414		22.8		0.962	43.0	
						0.405		21.4		0.933	43.4	
14	column	0.493	1.6	0	62	0.168	10.89	10.89		0.709	23.7	
						0.160		10.64		0.700	22.9	
						0.110		9.46		0.619	17.8	

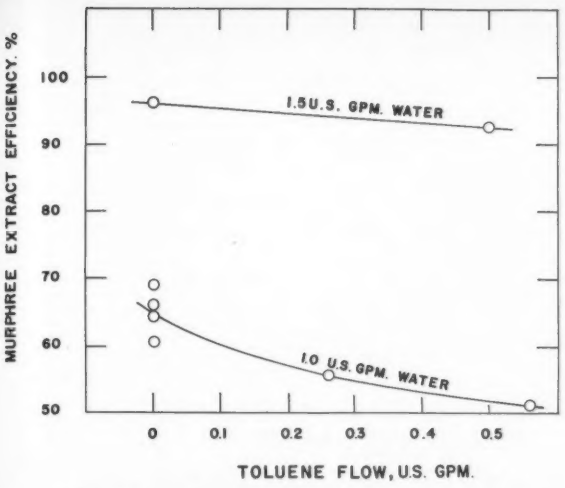

Figure 9—Effect of toluene rate on stage efficiency in 4-in. column, using ⅛-in. schedule-40 spout pipe.

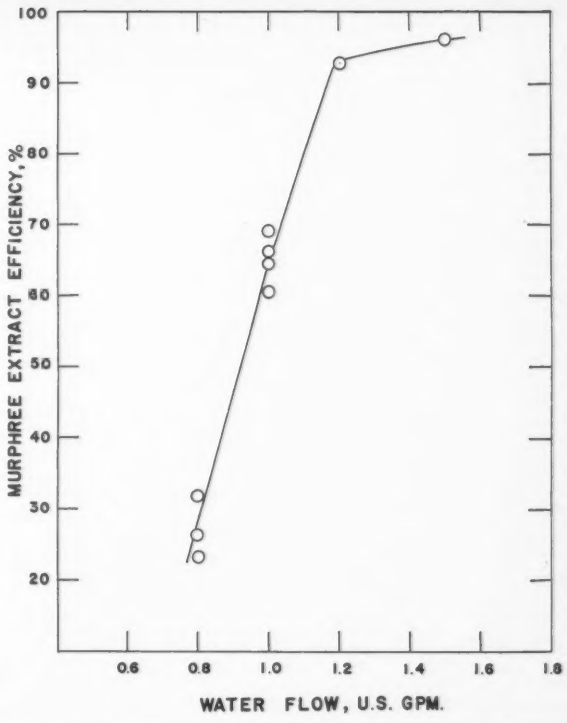

Figure 10—Effect of water spouting rate on stage efficiency in static toluene, using ⅛-in. schedule-40 spout pipe in 4-in. column.

therefore recalculated by material balance on the assumption that only the toluene occupying a cylindrical volume of length and diameter equal to that of the spout height and spread respectively (see Figure 1b) participated in the mass transfer significantly during the brief interval of a run. The excellent agreement of the resulting values of E_{ME}, listed immediately below the bracketed values in Table 1, with their respective initial values, appears to vindicate this assumption.

The same problem was avoided in the semi-batch column runs by using a toluene volume such that nearly all of it was caught in the turbulent dispersion process. Where successive data are listed in Table 1 for these runs, which lasted either five or ten minutes, these apply to the start of a run, the 5-minute mark, and the end of a run. The discrepancies in successive values of E_{ME} for a given run can be accounted for on the basis of experimental error[10], equilibrium data uncertainties[8], and the finite time required to develop concentration boundary layers in the non-flowing toluene phase. The last factor would explain the consistently downward trend of the efficiency values with time near the start of a run. The two or three values for a given run were given equal weight by including them all in subsequent plots.

Comparison of carboy run 6 with column run 7, both using a spout pipe i.d. of 0.180 in. and zero toluene flow, indicates a significantly higher stage efficiency in the column (64% average) than in the carboy (45%). It may be argued that much or all of this difference can be accounted for by the larger water flow rate in the column, where the water rate was 0.6 U.S. gal./min. as opposed to 0.5 U.S. gal./min. in the carboy. Comparison of carboy run 5 with column runs 8 and 9, all for a spout pipe i.d. of 0.269 in. and zero toluene flow, indicates however that even for the same water rate of 1.0 U.S. gal./min., the column efficiency (65% average) is considerably greater than the carboy efficiency (42%). This occurs, moreover, despite the fact that spout heights were lower in the column than in the carboy. The principal explanation for this difference is probably the fact that the average residence time of a droplet in the dispersion zone of the column is considerably greater than that of a droplet falling to the toluene-water interface in the carboy. In column runs 8 and 9 above, the height of the dispersion zone was 22 in., while in carboy run 5 the spout height was 13 in. For drops of similar size falling at equal velocities through a similar medium, simple mass transfer theory[11] dictates that for the settling process, $ln(1 - E_{ME})$ is directly proportional to the settling height. In this case the ratio of $ln(1 - E_{ME})$ for the overall column process to that for the overall carboy process is approximately 1.9, which is not much greater than the settling height ratio of 1.7. This near agreement gives support to the suggestion that droplet residence time is important in the overall mass transfer process. In addition, the added turbulence in the dispersion zone of the column probably increases the overall mass transfer coefficient around the droplets, while the stronger downflow currents of toluene probably increase the mass transfer coefficient about the rising spout, over that in the carboy.

Though the settling of droplets probably contributes substantially to the overall mass transfer process, there is evidence that it is not the sole contributor. This evidence is provided by Figure 9, which shows the effect of toluene flow rate on extraction efficiency for two constant water rates. If droplet settling were all-important, the effect of increasing toluene rate would be to increase mass transfer to the water drops, which are moving in a net direction opposite to that of the toluene. In fact, however, there is a slight decrease of E_{ME} with toluene rate, particularly at the lower water rate. This can only be explained by the contention that a significant portion, though not necessarily most, of the mass transfer occurs during the ascent of the spout and fountain rather than during the descent of the droplets. As noted previously in the discussion of Figure 4, increasing the toluene rate decreases the net relative velocity between the water spout and the cocurrent toluene, especially at the lower water rate. This causes a decrease in overall mass transfer coefficient between the water spout, the height of which increases only slightly (see Figure 4), and the cocurrent toluene, and hence apparently a small decrease in extraction efficiency for the overall process.

The effect of water spouting rate on E_{ME}, using 1/8-in. schedule - 40 spout pipe and no toluene flow, is shown in Figure 10. Increasing the water rate obviously has a most decided positive effect on E_{ME} up to about 1.2 U.S. gal./min. This can be explained by

(1) the increasing spout velocity which increases the overall mass transfer coefficient about the rising spout;

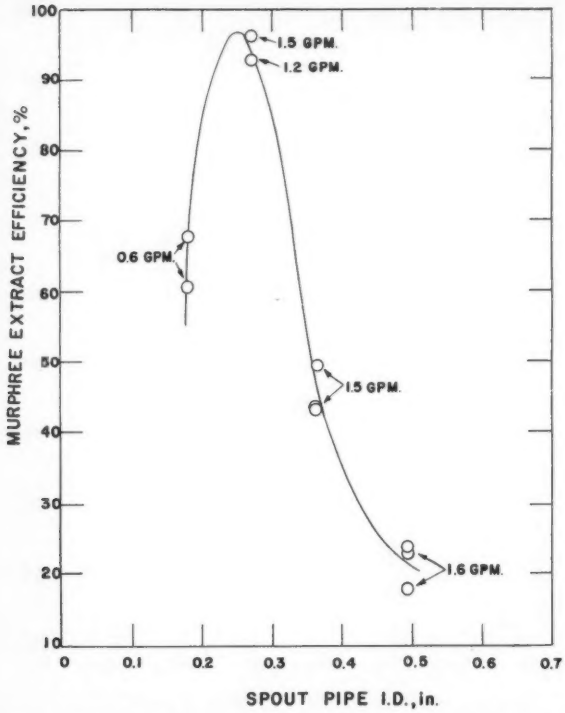

Figure 11—Effect of spout pipe diameter on stage efficiency in static toluene, operating near overhead entrainment point in 4-in. column.

(2) the increasing spout height (Figure 3), which counteracts the lowering of residence time per unit length of spout;

(3) the increasing formation of droplets (Figure 5), giving rise to more mass transfer surface; and

(4) the increasing depth of dispersion zone with water rate, a trend observed also by Ryon et al.[12] in their settlers, which results in raising the residence time of the droplets.

Above 1.2 gal. water/min., factors 2, 3 and to some extent 4 taper off, with the result that E_{ME} tapers off sharply. At 1.5 U.S. gal./min., overhead entrainment of water droplets starts (Figure 3). The plateau between 1.2 and 1.5 gal./min. is obviously the desirable operating region, using a 1/8-in. standard spout pipe.

The effect of spout pipe diameter on E_{ME}, operating at, or within 20% of, the overhead entrainment point in each case, presumably within a similar flat plateau region, is shown in Figure 11. The initial increase of E_{ME} with spout pipe inside diameter is undoubtedly due to the very large initial increase with spout pipe diameter of the allowable water rate before overhead entrainment will occur. This large increase in volumetric water rate more than counteracts several opposing tendencies, which only come into play decisively once an increase in spout pipe diameter is no longer accompanied by a large increase in allowable water rate. These tendencies, which result in the subsequent decrease of E_{ME} with spout pipe inside diameter, are the diminution of spout inlet velocity, of spout height, of droplet formation and of dispersion zone depth with an increase of spout pipe diameter. Clearly an optimum spout pipe inside diameter for mass transfer of about 0.25 in. is indicated by Figure 11.

Capacity Limitations

In picking an optimum operating spout pipe diameter, we have not only to consider mass transfer, but must also take into account capacity limitations. Capacity is restricted by operating instabilities caused by entrainment, or loading, and

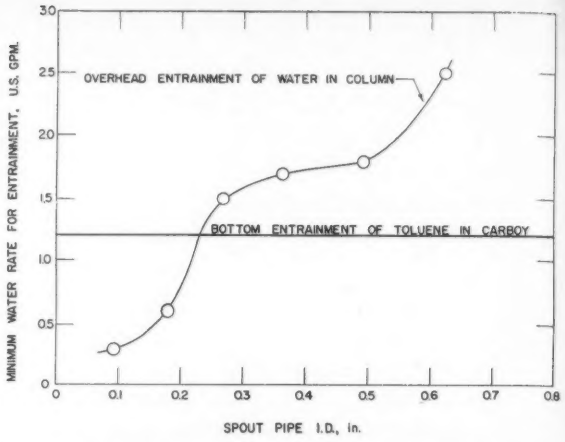

Figure 12—Initial entrainment points for water spouting in static toluene (overhead entrainment requires slight toluene flow).

eventual flooding of one phase by the other. Initial load points are shown in Figure 12, which is based largely on data from Figure 3. As spout pipe diameter increases, the water rate necessary to produce droplets sufficiently small to be entrained overhead by a slight toluene flow increases. On the other hand, bottom entrainment of toluene by water is independent of spout pipe diameter, and, under the severe conditions imposed by the contracting neck of the carboy, occurs at a water rate as low as 1.2 U.S. gal./min. If such unnecessarily severe conditions are imposed, then the maximum recommended spout pipe diameter, at the intersection of the two entrainment lines, would be about 0.23 in., a value which, by sheer coincidence, is very close to the 0.25 in. obtained by optimizing mass transfer.

Actually in the column, due to the transition piece at the bottom, the outlet water was slowed down sufficiently that bottom entrainment of toluene did not occur below about 3 gal. water/min. Even above this transition piece, however, there was no tendency for bottom entrainment to occur for water rates considerably in excess of 1.2 gal./min., the special figure for the carboy. Thus, in a design which involved neither end contractions or expansions, a spout pipe inside diameter of 0.23 in. could be safely exceeded, certainly up to the optimum value of 0.25 in., or even up to 0.269 in., as in a standard 1/8-in. schedule - 40 pipe.

If a design for spouting water into toluene continuously were based on a 1/8-in. schedule - 40 spout pipe, at a water flow of 1.2 U.S. gal./min., which is at the beginning of the plateau in Figure 10, then the corresponding toluene rate should be such that any possibility of flooding is precluded. Using the flooding correlation for spray towers of Minard and Johnson[13] as simplified by Treybal[14], applying the generous safety factors recommended, a toluene rate not exceeding 18 U.S. gal./(min.)(sq. ft.), corresponding to 35% of the calculated rate for water rejection, is indicated. In the 4-in. column this figure represents a toluene flow of 1.6 U.S. gal./min.

Design Proposals

One conception of a larger scale spouted mixer-settler is illustrated in Figure 13. The denser liquid is introduced to the bottom head through one or more inlet ports and moves upward through several equally spaced spout pipes in parallel, while the lighter liquid is introduced at the top head and moves downward through several pipes which surround the spout pipes symmetrically. The corresponding separated phases leave through ports immediately above the bottom sheet and below the top sheet, respectively. The heavy outlet phase passes over a sliding weir, which is used for interface control.

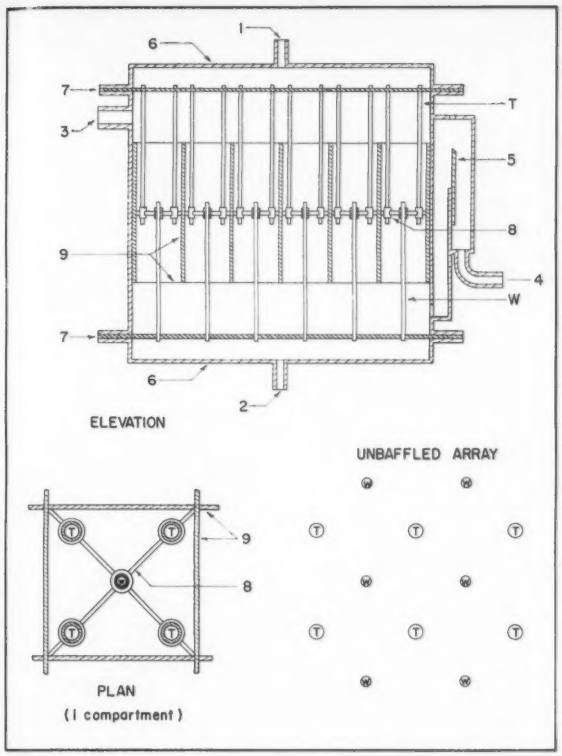

Figure 13 — Industrial-scale spouted mixer-settler. 1. Toluene-phase inlet; 2. Water-phase inlet; 3. Toluene-phase outlet; 4. Water-phase outlet; 5. Adjustable weir; 6. Bottom and top heads; 7. Bottom and top sheets; 8. Spider support; 9. Vertical baffles; T Toluene-phase inlet pipes; W Water-phase spout pipes.

In order to gain the enhancement of stage efficiency apparently contributed by confining walls, vertical baffles are provided in the primary design to completely encompass the dispersion zone. These baffles partition off each spout from its neighbours and are mounted on the outside walls of the unit. A typical baffled compartment, shown in Figure 13, would contain a central spout pipe surrounded by two or four light phase inlet pipes, all held by rings and spider supports from the baffles. Nozzle injectors could replace simple spout pipes to provide further insurance of high stage efficiency, but only at greater initial and operating cost.

To assign feasible dimensions to the above unit, the example of water spouting into toluene is considered. For this system it has been shown previously that 1/8-in. schedule - 40 spout pipes, operating with a water flow of 1.2 U.S. gal./min. per spout pipe and a toluene flow up to 18 U.S. gal./(min.) (sq. ft.), are indicated. The last figure in conjunction with the desired toluene throughput would determine the total cross-sectional area of the extractor, while the water rate per spout pipe in conjunction with the desired water capacity would determine the number of spout pipes. The toluene inlet pipes do not have a critical size and could be 1/4-in. schedule - 40, while a baffled compartment, in the light of the incomplete data on wall effect provided by the present study, could reasonably be four inches square. The distance between bottom and top sheets is set at 6 ft., thus allowing up to 3 ft. for the dispersion zone, though only 2 ft. are anticipated, and at least 1.5 ft. above and below this zone. The vertical baffles are 4 ft. high, leaving one foot of free space at top and bottom to permit removal of the raffinate and extract phases. The water and toluene inlet pipes each extend 3.2 ft. from their respective sheets and therefore overlap by almost five inches, which is ample vertical length for the ring supports.

It should be noted that it is quite possible and feasible to reverse the direction of spouting in any or all compartments, that is, to have in the present case downward spouting of toluene into water. In the above design, it would be necessary only to lower the toluene inlet pipes of a compartment to the same level as the original spout pipe, and to raise the spout pipe to the same level as the original toluene inlet pipes.

Another possibility is to use an unbaffled array of toluene and water inlet pipes, whereby the turbulence fostered by the presence of spout-confining walls is substituted by the turbulence created by the interaction of adjacent spouts. This would eliminate partitioning baffles and cut down on the necessary number of toluene inlet pipes, hence effecting economy. As illustrated in Figure 13, the ratio of the number of toluene inlet pipes to the number of spout pipes can be reduced from 4:1 (or 2:1) to 1:1 by use of an unbaffled array. Whether the stage efficiency of such an array would match that of a baffled unit is not, however, certain.

The unbaffled array could also lend itself to two-way spouting, water into toluene and toluene into water in this case. An increased vertical allowance, perhaps a foot, would be required for the dispersion zone. It is very likely that unbaffled two-way spouting, which bears a superficial resemblance to a Russian two-way injection column[15], could more than match the stage efficiency of baffled one-way spouting.

Comparisons and Conclusions

The relative compactness of an extractor can be measured as the contactor effectiveness E_f, defined by Coplan et al.[16] as

$$E_f = \frac{NF}{V} \qquad (4)$$

and having the dimensions of reciprocal time. Based on the system water-benzoic acid-toluene and the recommended design conditions above, for which the fractional stage efficiency and therefore N are estimated at 0.90, E_f for a spouted mixer-settler works out to be 35 hours^{-1}. This value, according to Mathers and Winter[17], is similar to those obtained in a pulsed column[18], in a pump-mix extractor[16], and in their own air-lift contactor, and three times that obtained in an unpulsed packed column[18], all for the system water-acetic acid-methyl isobutyl ketone. Since the unpulsed packed column figure is similar to those shown by the packed column data of Appel and Elgin[9] on the system water-benzoic acid-toluene, the procedure of comparing contactor effectiveness using data for the two different systems is considered legitimate.

A cascade of spouted mixer-settlers for a multistage operation would require inter-pumping of the phases. Making liberal allowances for various frictional head losses in the present equipment, the energy requirement for the recommended design conditions is computed to be less than 4×10^{-4} h.p./stage/litre/min. of total flow. According to Mathers and Winter[17], this value is about one-quarter that displayed by a mechanically agitated mixer[19], but about four times that shown by their own air-lift contactor. The degree of mixing was comparable in the three units, since the stage efficiencies were all close to 90% and the mixer retention time about 0.5 min. In the spouted contactor the "mixer" was taken as the middle 2 ft. dispersion zone.

A spouted mixer-settler has thus been shown to be an effective continuous-flow unit, which operates without the large energy losses inherent in mechanical agitation, performs both mixing and settling in a single relatively compact chamber, gives a high stage efficiency when optimally operated, and has a very simple design. Although its energy consumption is greater than that of an air-lift extractor[17], it has the advantage over the latter of not producing any air contaminated with

entrained liquid, an advantage which is pertinent in radiochemical work.

Liquid-liquid spouting may be characterized as bearing a similar relationship to conventional relatively bulky spray tower operation as up-down prilling does to the older bulkier one-way prilling, used for example in the manufacture of ammonium nitrate fertilizer as granular "nitraprills"[20].

Acknowledgements

The authors are indebted to the U.B.C. President's Committee on Research for grants-in-aid of this study, and to the National Research Council of Canada for supplementary financial support.

The authors wish to thank L. R. Galloway for the original suggestion which triggered this work and H. J. Bankes for practical assistance.

Nomenclature

C = bulk concentration of solute, lb.-moles/cu. ft.
C_T = value of C for toluene phase, lb.-moles/cu. ft.
C_W = value of C for aqueous phase, lb.-moles/cu. ft.
C_T^* = value of C_T in equilibrium with C_W, lb.-moles/cu. ft.
C_W^* = value of C_W in equilibrium with C_T, lb.-moles/cu. ft.
E = fractional stage efficiency, defined in Figure 7.
E_f = contactor effectiveness, defined by Equation (4), hours^{-1}.
E_{ME} = Murphree extract efficiency, defined in Figure 7
= Murphree spouted-phase efficiency in the present runs.
E_{MR} = Murphree raffinate efficiency, defined in Figure 7.
F = total flow rate of both phases, cu. ft./hr.
g = acceleration of gravity, ft./hr.^{2}
H = spout height, ft.
N = number of theoretical stages for a given operation
t = temperature, °F.
U_{avg} = space-average velocity of spouted liquid leaving spout pipe, ft./hr.
U_{max} = maximum local velocity of spouted liquid leaving spout pipe, ft./hr.
V = total volume of contactor (mixers plus settlers), cu. ft.
α = kinetic-energy correction factor to take account of radial velocity distribution in spout pipe.
α_t = ratio of C_W^* at temperature t to C_W^* at 59.9°F., for a given value of C_T
ρ = density of continuous-phase liquid, lb./cu. ft.
ρ_s = density of spouted liquid, lb./cu. ft.

Subscripts

1 = entrance
2 = exit
t = temperature

References

(1) Treybal, R. E., "Liquid Extraction", Chapter 9, McGraw-Hill, New York (1951).
(2) Davis, M. W., Hicks, T. E., and Vermeulen, T., Chem. Eng. Prog., **50,** 188 (1954).
(3) Treybal, R. E., "Mechanically Aided Liquid Extraction", from "Advances in Chemical Engineering", Vol. 1, edited by T. B. Drew and J. W. Hoopes, Jr., Academic Press, New York (1956).
(4) Mathur, K. B., and Gishler, P. E., A.I.Ch.E. Journal, **1,** 157 (1955).
(5) Kays, W. M., Trans. A.S.M.E., **72,** 1067 (1950).
(6) McCabe, W. L., and Smith, J. C., "Unit Operations of Chemical Engineering", p. 61, McGraw-Hill, New York (1956).
(7) Row, S. B., Koffolt, J. H., and Withrow, J. R., Trans. A.I.Ch.E., **37,** 559 (1941).
(8) Mayfield, F. D., and Church, W. L., Jr., Ind. Eng. Chem., **44,** 2253 (1952).
(9) Appel, F. J., and Elgin, J. C., Ind. Eng. Chem., **29,** 451 (1937).
(10) Johnston, T. R., B.A.Sc. Thesis, University of British Columbia, April 1959.
(11) Sherwood, T. K., and Pigford, R. L., "Absorption and Extraction", 2nd. ed., p. 155, McGraw-Hill, New York (1952).
(12) Ryon, A. D., Daley, F. L., and Lowrie, R. S., Chem. Eng. Prog., **55,** 70 (1959).
(13) Minard, G. W., and Johnson, A. I., Chem. Eng. Prog., **48,** 62 (1952).
(14) Treybal, R. E., "Mass-Transfer Operations", p. 371, McGraw-Hill, New York (1955).
(15) Gelperin, N. I., Volynetz, M. P., and Kolosova, G. M., Khim. Nauka i Prom., **1,** 560 (1956).
(16) Coplan, B. V., Davidson, J. K., and Zebroski, E. L., Chem. Eng. Prog., **50,** 403 (1954).
(17) Mathers, W. G., and Winter, E. E., Can. J. Chem. Eng., **37,** 99 (1959).
(18) Chantry, W. A., Van Berg, R. L., and Wiegandt, H. F., Ind. Eng. Chem., **47,** 1153 (1955).
(19) Overcashier, R. H., Kingsley, M. A., Jr. and Olney, R. B., A.I.Ch.E. Journal, **2,** 529 (1956).
(20) Cominco feature issue of Can. Min. J., **75,** 301 (1954).

★ ★ ★

Mass Transfer from Fluid and Solid Spheres at Low Reynolds Numbers[1]

C. W. BOWMAN[2], *D. M. WARD*[2], *A. I. JOHNSON*[2]
and O. TRASS[2]

Predicted continuous phase mass transfer coefficients for fluid and solid spheres in the Stokes region of flow are correlated as Sherwood numbers plotted against Peclet numbers. These correlations permit a study of the effect of internal circulation on the rate of mass transfer from fluid spheres. At a Peclet number of 10^4, the theory predicts a three-fold increase in transfer due to the circulation movements within a gas bubble. At a Peclet number below 10^{-2}, the difference between a circulating and non-circulating (or solid) sphere is indiscernible.

The analysis presented in this paper for fluid spheres is based on a study by Friedlander [1] of mass transfer around solid spheres. A more elaborate concentration profile through the boundary layer has been used in the present investigation and the result reported for solid spheres differs about 8% from that given by Friedlander.

The more interesting details of the mathematical treatment and the machine computation of the resulting differential equations are included.

The rate of mass transfer from spherical particles moving uniformly in a continuous fluid medium has direct application in many types of two-phase contacting equipment. Unfortunately precise mathematical formulation of this problem is exceedingly difficult in the flow regime of practical significance. However some theoretical studies on diffusion from solid spheres at low Reynolds numbers have been carried out[1,2,3].

This paper is a mathematical analysis of the influence of the internal circulation predicted by Hadamard[4] on the transfer rate from spherical fluid particles at $Re < 1$. Specifically, the continuous phase mass transfer coefficient was calculated for a typical liquid-liquid and a gas-liquid system and compared with that obtained for the analogous solid sphere case. This work was suggested in part by the observation of Hammerton and Garner[5] that the transfer rate from circulating bubbles of slightly soluble pure gases was about five times as large as from non-circulating bubbles. This increase cannot be attributed to improved mixing inside the sphere (since the entire resistance to transfer is in the continuous phase) and therefore must be due to the effect of internal circulation on the external flow pattern.

[1]*Manuscript received May 14; accepted October 10, 1960.*
[2]*Department of Chemical Engineering, University of Toronto, Toronto, Ont.*

Diffusion Model

The model used in this work is similar to that used by Friedlander[1] and is illustrated in Figure 1.

It is assumed that steady state diffusion is occurring from a fixed spherical particle of radius 'a' to a continuous fluid medium in laminar flow.

Two cases will be considered both of which have resistance to transfer present in the external fluid only. Case 1, illustrated on the left side of Figure 1, represents diffusion from a solid sphere where the velocity distribution in the continuum is obtained from the Stokes[6] solution of the linearized Navier-Stokes equations. Case 2, on the right side of Figure 1, considers diffusion from a two-component fluid system where the circulating disperse particle is saturated with the continuous phase and where the velocity distribution in the continuum is obtained from the Hadamard[4] solution of the linearized Navier-Stokes equations.

A concentration boundary layer is defined having a radius y', which is a function of the angle θ, with the concentration varying from the saturation value at the surface to the main stream value at the outer edge. Natural convection is neglected.

Mathematical Relationships

The amount of solute passing any section as indicated by the line A–A in Figure 1 is given by $\int_o^{\psi'_y} 2\pi c'\, d\psi'$ where ψ' is the stream function, $2\pi\psi'$ is the volumetric rate of flow, and c' is the concentration with respect to a main stream concentration of zero.

Assuming molecular diffusion in the θ direction is negligible, the difference in this quantity between any two sections separated by the angle $d\theta$ can be equated to the amount diffused from the surface as expressed by Fick's first law. Thus

$$\frac{-d\left[\int_o^{\psi'_y} 2\pi c'\, d\psi'\right]}{d\theta} = -D\left(\frac{\partial c'}{\partial r'}\right)_{r'=a} 2\pi a^2 \sin\theta \qquad (1)$$

When the non-dimensional symbols of Friedlander are used:

$$r = \frac{r'}{a} \quad (2a) \qquad c = \frac{c'}{c_o} \quad (2b) \qquad \psi = \frac{\psi'}{a^2 U} \quad (2c)$$

then Equation (1) becomes:

$$\frac{d\left[\int_o^{\psi_y} c\, d\psi\right]}{d\theta} = \frac{2}{Pe}\left(\frac{\partial c}{\partial r}\right)_{r=1} \sin\theta \qquad (3)$$

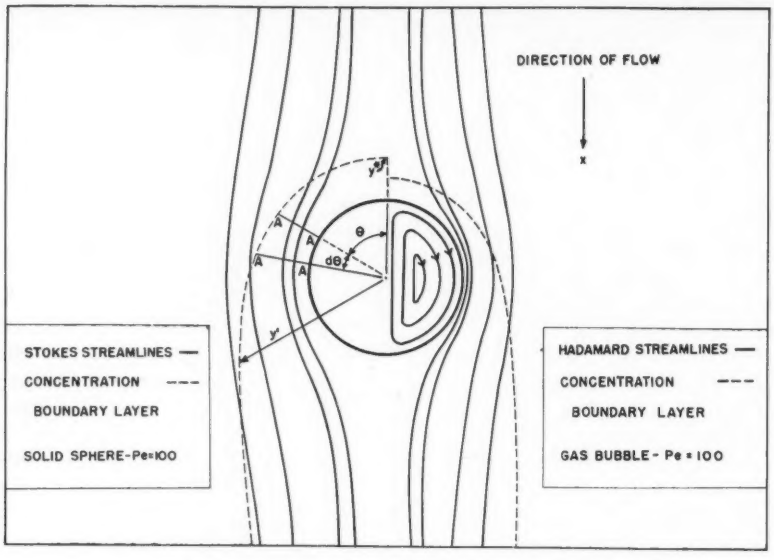

Figure 1—Comparison of solid and gas sphere in forced convection ($Re < 1$).

The important quantity in this study is the amount diffused from the total surface of the sphere which is given by $\int_a^{\psi_y} c d\psi$ at 180°. This integral, evaluated by the methods to be discussed in the next section, contains the unknown boundary layer thickness y. However, further substitution into Equation (3) gives rise to an ordinary non-linear differential equation which can be solved numerically for y.

Evaluation of $\int c d\psi$

To solve this integral, it is first necessary to express both ψ and c in terms of r and θ.

(a) **Stream Function ψ (r, θ)**

The linearized form of the Navier-Stokes equations can be expressed as:

$$\left(\frac{\partial^2}{\partial r'^2} - \frac{1}{r'}\frac{\partial}{\partial r'} + \frac{\partial^2}{\partial x^2}\right)^2 \psi' = 0 \quad \ldots\ldots(4)$$

This equation has the general solution

$$\psi' = \left(\frac{\alpha}{r'} + \beta r' + \gamma r'^2 + \Delta r'^4\right) \sin^2\theta \quad \ldots\ldots(5)$$

The specific solution for solid spheres obtained by Stokes[6] is as follows:

$$\psi' = -\frac{1}{2} U r'^2 \left(1 - \frac{3}{2}\frac{a}{r'} + \frac{1}{2}\frac{a^3}{r'^3}\right) \sin^2\theta \quad \ldots\ldots(6)$$

or in non-dimensional form:

$$\psi = -\frac{1}{2} r^2 \left(1 - \frac{3}{2}\left(\frac{1}{r}\right) + \frac{1}{2}\left(\frac{1}{r}\right)^3\right) \sin^2\theta \quad \ldots\ldots(7)$$

The boundary conditions for a circulating fluid sphere given by Hadamard[4] were applied to Equation (5) giving the following:

$$\psi' = -\frac{1}{2} U r'^2 \left(-\frac{3}{2}\frac{a}{r'}\left(\frac{3\mu_1 + 2\mu}{3\mu_1 + 3\mu}\right) + \frac{1}{2}\left(\frac{a}{r'}\right)^3 \left(\frac{\mu_1}{\mu_1 + \mu}\right)\right) \sin^2\theta \quad \ldots(8)$$

where μ and μ_1 are the continuous and disperse phase viscosities respectively. Since Equation (8) represents the stream function for a particle moving in a quiescent liquid it was necessary to superimpose on the flow field a negative velocity equal to the Hadamard velocity of fall. The resulting equation written in non-dimensional form is:

$$\psi = -\frac{1}{2} r^2 \left(1 - \frac{3}{2r}\left(\frac{3\mu_1 + 2\mu}{3\mu_1 + 3\mu}\right) + \frac{1}{2r^3}\left(\frac{\mu_1}{\mu_1 + \mu}\right)\right) \sin^2\theta \quad \ldots\ldots(9)$$

For simplicity, both Equations (7) and (9) can be written as

$$\psi = -\frac{1}{2} r^2 \left(1 - \frac{A}{r} + \frac{B}{r^3}\right) \sin^2\theta \quad \ldots\ldots(10)$$

where $A = \frac{3}{2}$ for Equation (7); $\frac{3}{2}\left(\frac{3\mu_1 + 2\mu}{3\mu_1 + 3\mu}\right)$ for Equation (9)

$B = \frac{1}{2}$ for Equation (7); $\frac{1}{2}\left(\frac{\mu_1}{\mu_1 + \mu}\right)$ for Equation (9)

(b) **Concentration c (r, θ)**

A mass balance on an elemental cube in the boundary layer, considering bulk flow in both the radial and tangential directions and diffusional flow in the radial direction, gives rise to the following equation in polar coordinates.

$$r'^2 V_r \frac{\partial c'}{\partial r'} + r' V_\theta \frac{\partial c'}{\partial \theta} = \frac{D\partial\left(r'^2 \dfrac{\partial c'}{\partial r'}\right)}{\partial r'} \quad \ldots\ldots(11)$$

where V_r and V_θ are the radial and tangential velocities respectively.

This partial differential equation leads to $c(r, \theta)$ as required but the solution is quite complex. To obtain an expression more suitable for the subsequent calculations, an arbitrary concentration polynomial was adopted which satisfied known boundary conditions. These conditions were as follows:

at $r = 1$ (surface of the sphere) (1) $c = 1$ (2) $\dfrac{\partial(r^2 \partial c/\partial r)}{\partial r} = 0$ ....(12)

at $r = y$ (outer edge of B.L.) (3) $c = 0$ (4) $\partial c/\partial r = 0$

Of the above, (1), (3) and (4) came directly from the physical model. Condition (2) was obtained by applying Equation (11) at the sphere's surface. It will be noted that since

V_r and $\partial c'/\partial\theta$ are zero at the surface for the solid and fluid spheres considered in this work, Equation (11) reduces to (2) for both cases.

The various polynomials investigated are shown in Table 1. Most did not satisfy one or more of the following additional requirements:

(a) boundary conditions must be independently satisfied.

(b) no discontinuities can occur within the boundary layer.

(c) $(\partial c/\partial r)_{r=1}$ must equal -1 as $y \to \infty$. This condition corresponds to diffusion into a stagnant fluid and must be satisfied.

As noted in column four of Table 1, only polynomials (2), (5) and (10) met these added conditions.

Polynomial (10) satisfied the four boundary conditions and was therefore used in the subsequent calculations. In addition polynomial (2) was also carried through to a final solution to see if a two-term profile was sufficiently accurate to characterize the concentration in the boundary layer. This latter profile is the one used by Friedlander (in slightly different form) for mass transfer from solid spheres and his work served as a guide and comparison for that portion of the present study.

The concentration profiles obtained from polynomials (2) and (10) are respectively:

$$\text{Profile 2: } c = \frac{y - r}{r(y-1)} \qquad (13)$$

$$\text{Profile 10: } c = \frac{(y-r)^2(r+2y-3)}{2r(y-1)^3} \qquad (14)$$

(c) Evaluation of $\int \psi\, dc$

To simplify the boundary limits, Friedlander transformed the $\int c\,d\psi$ as follows:

TABLE 1

No.	Form of Polynomial	Boundary Conditions Satisfied	Reason for Eliminating*
1.	$c = a + br$	(1), (3)	(c)
2.	$c = a + \frac{b}{r}$	(1), (3)	√
3.	$c = a + br + cr^2$	(1), (3), (4)	(c)
4.	$c = a + br + cr^2$	(1), (2), (3)	(b) and (c)
5.	$c = a + \frac{b}{r} + cr$	(1), (3), (4)	√
6.	$c = a + \frac{b}{r} + cr$	(1), (2), (3)	(a)
7.	$c = a + \frac{b}{r} + \frac{c}{r^2}$	(1), (3), (4)	(c)
8.	$c = a + \frac{b}{r} + \frac{c}{r^2}$	(1), (2), (3)	(a)
9.	$c = a + br + cr^2 + dr^3$	(1), (2), (3), (4)	(b) and (c)
10.	$c = a + \frac{b}{r} + cr + dr^2$	,,	√
11.	$c = a + \frac{b}{r} + \frac{c}{r^2} + \frac{d}{r^3}$	,,	(c)

*(a) Boundary conditions must be independently satisfied.
(b) No discontinuities can occur within the boundary layer.
(c) $\left(\frac{\partial c}{\partial r}\right)_{r=1}$ must equal -1 as $y \to \infty$

TABLE 2

	Profile 2			Profile 10		
	Solid	Liquid	Gas	Solid	Liquid	Gas
c_1	.7500	.5855	.5046	10.00	12.19	13.28
c_2	.1250	.04277	.002022	0	3.947	5.903
c_3	.3750	.4572	.4980	6.00	2.053	.09706
c_4				10.00	4.299	1.474
c_5				18.00	14.05	12.10
c_6				12.00	9.369	8.065
c_7				6.00	2.053	.09706

$$\int_o^{\psi_y} c\,d\psi = \int_o^{(c\psi)_y} d(c\psi) - \int_1^o \psi\,dc = -\int_1^o \psi\,dc \qquad (15)$$

Substituting for ψ in the form of Equation (10) and c from Equations (13) and (14), the following two expressions are obtained:

Using Equation (13)

$$\int c\,d\psi = \frac{-y}{2(y-1)}\left[y - A\ln y - \frac{B}{2y^2} - 1 + \frac{B}{2}\right]\sin^2\theta \qquad (16)$$

Using Equation (14)

$$\int c\,d\psi = \frac{1}{4(y-1)^3}\left[-\frac{3}{2}y^4 + \left(4 - \frac{2}{3}A - B\right)y^3 + \left(\frac{3}{2}A + \frac{3}{2}B - 3\right)y^2 + 3By - \frac{7}{2}B - \frac{5}{6}A + \frac{1}{2} - (3Ay^2 - 2Ay^3 + 3B)\ln y\right]\sin^2\theta \qquad (17)$$

For convenience in later computations, these equations were simplified to

$$\int c\,d\psi = \frac{-y}{y-1}\left[\frac{y}{2} - c_1\ln y - \frac{c_2}{y^2} - c_3\right]\sin^2\theta \qquad (18)$$

$$\int c\,d\psi = \frac{1}{16(y-1)^3}\left[-6y^4 + c_1y^3 - c_2y^2 + c_3y - c_4 - (c_5y^2 - c_6y^3 + c_7)\ln y\right]\sin^2\theta \qquad (19)$$

The coefficients ($c_1 \ldots c_7$) were evaluated for the three cases of a solid, liquid and gaseous spherical particle and are given in Table 2. The specific examples were chosen to be:

(a) solid (in any fluid)

(b) liquid (ethyl acetate drop rising in water)

(c) gas (carbon dioxide bubble rising in water)

Determination of Mass Transfer Coefficient

Equations (18) and (19) when substituted into Equation (3) give respectively the following differential equations in general form:

$$\frac{d\left[\left(\frac{y}{y-1}\right)\left(\frac{y}{2} - c_1\ln y - \frac{c_2}{y^2} - c_3\right)\sin^2\theta\right]}{d\theta} = \frac{2}{Pe}\left(\frac{y}{y-1}\right)\sin\theta \qquad (20)$$

$$\frac{d\left[\frac{1}{16(y-1)^3}\left[-6y^4 + c_1y^3 - c_2y^2 + c_3y - c_4 - (c_5y^2 - c_6y^3 + c_7)\ln y\right]\sin^2\theta\right]}{d\theta} = \frac{2y+1}{Pe(1-y)}\sin\theta \qquad (21)$$

Now Fick's first law written in dimensionless form becomes:

$$Sh = -\int_o^\pi \left(\frac{\partial c}{\partial r}\right)_{r=1} \sin\theta\, d\theta \quad \ldots\ldots\ldots\ldots (22)$$

and substituting from Equation (3), one obtains

$$Sh = -\int_o^\pi \frac{Pe}{2}\frac{d[\int cd\psi]}{d\theta}\, d\theta = -\frac{Pe}{2}\left[\int_o^{\psi_y} cd\psi\right]_\pi \quad \ldots\ldots\ldots (23)$$

The final results will be reported in this form.

(a) Analytical Solutions of Equations (20) and (21).

Friedlander in his sphere analysis (using profile 2) showed that certain order of magnitude approximations were possible for thick and for thin boundary layers and, for these limiting cases, obtained analytical solutions of Equation (20). The same techniques were applied in the present study to Equation (21)—again for the solid sphere case. These analytical solutions are shown in Table 3. No general analytical thin boundary layer solutions were possible for fluid spheres. However the thick boundary layer solutions for both solid and fluid spheres reduced to $Sh = 2$. This would be expected since a very thick boundary layer implies diffusion into a stagnant medium.

(b) Numerical Solutions of Equations (20) and (21).

Except in the restricted regions mentioned above, these equations required numerical solution. The method used by the authors is discussed below in some detail as several interesting points arose. The entire calculation was programmed on the I.B.M. 650 computer.

Both Equation (20) and (21) can be expressed in the following form

$$\frac{dy}{d\theta} = \frac{2/Pe - f_2\cos\theta}{f_1\sin\theta} \quad \ldots\ldots\ldots\ldots (24)$$

where f_1 and f_2 are given in Table 4.

TABLE 3

	Profile 2	Profile 10
Thin B.L.–Solid (Large Pe)	$Sh = 0.89\ Pe^{1/3}$	$Sh = 0.978\ Pe^{1/3}$
Thick B.L.–Solid and Fluid (Small Pe)	$Sh = 2 + \frac{Pe}{2} + \frac{Pe^2}{6} + \ldots$	$Sh = 2 + \frac{9}{16}Pe + \frac{9}{64}Pe^2 + \ldots$

From physical considerations $dy/d\theta$ must be positive for the region $0° \leqq \theta \leqq 180°$. Now $f_1 \sin\theta$ vanishes for $\theta = 0$ and $dy/d\theta$ is infinite unless $(2/Pe - f_2\cos\theta)$ also vanishes in which case $dy/d\theta$ is indeterminate. Thus the solution of the equation passing through the point $y = 1$, $\theta = 0$ will follow the line $\theta = 0$ (corresponding to infinite slope) until a value of y is reached which solves the equation

$$2/Pe - f_2 = 0 \quad \ldots\ldots\ldots\ldots (25)$$

At this point, the slope of the required solution will change discontinuously and will swing into the region $\theta > 0$. Thus until a critical value of y (say y^* — see Figure 1) is reached, a solution cannot be initiated. The first step was therefore to solve Equation (25) for y^* (the Newton-Raphson iterative process[7] was found convenient for machine computation) and to start the solution from the point $y = y^*$, $\theta = 0$.

The numerical computation itself used a power series (Equation (27)) to obtain four starting values (at $\theta = 0.5$, 1, 1.5, 2°) and employed these in new predictor-corrector formulae suggested by Hamming[8]. The frequently used Milne method proved unstable for this problem.

For convenience, the substitution $z = 1 - \cos\theta$ was made in Equation (21) giving

$$f_1(2 - z)\frac{dy}{dz} = f_2 + \frac{2/Pe - f_2}{z} \quad \ldots\ldots\ldots\ldots (26)$$

The solution was assumed to have the form

$$y = y^* + a_1 z + a_2 z^2 \quad \ldots\ldots\ldots\ldots (27)$$

and hence

$$dy/dz = a_1 + 2a_2 z \quad \ldots\ldots\ldots\ldots (28)$$

Also f_1 and f_2 can be expanded as a Taylor Series as follows:

$$f(y) = f(y^*) + (a_1 z + a_2 z^2) f'(y^*) + \frac{(a_1 z + a_2 z^2)^2}{2} f''(y^*) \ldots (29)$$

Substituting Equations (27), (28) and (29) into Equation (26) and collecting like powers of z, one obtains the following expressions for a_1 and a_2.

$$a_1 = \frac{f_2}{2f_1 + f_2'}\ ;\ a_2 = \left[(f_1 + f_2') - \frac{f_2(4f_1' + f_2'')}{(4f_1 + 2f_2')}\right]\frac{a_1}{4f_1 + f_2'} \quad \ldots (30)$$

After the four starting values were obtained, predictor Equation (31) and corrector Equation (32) given below were applied. The corrector equation was repeated until two successive values of y agreed to four significant figures.

$$y_{n+1} = y_{n-3} + \frac{4h}{3}\left\{2\left(\frac{dy}{d\theta}\right)_n - \left(\frac{dy}{d\theta}\right)_{n-1} + 2\left(\frac{dy}{d\theta}\right)_{n-2}\right\} \quad \ldots\ldots (31)$$

$$y_{n+1} = \frac{1}{8}\left[9y_n - y_{n-2} + 3h\left\{\left(\frac{dy}{d\theta}\right)_{n+1} + 2\left(\frac{dy}{d\theta}\right)_n - \left(\frac{dy}{d\theta}\right)_{n-1}\right\}\right] \quad \ldots\ldots (32)$$

The increment "h" was the angle in radians corresponding to ½°.

TABLE 4

	Using Equation (13) (Profile 2)
f_1	$\left[\frac{y^2}{2} - y - c_1(y-1) + c_2\left(\frac{2y-1}{y^2}\right) + c_3 + c_1 \ln y\right]\left[\frac{1}{y(y-1)}\right]$
f_2	$y - 2c_1 \ln y - \frac{2c_2}{y^2} - 2c_3$
	Using Equation (14) (Profile 10)
f_1	$\frac{6y^4 - y^3(c_6 + 24) + y^2(3c_1 - c_2 + c_5 + c_6) + y(2c_3 - 2c_2 - c_5) + c_3 + c_7 - 3c_4 - c_7/y + (y^2(3c_6 - c_5) - 2c_5 y - 3c_7)\ln y}{(y-1)^3(2y+1)}$
f_2	$-2\left\{\frac{(-6y^4 + c_1 y^3 - c_2 y^2 + c_3 y - c_4) - (c_5 y^2 - c_6 y^3 + c_7)\ln y}{(y-1)^2(2y+1)}\right\}$

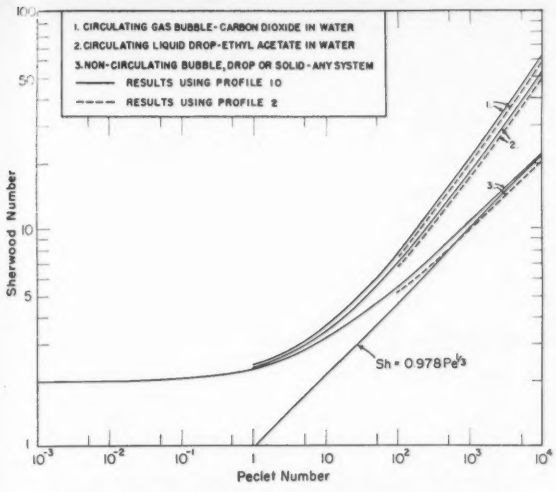

Figure 2—Transfer from fluid and solid spheres.

In this manner values of y were obtained at $\frac{1}{2}°$ intervals from $\theta = 2°$ up to $\theta = 179.5°$. As part of the machine calculation, the $\int c d\psi$ was also obtained (using Equation 18 or 19) and the value of the integral at 180° estimated by extrapolation. This latter quantity was then substituted into Equation (23) to obtain the Sherwood number and hence the mass transfer coefficient. The results for solid, liquid and gas particles for both concentration profiles are shown in Figure 2.

Discussion and Conclusions

The results show that at a Peclet number of 10^4 circulation movements within a gas bubble increase the mass transfer rate about threefold over that of a non-circulating bubble or a solid particle. The enhancement of a typical circulating liquid drop at the same Peclet number is about two and one-half times that of a solid particle. For any particular system, the exact degree of improvement depends on the viscosity ratio of the disperse and continuous phases. The increase due to circulation decreases with decreasing Peclet number and almost vanishes for $Pe < 10^{-2}$. This is to be expected since a low Peclet number (i.e., high diffusivity) indicates a very thick concentration boundary layer where the relative effects of circulation are much less pronounced.

Hammerton and Garner[5] reported that a fivefold reduction in mass transfer occurred when ethylene bubbles rising in water had previously contacted petroleum jelly. This contaminant presumably prevented circulation. Since their work was at a much higher Reynolds number than that considered in the present study, quantitative comparisons are not possible. However the general agreement with the results reported above suggests that circulation at higher Reynolds numbers may play a similar role. It should be pointed out that a circulating fluid sphere has a higher Peclet number due to its increased terminal velocity and hence some increase in transfer rate over its non-circulating partner would be expected. The curves in the present investigation, however, are independent of this effect since they have been plotted against the Peclet number.

Part of the present study was an evaluation of various assumed concentration profiles and their effect on the final solution. As shown in Table 3, many of the polynomial forms attempted gave profiles which were consistent with the physical picture. The four term profile (No. 10) yields a slightly different Sherwood-Peclet number relationship than the two term profile (No. 2). The greater complexity involved in the former must be weighed against the accuracy desired, taking into account the inherent limitations of the defining model. If effects such as tangential diffusion, natural convection and interfacial tension could mathematically be included, the more complete profile would undoubtedly be warranted. Yuge[9] in a solid sphere heat transfer study for Peclet numbers less than 10 obtained theoretical results identical to those given here for profile 10.

The quantity y^*, although its use here was to overcome a mathematical hurdle, can be given the physical significance of back diffusion from the forward stagnation point into the on-coming fluid stream. Since an infinite concentration boundary layer is realized as the Pe number approaches zero, this hypothesis seems reasonable. Indeed y^* approaches infinity for this condition as can be seen from Equation (25).

Further details of the mathematics derivations given in this paper may be found in either reference (10) or (11).

Nomenclature

a = sphere radius, cm.
a,b,c,d = constants in concentration polynomial
A,B = constants in stream functions
c = c'/c_o, dimensionless
c' = concentration, g.-moles/cc.
c_o = saturation concentration, g.-moles/cc.
D = diffusivity, cm.²/sec.
h = angle in radians
k = mass transfer coefficient, cm./sec.
Pe = Peclet number, $2aU/D$, dimensionless
r = r'/a, dimensionless
r' = radial distance, cm
Re = Reynolds number, $2a\rho U/\mu$, dimensionless
Sc = Schmidt number, $\mu/\rho D$, dimensionless
Sh = Sherwood number, $2ka/D$, dimensionless
U = main stream velocity, cm./sec.
V_r = radial velocity, cm./sec.
V_θ = tangential velocity, cm./sec.
x = distance in direction of flow, cm.
y = y'/a dimensionless
y' = distance from centre of sphere to outer edge o_2 boundary layer, cm.
z = $1 - \cos\theta$
ρ = fluid density, gm./cc.
θ = angle from negative x-axis
μ = continuous phase fluid viscosity, gm./cm.-sec.
μ_1 = disperse phase fluid viscosity, gm./cm.-sec.
ψ = stream function, ψ'/a^2U, dimensionless
ψ_s = stream function at outer edge of boundary layer, dimensionless
ψ' = stream function, cc./sec.
$\alpha,\beta,\gamma,\Delta$ = constants

References

(1) Friedlander,S. K., A.I.Ch.E. Journal, **3,** 43 (1957).
(2) Frisch, H. L., J. Chem. Phys., **22,** 123 (1954).
(3) Kronig, R.and Bruijsten, J., Appl. Sci. Research, **A2,** 439 (1951).
(4) Hadamard, J., Compt. Rend. **152,** 1735 (1911).
(5) Hammerton, D., and Garner, F. H., Trans. Inst. Chem. Eng. (London) **32,** (Supplement) S-18 (1954).
(6) Stokes, G. G., Math. and Phys. Papers—Vol. 1, Cambridge University Press—1880.
(7) Hartree, D. R., Numerical Analysis, Oxford 1958.
(8) Hamming, R. W., Journ. Assoc. Computing Machinery, **6,** 73 (1959).
(9) Yuge, T., Reports of the Institute of High Speed Mechanics (Tohoku University) **6,** 143 (1956).
(10) Bowman, C. W., Ph.D. Thesis, University of Toronto, (1960).
(11) Ward, D. M., Ph.D. Thesis, University of Toronto, (1961).

★ ★ ★

Dynamic Analysis of Bubble Plate Performance[1]

H. S. MICKLEY[2], L. A. GOULD[3] and L. M. SCHWARTZ[4]

A frequency response method is examined as a possible experimental method for the simultaneous determination of liquid mixing, plate efficiency, vapor-liquid equilibrium, and liquid holdup on a single bubble tray. The method depends upon the introduction of sinusoidal fluctuations in the concentration of a species in the liquid and vapor fed to the plate and the measurement of the induced concentration variations of the same species in the effluent liquid. It is applicable to multi-component systems.

The analytical results used to interpret the measurements are based on a linearized model. Despite this idealization, systems exhibiting marked curvature of the liquid-vapor equilibrium relation are adequately represented. Systems showing very significant enthalpy effects are treated quantitatively when the liquid on the plate is perfectly mixed. This is done with the aid of the "signal flow graph" technique.

With incompletely mixed plate liquid, mathematical difficulties have so far prevented the quantitative interpretation of measurements of the frequency response when enthalpy effects are large. At present it appears that the frequency response technique is limited to perfectly mixed plates, i.e., to small laboratory sized plates, or to incompletely mixed systems in which the heat effects are small, i.e., gas absorption plates and distillation systems in which the volatilities and latent heats of all components are of comparable magnitude.

Technological advances in the fields of process design and control have increased the need for more complete information concerning the behavior of chemical engineering systems. In particular, it is now recognized that the optimization of the design and operation of a chemical plant requires the specification of its transient behavior. The information needed to predict the unsteady-state performance of a plant component is not easy to obtain and faster, cheaper methods than now available are much to be desired. The motivation of the work reported here stemmed from the need to predict the dynamic response of bubble plate contactors, a class of equipment which is found in all branches of the chemical process industry.

In this paper, the feasibility of using a frequency response technique for the simultaneous experimental determination of liquid mixing, plate efficiency, vapor-liquid equilibrium and liquid holdup on a single experimental bubble tray is investigated. The method involves the introduction of sinusoidal composition fluctuations in the concentration of one of the species entering the plate with the liquid and vapor feed and the measurement of the composition fluctuations of that same species in the effluent liquid from the plate. The method is applicable to multi-component systems.

Well developed techniques exist for the analysis of the dynamic response of linear systems and the form of the perturbation imposed on a linear system for the purpose of determining its dynamic behavior is relatively unimportant. Neither of these circumstances apply in the case of a non-linear system and unfortunately a bubble plate contactor is a non-linear device. For small fluctuations, however, a linearized model can be expected to approximate the behavior of the actual plate. Under such circumstances, the correspondence between the behavior of the actual plate and that predicted on the basis of a linearized model needs to be known as a function of the amplitude and type of disturbance imposed. In the present paper, the form of the disturbance is limited to a sinusoid and attention is focussed upon the information that can be obtained from applying such a disturbance to an actual plate.

Two important considerations led to the choice of a sinusoidal disturbance:

1. Should it prove capable of producing useful results, a sinusoidal forcing technique would be an important experimental tool. Firms concerned with the design and control of separation equipment using bubble contacting plates might find it profitable to build both laboratory and commercial sized plates on which critical separations could be studied by means of the measurement of the response of the plate to sinusoidal oscillations of the input streams.

2. Ultimately it is to be hoped that the characteristics of an operating plate can be ascertained from measurements of the response of the plate to the "random" fluctuations in input quantities which occur as a normal part of its commercial operation. If this were possible, no artificial disturbances would be required. However, at present the feasibility of such a technique rests on the use of correlation techniques which require that the response of the system to sinusoidal perturbations be understood. This suggests that the response of the system to sinusoid variations be studied before an investigation of the utility of a random fluctuation technique is undertaken.

[1]*Manuscript received April 27; accepted September 20, 1960.*
[2]*Professor of Chemical Engineering, Massachusetts Institute of Technology, Cambridge, Mass.*
[3]*Associate Professor of Electrical Engineering, Massachusetts Institute of Technology, Cambridge, Mass.*
[4]*Esso Research and Engineering Company, Linden, N.J.*
Contribution from the Massachusetts Institute of Technology, Cambridge, Mass.

The Linearized Model

Consider a single bubble plate. Idealize the plate as follows.

1. Represent the liquid mixing on the plate by the Kirschbaum idealization as a series of N perfectly mixed pools[1,2,3], each pool containing $\frac{\bar{H}}{N}$ moles of liquid as shown in Figure 1.

The liquid flows from one pool to the next without bypassing pools or back-mixing. Although this simplification of the mixing process is a gross approximation to the actual state of affairs, it is shown in Reference 18 that in the range of customary commercial operation, the pool concept is essentially equivalent to such alternate mixing hypotheses as eddy-diffusion[4,5,6,7,8,9,10,11] splashing[12] and recycling[13,14,15,16].

2. The vapor enters the plate with a uniform composition and divides equally among the N pools.

3. The liquid flow rate $\bar{L}$ and the vapor flow rate $\bar{V}/N$ are unchanged by passage through a pool and are invariant with time. It is important to note that this assumption ignores the fact that unequal heats of vaporization and sensible heat effects can change the vapor flow rate at the expense of the liquid flow rate. Later, it will be shown that such energy effects can be significant and may have an important influence on the dynamics of plate behavior.

4. It is assumed that the vapor composition in equilibrium with the liquid can be represented by a linear relation over the composition range found on the plate:

$$y^* = mx + b \qquad (1)$$

It is *not* assumed here that the vapor-liquid equilibrium relation is truly linear. Rather, that over a limited composition range, the true curve can be approximated by its cord. m and b then are actually functions of composition which can be approximated by average values for small variations in x. Later, the validity of this approximation is explored.

5. The composition of the vapor leaving pool k, y_k, is related to y_k^* by an efficiency expression

$$\frac{y_i - y_k}{y_i - y_k^*} = E \qquad (2)$$

and E is assumed constant across the plate.

With the above idealizations, a mass balance written about pool k for the same component in gas and liquid gives

$$\bar{L}(X_{k-1} - x_k) + \frac{\bar{V}}{N}(y_i - y_k) = \frac{\bar{H}}{N}\frac{dx_k}{d\theta} \qquad (3)$$

In Equation (3), the subscript k refers to the k^{th} pool. x and y refer to chemically identical species in the liquid and vapor respectively. Equations of the form of 1, 2, and 3 apply to each component of the system and no restriction is placed on the number of components present.

By eliminating y_k^* and y_k from Equations (1), (2), and (3) there results

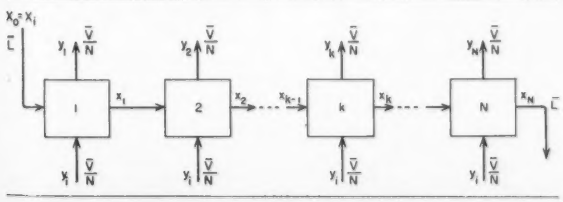

Figure 1—The representation of liquid mixing by a series of perfectly mixed pools.

$$x_{k-1}\bar{L} - x_k\left(\bar{L} + \frac{mE\bar{V}}{N}\right) + \frac{E\bar{V}}{N}(y_i - b) = \frac{\bar{H}}{N}\frac{dx_k}{d\theta} \qquad (4)$$

When the inlet vapor and/or liquid composition is varied sinusoidally, x_k and/or y_i is a function of time. Each of these is the sum of a mean value $\bar{x}_k$, $\bar{y}_i$ and a time-dependent value x_k', y_i'; i.e., $x_k = \bar{x}_k + x_k'$. The mean values correspond to a steady-state operation of the plate. With the above substitutions Equation (4) becomes

$$(\bar{x}_{k-1}+x'_{k-1})\bar{L} - (\bar{x}_k+x'_k)\left(\bar{L}+\frac{mE\bar{V}}{N}\right) + \frac{E\bar{V}}{N}(\bar{y}_i+y'_i-b) = \frac{\bar{H}}{N}\left(\frac{dx'_k}{d\theta}\right) \qquad (5)$$

If the steady-state expression,

$$\bar{x}_{k-1}\bar{L} - \bar{x}_k\left(\bar{L} + \frac{mE\bar{V}}{N}\right) + \frac{E\bar{V}}{N}(\bar{y}_i - b) = 0$$

is subtracted from Equation (5), the relationship amongst the time-dependent values is found to be

$$x'_{k-1}\bar{L} - x'_k\left(\bar{L} + \frac{mE\bar{V}}{N}\right) + \frac{E\bar{V}}{N}y'_i = \frac{\bar{H}}{N}\frac{dx'_k}{d\theta} \qquad (6)$$

Taking initial conditions of Equation (1) to be steady-state operation, then the initial conditions of Equation (6) are

$$x'_i = x'_1 = x'_2 = \ldots = x'_N = y'_1 = 0;\ \theta = 0 \qquad (7)$$

The Laplace transform of Equation (6) with the initial conditions (7) is

$$x_{k-1}(s)\bar{L} - x_k(s)\left(\bar{L} + \frac{mE\bar{V}}{N}\right) + \frac{E\bar{V}}{N}y_i(s) = \frac{\bar{H}}{N}sx_k(s) \qquad (8)$$

$$x_o(s) = x_i(s)$$

Equation (8) is a linear finite-difference equation with constant coefficients whose solution is readily found to be

$$x_k(s) = x_i(s)\left[\frac{\bar{L}}{\frac{\bar{H}s}{N} + \bar{L} + \frac{\bar{V}Em}{N}}\right]^k + \frac{E\bar{V}y_i(s)}{(\bar{H}s + \bar{V}Em)}\left[1 - \left(\frac{\bar{L}}{\frac{\bar{H}s}{N} + \bar{L} + \frac{\bar{V}Em}{N}}\right)^k\right] \qquad (9)$$

Equation (9) is the desired result. When k is replaced by N and s by $j\omega$, the result expresses the response of the outlet liquid composition x_N to sinusoidal composition variations in either the inlet liquid x_i or the inlet vapor y_i.

If $(AR)_{x/x}$ is used to denote the ratio of the amplitude of the outlet liquid composition variation to the amplitude of a sinusoidal variation of frequency ω imposed on the entering liquid composition when the inlet vapor composition and all flow rates are maintained constant, Equation (9) gives

$$(AR)_{x/x} = \frac{x(\omega)}{x_i(\omega)} = \left\{\left[1 + \left(\frac{mE\bar{V}}{\bar{L}N}\right)\right]^2 + \left(\frac{\bar{H}\omega}{\bar{L}N}\right)^2\right\}^{-N/2} \qquad (10)$$

Rearrangement of Equation (10) yields

$$(AR)^{-2/N}_{x/x} = \left(1 + \frac{mE\bar{V}}{\bar{L}N}\right)^2 + \left(\frac{H\omega}{\bar{L}N}\right)^2 \qquad (11)$$

This statement predicts that if several frequency response experiments are performed and the results plotted as $(AR)^{-2/N}_{x/x}$ vs. ω^2, a straight line is formed whose slope is $\left(\frac{\bar{H}}{\bar{L}N}\right)^2$ and

whose intercept is $\left(1 + \frac{mE\overline{V}}{\overline{L}N}\right)^2$. Since N is not known, curves must be plotted for several values of N and that one which yields the best straight line selected as the correct one. With $\left(1 + \frac{mE\overline{V}}{\overline{L}N}\right)^2$, $\left(\frac{\overline{H}}{\overline{L}N}\right)^2$, N, $\overline{L}$, and $\overline{V}$ known, $\overline{H}$ and mE can be determined. There remains only to separate E and m from the product mE.

Paranthetically, it should be mentioned here that Equation (11) implies a method of determining liquid holdup and liquid mixing on an imperfectly mixed bubble plate by sinusoidal variation of the concentration of a nonvolatile solute tracer. It is easily seen that although Equation (11) was derived for a volatile component, it can be applied equally well to a nonvolatile one by simply ignoring the term $\frac{mE\overline{V}}{\overline{L}N}$ in the expression for the intercept. The nonvolatile species may be thought of as a component whose vapor-liquid equilibrium curve is a horizontal line ($m = 0$) coincident with the x axis. The liquid holdup and mixing parameter N are determined as described above, by guessing N, plotting $(AR)_{x/x}^{-2/N}$ vs. ω^2, and finding the slope $\left(\frac{\overline{H}}{\overline{L}N}\right)^2$.

Return now to the case of volatile components and the problem of separating m and E from the product mE. Let $(AR)_{x/y}$ represent the ratio of the amplitude of the outlet liquid composition variation to the amplitude of a sinusoidal variation of frequency ω imposed on the entering vapor composition when the entering liquid composition and all flow rates are held constant. Then Equation (9) gives

$$(AR)_{x/y} = \left[\frac{x(\omega)}{y_i(\omega)}\right] = E\overline{V}\left[\frac{1-\phi}{mE\overline{V} + j\omega\overline{H}}\right] \quad \ldots\ldots\ldots (12)$$

where

$$\phi = \left[1 + \frac{mE\overline{V}}{\overline{L}N} + \frac{j\omega\overline{H}}{\overline{L}N}\right]^{-N} \quad \ldots\ldots\ldots\ldots\ldots\ldots (13)$$

Three alternative methods may be used to obtain the values of m or E from the procedure represented by Equation (12).

First, if $(AR)_{x/y}$ is determined at a sufficiently high frequency such that

$$|\phi| \ll 1$$

then Equation (12) implies

$$(AR)_{x/y} = \frac{E\overline{V}}{\sqrt{(mE\overline{V})^2 + (\overline{H}\omega)^2}} \quad \ldots\ldots\ldots\ldots (14)$$

With knowledge of mE and $\overline{L}\overline{t}$ from the results of a set of $(AR)_{x/x}$ experiments, a single determination of $(AR)_{x/y}$ in this high ω range is sufficient to determine E from Equation (14).

If it is possible to obtain more than one $(AR)_{x/y}$ value at different frequencies, then independent estimates of both m and E are available by plotting $(AR)_{x/y}^{-2}$ vs. ω^2. since the inverted square of Equation (14) is

$$\frac{1}{(AR)^2_{x/y}} = m^2 + \left(\frac{\overline{H}\omega}{E\overline{V}}\right)^2 \quad \ldots\ldots\ldots\ldots (15)$$

A straight line fitted to such a plot should have an intercept m^2 and a slope $\left(\frac{\overline{H}}{E\overline{V}}\right)^2$ from which both m and E could be calculated.

If $(AR)_{x/x}$ is determined at the same mean conditions and frequencies as $(AR)_{x/y}$, comparison of Equations (10) and (13) shows that $(AR)_{xx} = |\phi|$. Hence, the frequency range required to satisfy $|\phi| \ll 1$ can be ascertained from measurements of the output response to liquid input composition variation.

The disadvantage of the above method lies in the fact that at high frequencies, $(AR)_{x/y}$ as well as $(AR)_{x/x}$ becomes small and the difficulty of actual measurement increases when a small variation must be detected precisely. However, relatively simple experimental techniques are available for detecting the amplitude and phase of a sinusoid of known frequency in the presence of a quite high level of noise and distortion.

The second method of extracting information from Equation (12) involves experiments with very low frequencies or long sinusoidal periods. It is seen that when ϕ is substituted into Equation (12) and $(AR)_{x/y}$ evaluated at vanishingly small values of ω, there results

$$\lim_{\omega \to 0} (AR)_{x/y} = \frac{1}{m}\left[1 - \left(1 + \frac{mE\overline{V}}{\overline{L}N}\right)^{-N}\right] \quad \ldots\ldots\ldots (16)$$

This implies that a curve of $(AR)_{x/y}$ vs. ω extrapolated to $\omega = 0$ yields the value

$$\frac{1}{m}\left[1 - \left(1 + \frac{mE\overline{V}}{\overline{L}N}\right)^{-N}\right] \text{ as } \omega \to 0$$

If then $1 + \frac{mE\overline{V}}{\overline{L}N}$ is known as the square root of the intercept in Equation (11), a value of m can be determined.

A third approach is available if neither sufficiently high nor low frequency experiments are practicable. This involves a direct determination of the absolute value of $1 - \phi$ in Equation (12). It is seen that if $|1 - \phi|$ is known as a function of frequency, a plot of

$$\frac{|1-\phi|^2}{(AR)^2_{x/y}} \text{ vs. } \omega^2$$

yields a straight line,

$$\frac{|1-\phi|^2}{(AR)^2_{x/y}} = m^2 + \left(\frac{\overline{H}\omega}{E\overline{V}}\right)^2 \quad \ldots\ldots\ldots\ldots (17)$$

from which m^2 and $\left(\frac{\overline{H}}{E\overline{V}}\right)^2$ are easily found. In order to find $|1 - \phi|$, both the absolute value and the argument of the complex number ϕ must be known as functions of frequency. The absolute value is simply $(AR)_{x/x}$. The argument may be found by De Moivre's theorem. For

$$\phi = \left(1 + \frac{mE\overline{V}}{\overline{L}N} + \frac{j\omega\overline{H}}{\overline{L}N}\right)^{-N}$$

$$\phi = \frac{|\phi|}{(\cos\alpha + j\sin\alpha)^N} = \frac{|\phi|}{(\cos N\alpha + j\sin N\alpha)}$$

and

$$|1-\phi|^2 = \left[\frac{\cos N\alpha - |\phi| + j\sin N\alpha}{\cos N\alpha + j\sin N\alpha}\right]^2 =$$

$$[\cos N\alpha - (AR)_{x/x}]^2 + \sin^2 N\alpha$$

where

$$\alpha = \tan^{-1}\frac{\omega\overline{H}}{\overline{L}N\left(1 + \frac{mE\overline{V}}{\overline{L}N}\right)}$$

With this, Equation (17) becomes

$$\psi = \frac{[\cos N\alpha - (AR)_{x/x}]^2 + \sin^2 N\alpha}{(AR)^2_{x/y}} = m^2 + \left(\frac{\overline{H}\omega}{E\overline{V}}\right)^2 \quad \ldots\ldots (18)$$

The values of N and $\frac{\omega\overline{H}}{\overline{L}N\left(1 + \frac{mE\overline{V}}{\overline{L}N}\right)}$ needed for the evaluation

of the angle $N\alpha$ must be obtained from a determination of the slope and intercept of Equation (11).

The validity of Equation (18) depends upon the requirement that ϕ in Equation (17) has the same values as the ϕ which replaces it, the transfer function of liquid outlet composition with respect to liquid inlet composition. This means that the two amplitude ratios which are combined in the calculation of the left-hand member of Equation (18) must be the result of a pair of experiments in which the expression

$$\left(1 + \frac{mE\overline{V}}{\overline{L}N} + \frac{j\omega\overline{H}}{\overline{L}N}\right)^{-N}$$

is equal for both. This implies that the frequency and mean value of all input variables in both experiments should be the same.

Testing of the Linear Model

The previous discussion makes it clear that if the linear model is obeyed the frequency response method is indeed a powerful experimental tool.

A preliminary evaluation of the linear model was carried out by comparing the linear model predictions with the results of a digital computer simulation of an operating bubble plate.

Computer simulation is not a replacement for an experimental test using an operating plate. Rather, it is a very useful means of initial evaluation and exploration. Wide ranges of operating and physical parameters may be covered under conditions that facilitate interpretation of their effect. If the linearized model shows satisfactory correspondence with a realistic computer simulation of an actual plate, it is then necessary and desirable to test the method by means of physical measurements on an operating plate whose characteristics have been determined by conventional procedures.

Non-Linear Vapor-Liquid Equilibria

One of the most questionable assumptions required by the linear model is that of a linear vapor-liquid equilibrium relationship over the range of the plate composition. Consequently, a simulation was built which included an unusually severe local curvature in the vapor-liquid equilibrium line. The equilibrium line chosen was at $\bar{x}_i = 0.60$ on Figure 2. The quadratic expression

$$y_k^* = -3.2 + 14x_k - 12x_k^2 \quad \ldots\ldots\ldots\ldots\ldots\ldots (19)$$

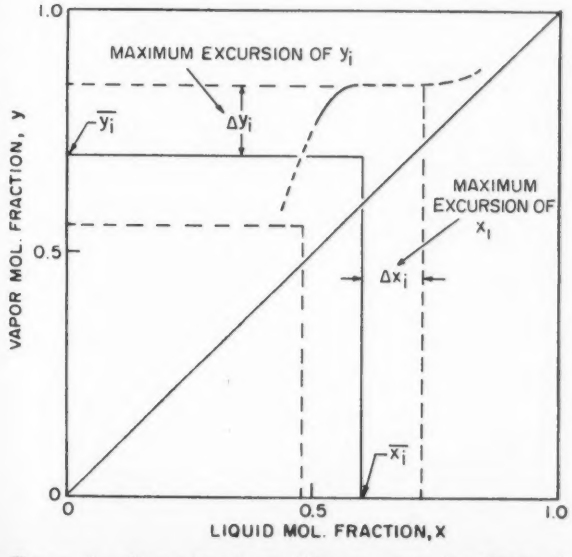

Figure 2 — Vapor-liquid equilibrium curve for Series *C* and *D*.

coincides with the equilibrium line on the solid segment at the sharp bend near $x = 0.55$. An equilibrium line of this form corresponds to incipient phase separation. The simulation was run on the IBM 704 computer at the M.I.T. Computation Center and was subjected to sinusoidal composition disturbances as required by the linear analysis methods. The digital response waves obtained from the simulation were analyzed for harmonic content by the discrete Fourier approximation method described by Hildebrand[19]. The details of the simulation program and complete numerical results are available in Reference 18.

Inlet conditions to the plate were chosen so that the liquid composition range across the plate also coincided with the bend of Figure 2. The calculations were carried out using $\bar{x}_i = 0.60$, $\bar{y}_i = 0.70$, $\overline{L} = \overline{V} = 1.5$ mols/sec., $E = 0.70$ and $N = 20$. The *steady-state* liquid composition for each pool was computed using the *actual* equilibrium curve (Equation (19); the results are given in Table 1.

Two sets of computer simulation of sinusoidal forcing of the input streams were carried out. Series C employed a constant excitation frequency of 0.632 radians/second and a total of six calculations were made. Three involved variation of the inlet liquid composition at 0.5%, 5.0% and 20.0% normalized amplitude about $\bar{x}_i = 0.60$ with $\bar{y}_i$ held constant at $\bar{y}_i = 0.70$. Three involved fluctuation of the inlet vapor composition at 0.5%, 5.0% and 20.0% normalized amplitude about $\bar{y}_i = 0.70$ with $\bar{x}_i$ held constant at $\bar{x}_i = 0.60$. The results are given in Table 2.

The simulation of Series *D* was made at varying frequency ω was varied from 0.2 to 3.0 radians per second. Six calculations were made employing fluctuation of x_i about $\bar{x}_i = 0.60$ with y_i held constant at 0.70 and six calculations were made employing fluctuation of y_i about $\bar{y}_i = 0.70$ with x_i held constant at 0.60. The results are given in Table 3.

Examination of Table 2 discloses two interesting results. The non-linear vapor-liquid equilibria generates a mean value of the reponse wave which differs from the steady-state value. The differences are reflected in the column marked "Zeroth harmonic amplitude". The entries in that column are the quantities $(\overline{X}_{20} - 0.495725)/0.495725$; $\overline{X}_{20}$ is the mean value of the liquid composition leaving the plate (the 20th pool) and 0.495725 is the corresponding liquid composition leaving the plate under steady-state operation as shown by Table 1. The harmonic analyses of the results shown in Table 2 show that despite the highly non-linear equilibrium curve the wave forms are slightly distorted fundamental sinusoids. In all cases the distortion is chiefly due to the second harmonic and the amplitudes of the third harmonics are small in comparison with those of the first and second. As a result, the amplitude of the fundamental wave, which is the value required by the linear analysis methods, can be obtained without resorting to Fourier analysis. To a good approximation it may be taken to be one-half the peak-to-peak distance on the distorted wave.

TABLE 1

STEADY-STATE LIQUID COMPOSITION ACROSS PLATE FOR $\bar{x}_i = 0.60$, $\bar{y}_i = 0.70$, $\overline{L} = \overline{V} = 1.5$ MOLS/SEC., $E = 0.70$, $N = 20$, EQUILIBRIUM ACCORDING TO EQUATION (19).

Pool	Liquid Mol Fraction	Pool	Liquid Mol Fraction
1	0.593628	11	0.533135
2	0.587217	12	0.528004
3	0.580804	13	0.523111
4	0.574420	14	0.518461
5	0.568101	15	0.514060
6	0.561878	16	0.509908
7	0.555780	17	0.506003
8	0.549834	18	0.502341
9	0.544065	19	0.498918
10	0.538493	20	0.495725

TABLE 2

SERIES C: AMPLITUDES OF THE HARMONIC COMPONENTS OF THE RESPONSE WAVES AT CONSTANT EXCITATION FREQUENCY $\omega = 0.632$ RADIANS/SEC.

Run No.	Excited Input	Normalized Input Amplitude	Amplitudes of Harmonic Components*				
			Zeroth	First	Second	Third	Fourth
*C*1	x_i	0.005	0.000014	0.001221	0.000002	——	——
*C*2	x_i	0.050	0.002425	0.012226	0.000290	0.000003	——
*C*3	x_i	0.200	0.028356	0.061507	0.004946	0.000266	0.000065
*C*4	y_i	0.005	0.000001	0.000595	——	——	——
*C*5	y_i	0.050	0.000092	0.005953	0.000004	0.000001	——
*C*6	y_i	0.200	0.001479	0.023770	0.000070	0.000001	——

*These amplitudes are those of the response wave $\frac{x_{20} - 0.495725}{0.495725}$, where 0.495725 is the steady-state mol fraction from the last (twentieth) pool.

In Figure 3 the $(AR)_{x/x}$ data of Series *D*, Table 3 are plotted in accordance with Equation (11) for various assumed values of the number of pools, *N*. The results of a least squares evaluation of the "fit" of the results to the straight lines predicted by Equation (11) are given in Table 4. It appears that the correct value of *N* can be determined by a least squares treatment of Equation (11) despite the non-linearity in the equilibrium curve. Near the correct *N* the variances are small and conceivably could be masked by experimental errors in an actual application but as will be shown this does not appear to be a serious practical limitation. An accurate value of the holdup $\bar{H}$ can be found from the slope of the correct *N* line of Equation (11) using $(AR)_{x/x}$ results. The wrong *N* lines shift the $\bar{H}$ determination moderately.

The $(AR)_{x/x}$ results of Table 3 were used to separate *E* and *m*. All of the methods discussed earlier were tested and were found to give similar results. Only the phase angle technique employing Equation (18) will be covered here. Values of ψ were computed as a function of ω^2 using Table 3 and several assumed values of *N*. Figure 4 shows the values of ψ plotted versus ω^2 in accordance with Equation (18). A graph of reasonable size cannot resolve the differences between the "best" (on a least squares basis) straight lines corresponding to the differing assumed values of *N* and hence only one line is shown. However, a least squares analysis did give somewhat different values of slope and intercept for different values of *N* and these results were used in obtaining the values reported in Table 5. The columns in Table 5 are: (1) the assumed *N*; (2) the value of m_e as obtained from the intercept of the data treated by Equation (18); (3) the liquid mol fraction calculated from $m_e = dy^*/dx = 14 - 24\bar{x}_e$ (obtained by differentiation of Equation (19); (4) the point efficiency *E* obtained from the slope $\left(\frac{\bar{H}}{E\bar{V}}\right)^2$ of the data treated by Equation (18) and using values of $\bar{H}$ from Table 4; (5) m_e^*E transcribed from the m_eE column of Table 4; (6) m_e^*, the slope derived from m_e^*E and *E* of column (4); (7) $\bar{x}_e^*$ obtained from $m_e^* = 14 - 24\bar{x}_e^*$.

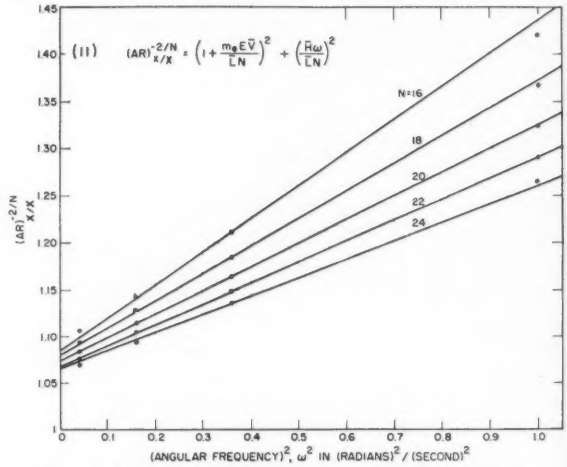

Figure 3—Series *D*: Least-squares straight lines of Equation (11).

TABLE 3

SERIES D: MEAN VALUES OF THE RESPONSE AND AMPLITUDE RATIOS

Run No.	Excited Input	Normalized Input Amplitude	Frequency rad./sec.	Mean Liquid outlet composition	Amplitude Ratio of response with respect to excited input
*D*1	x_i	0.10	3.0	0.495889	1.218×10^{-5}
*D*2	x_i	0.10	2.0	0.494928	0.0006764
*D*3	x_i	0.02	1.0	0.495788	0.059970
*D*4	x_i	0.02	0.6	0.495836	0.217713
*D*5	x_i	0.02	0.4	0.495892	0.338157
*D*6	x_i	0.02	0.2	0.495938	0.444879
*D*7	y_i	0.20	3.0	0.495752	0.023279
*D*8	y_i	0.20	2.0	0.495877	0.034840
*D*9	y_i	0.06	1.0	0.495749	0.072533
*D*10	y_i	0.06	0.6	0.495800	0.088377
*D*11	y_i	0.06	0.4	0.495911	0.187171
*D*12	y_i	0.06	0.2	0.496107	0.348895

TABLE 4

LEAST SQUARES EVALUATION OF FIT OF RESULTS OF TABLE 3 TO EQUATION 11

N Assumed	$\left(1+\frac{m_eE\bar{V}}{\bar{L}N}\right)^2$	$\left(\frac{\bar{H}}{\bar{L}N}\right)^2$	m_eE	$\bar{H}$ in mols	Sum of Squares of Deviations
16	1.084950	0.350466	0.83218	14.2080	278×10^{-6}
18	1.079777	0.292278	0.78246	14.5969	36×10^{-6}
20	1.074580	0.250079	0.73240	15.0024	3×10^{-6}
22	1.069732	0.218187	0.68558	15.4145	19×10^{-6}
24	1.065289	0.193339	0.64256	15.8293	46×10^{-6}

TABLE 5

SERIES D: RESULTS OF ANALYSIS USING EQUATION 18

N Assumed	m_e	$\bar{x}_e$	E	$(m_e{}^*E)$†	$m_e{}^*$	$\bar{x}_e{}^*$
16	3.183	0.451	0.66358	0.83218	1.2541	0.531
18	3.374	0.442	0.68193	0.78246	1.1474	0.536
20	3.241	0.448	0.70056	0.73240	1.0455	0.540
22	3.054	0.456	0.71950	0.68558	0.9528	0.544
24	2.804	0.467	0.73856	0.64256	0.8700	0.547

†m_eE transcribed from Table 4.

It is seen from Table 5 that satisfactory values of the point efficiency E are obtained even if the value of N chosen differs from the correct one. On the other hand, when the intercept of a ψ vs. ω^2 line is used to find m_e, the value is unreliable. Comparison of the $\bar{x}_e$ value of Table 5 with the steady-state values of the liquid composition shows that the $\bar{x}_e$ values fall below the range on the plate. On the other hand, the slopes $m_e{}^*$ calculated from the $m_e{}^*E$ values obtained using the $(AR)_{x/x}$ results and Equation (11) together with E values from $(AR)_{x/y}$ results correspond to liquid mol fractions near the center of the plate.

From these results it appears that even when the vapor-liquid equilibrium line shows marked curvature, frequency response measurements may be coupled with analytical predictions based upon a linear model in order to obtain plate parameters if the following procedures are used: N, $\bar{H}$ and the product mE are to be obtained from experimental measurements

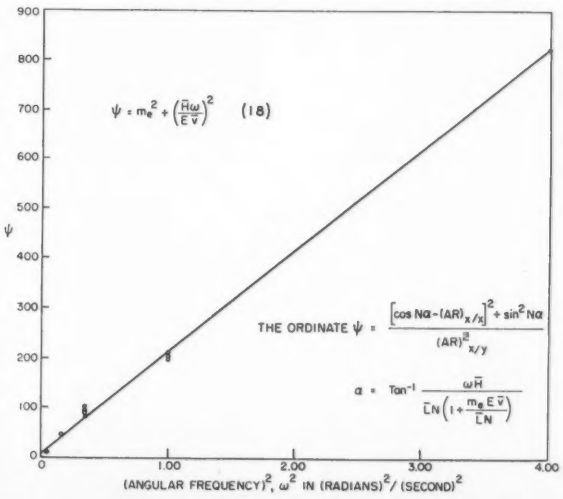

Figure 4—Series *D*: Least-squares straight lines of Equation (18) for $N = 16, 18, 20, 22,$ and 24.

eof $(AR)_{x/x}$ vs. ω in conjunction with Equation (11). The plat efficiency E is to be obtained by means of $(AR)_{x/y}$ vs. ω measurements used in conjunction with either Equations (15) or (18). The slope, m, of the equilibrium curve is computed from the mE value obtained from $(AR)_{x/x}$ data alone and the E value determined above and is to be applied to a central or average liquid composition on the plate.

The $(AR)_{x/y}$ data coupled with Equations (15) or (18) will also yield a value of m. If this differs significantly from that found above, the curvature of the vapor-liquid equilibrium line is pronounced.

The physical basis for the superiority of the linear approximation analysis using $(AR)_{x/x}$ data is due to the following. When a fluctuation is introduced into the inlet liquid, the induced fluctuations must "flow" across the entire plate before reaching the outlet where they are measured. Consequently, the outlet fluctuations should reflect average parameters across the plate and in particular, an average slope m corresponding to an average or central composition. On the other hand, when fluctuations are introduced into the incoming vapor in order to make $(AR)_{x/y}$ measurements, the uniform distribution of vapor across the entire plate causes the composition fluctuations to be introduced

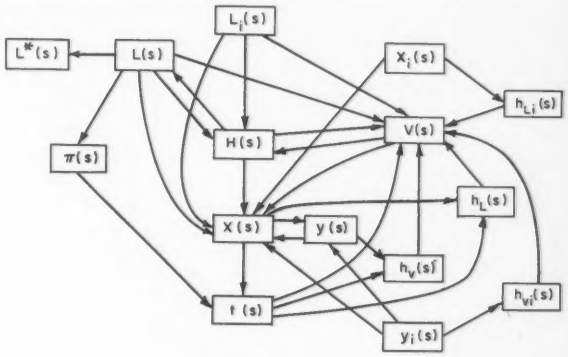

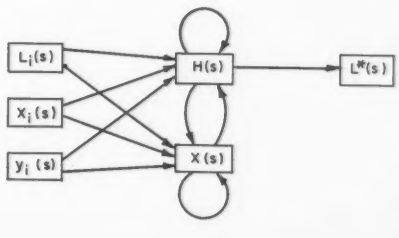

Figure 5—Flow graphs *A* and *B*.

uniformly across the plate also. As a result, the effect of the forcing fluctuation is a maximum at the down-stream end of the plate and the attenuation measured at the outlet is heavily weighted by the characteristics of the downstream liquid.

The linearized frequency response method gives satisfactory values of $\overline{H}$, N, and E even when the equilibrium curve exhibits marked curvature. The vapor-liquid equilibrium values obtained under such circumstances are less satisfactory. This is primarily due to incomplete mixing on the plate and the resulting plate concentration gradient. With a well-mixed plate, the vapor-liquid equilibrium results approach the precision of the $\overline{H}$, N and E results. However, even with imperfect mixing the frequency response results may be used to estimate the vapor-liquid equilibria as follows. Presumably an experimenter does not know beforehand that the curve is non-linear nor does he know the liquid composition distribution on the plate. However, the mean inlet and outlet liquid compositions, the mean inlet vapor composition, and the liquid and vapor flow rates are measured. From these parameters, a steady-state mass balance around the plate determines the average effluent vapor composition, $\bar{y}$, where average refers to both time and plate area. Now the point efficiency is defined by

$$E = \frac{y_i - y}{y_i - y^*} \quad \ldots\ldots(2)$$

However, on the experimental plate the distribution and composition of the incoming vapor stream y_i is to be uniform and the point efficiency is assumed uniform over the tray area. Hence, when Equation (2) is averaged over both time and tray area the result is

$$E = \frac{\bar{y}_i - \bar{y}}{\bar{y}_i - \bar{y}^*} \quad \ldots\ldots(20)$$

E is still the point efficiency and is determined from the dynamic analysis. Since E, $\bar{y}_i$, $\bar{y}$ are known, $\bar{y}^*$ may be calculated and provides a "point" on the vapor-liquid equilibrium curve.

The abscissa is not known precisely if there is a significant concentration gradient across the plate. If a single time mean composition sample is taken just downstream of the inlet section, a comparison of this composition with the outlet composition will indicate the magnitude of the composition gradient. If it is inconvenient to traverse the plate to find the steady-state liquid composition distribution, the average of the entrance sample composition and the outlet composition may serve as a reasonable approximation to the area average liquid composition. This composition is the abscissa which is sought for the point on the vapor-liquid equilibrium curve. In plotting a curve from a series of such $\bar{x}$, $\bar{y}^*$ determinations, the values of m also determined in the course of the frequency analysis experiment fix the local slope of the equilibrium curve and facilitate the construction of the curve.

Significant Latent and Sensible Heat Effects

In addition to a linear approximation to the equilibrium curve, the linearized analysis has assumed that the liquid flow rate $\overline{L}$ and the vapor flow rate $\overline{V}/N$ are unchanged by passage through a pool. These flow rates can, of course, change in practice as a result of energy effects. In order to ascertain the importance of such effects, an extreme case was examined. A commercial scale extractive distillation plate separating C_4 hydrocarbons with the aid of a furfural-water stream was simulated on the IBM 704 Digital Computer. The simulation included the actual vapor-liquid equilibrium curve and the latent and sensible heat effects associated with all streams. However, in order to understand the complicated interactions, the plate was taken to be perfectly mixed, i.e., $N = 1$.

With $N = 1$, the linearized relations Equations (10 and (12) become

$$(AR)_{x/x} = \left[\frac{\overline{L}^2}{(\overline{H}\omega)^2 + (\overline{L} + mE\overline{V})^2}\right]^{1/2} \quad \ldots\ldots(21)$$

$$(AR)_{x/y} = \frac{E\overline{V}}{[(\overline{H}\omega)^2 + (\overline{L} + mE\overline{V})^2]^{1/2}} \quad \ldots\ldots(22)$$

It is apparent that on a perfectly mixed plate for which the linearizing assumptions are valid it is not necessary to run frequency response experiments over a range of sinusoidal frequencies in order to determine plate efficiency and vapor-liquid equilibria. A single pair of experiments at the same frequency is sufficient provided liquid feed composition is fluctuated in one experiment and feed vapor composition is fluctuated in the other, but the time-mean values of all variables are the same in both. Under these conditions, the ratio of Equation (22) to Equation (21) gives

$$\frac{(AR)_{x/y}}{(AR)_{x/x}} = \frac{E\overline{V}}{\overline{L}} \quad \ldots\ldots(23)$$

When the predictions of Equations (21), (22) and (23) were compared with the performance of the simulated extractive distillation plate, the correspondence was poor for $(AR)_{x/x}$ and $(AR)_{x/y}$ considered separately, but their ratio, Equation (23) was in good agreement. In order to define the cause of the discrepancies, a theoretical analysis was made of the plate behavior, taking into account the energy effects. The details of the analysis are given in the appendix.

The principal finding is that Equations (21), (22) and (23) should be replaced by

$$(AR)_{x/x} = \frac{\overline{L}_i}{\overline{H}(j\omega) + \overline{L} + mE\overline{V} + \overline{Q}(j\omega)} \quad \ldots\ldots(24)$$

$$(AR)_{x/y} = \frac{\overline{V}_i - \overline{V} + E\overline{V}}{\overline{H}(j\omega) + \overline{L} + mE\overline{V} + \overline{Q}(j\omega)} \quad \ldots\ldots(25)$$

$$\frac{(AR)_{x/y}}{(AR)_{x/x}} = \frac{\overline{V}_i - \overline{V} + E\overline{V}}{L_i} \quad \ldots\ldots(26)$$

$$\overline{L}_i + \overline{V}_i = \overline{L} + \overline{V} \quad \ldots\ldots(27)$$

Equations (24), (25) and (26) are approximations in that certain of the energy terms have been discarded in order to obtain the simple form shown. However, the examination of the omitted terms made in the appendix indicates that in nearly all practical cases their omission is justified.

Two different types of heat effects appear in these equations. The first is the change in the steady-state liquid and vapor flow rates $(\overline{V}_i - \overline{V})$ and $(\overline{L}_i - \overline{L})$ upon passage through the plate. This is the familiar steady-state behavior usually resulting from differing heats of vaporization among the plate components. The second effect, denoted by the function $\overline{Q}(j\omega)$, is wholly a transient phenomenon. Physically, $\overline{Q}(j\omega)$ is associated with transient boiling and condensing action on a tray. When the concentration of one component in a constant pressure boiling mixture fluctuates, the temperature of the liquid on the tray must also fluctuate if the vapor pressure of that pure component differs from the vapor pressure of the mixture at the mean plate temperature. Since the mixture is boiling, the fluctuating temperature causes flashing and condensing in the system which, in turn, fluctuates the flow rates of liquid and vapor. The heat source or sink is the sensible heat in the mass of the liquid on the plate and the plate metal.

These simulation results have implications in the field of distillation column control. It is common practice to assume that liquid and vapor flow rates in the column vary only when reflux and reboil conditions are varied. The present results indicate composition fluctuations can also induce considerable variation in flow rates and this possibility should not be ignored. Frequency response tests on a small laboratory size plate which

is well mixed can be used in conjunction with Equations (24) and (25) to determine the value of $\overline{Q}(j\omega)$ and hence the importance of this effect.

The response of the simulated extractive distillation tray was used with Equation (26) to predict the plate efficiency, E, and this value in turn was used to obtain the equilibrium curve by means of Equation (20). The prediction proved to be excellent.

The energy effects test used here is an unusually severe one. 90% of the liquid on the plate was high boiling extractive agent and slight fluctuations in plate temperature caused relatively large quantities of C_4 hydrocarbons to flash or condense in order to supply heat to or remove heat from the large mass of low volatility extractive agent. In an ordinary distillation system where all of the components exhibit comparable volatilities, the effects would be much smaller and in many systems insignificant.

Energy Effects on an Imperfectly Mixed Plate

Unfortunately, the problem of treating the energy effects on a plate which is imperfectly mixed has not yet been resolved in a satisfactory manner. Until such a solution is obtained, the frequency response technique is limited to perfectly mixed plates, i.e., to small laboratory sized plates, or to systems in which the heat effects are small, i.e., gas absorption plates and distillation systems in which the volatilities and latent heats of all components are of comparable magnitude. Despite these limitations, the method in its present form would appear to be an adjunct to the standard procedures. Further analytical and experimental work is indicated. In time it is hoped that a frequency reponse procedure of general validity can be developed and tested.

Acknowledgement

The writers wish to thank the National Science Foundation for a Fellowship awarded to L. M. Schwartz, the International Business Machines Corporation for additional financial support, the M.I.T. Computation Center for the use of the IBM 704 computer, and the Texas Butadiene and Chemical Corporation for providing information concerning their extractive distillation towers.

Nomenclature

$(AR)_{x/x}$ = amplitude ratio of the effluent liquid concentration sinusoid to the feed liquid concentration sinusoid, concentrations expressed as mol fractions
$(AR)_{x/y}$ = amplitude ratio of the effluent liquid concentration sinusoid to the feed vapor concentration sinusoid, concentrations expressed as mol fractions
b = a constant
C = molal heat capacity
C_M = heat capacity of plate which thermally interacts with fluids on the plate
C_L = $C_{L1}\bar{x} + C_{L2}(1 - \bar{x})$
C_V = $C_{V1}\bar{y} + C_{V2}(1 - \bar{y})$
ΔC_L = $C_{L1} - C_{L2}$
ΔC_V = $C_{V1} - C_{V2}$
E = point efficiency
H = mols of liquid holdup
h = molal enthalpy
Δh_m = $\bar{h}_{m1} - \bar{h}_{m2}$
j = $\sqrt{-1}$
L = molal flow rate of liquid
l = liquid level
m = slope of a linear approximation to the vapor-liquid equilibrium line
N = the mixing parameter of Kirschbaum pool concept: the total number of equally sized, perfectly mixed stages which represents the liquid mixing on the plate
P = vapor pressure of a component
R = universal gas constant
s = Laplace transform variable
T = absolute temperature of liquid
t = temperature
Δt = $\bar{t} - t^\circ$
V = molal flow rate of vapor
x = liquid mol fraction
y = vapor mol fraction
y^* = vapor mol fraction in equilibrium with liquid
Z = length of liquid flow path in contact with vapor

Greek Letters

α = phase angle
α_j = a constant. Each value of j (1,2,...) denotes a different constant.
γ = activity coefficient
θ = time
λ = molal heat of vaporization
$\Delta\lambda^\circ_V$ = $\lambda^\circ_{V1} - \lambda^\circ_{V2}$
π = total pressure
ω = sinusoidal angular frequency

Subscripts

1 = molecular species 1
2 = molecular species 2
i = property of a feed or incoming stream
k = index of liquid mixing stages, counting from the inlet
L = liquid
M = plate metal
m = partial molal quantity
V = vapor

Superscripts

$-$ = time mean value
$=$ = time and area mean value
$'$ = the time-dependent component of a variable
$^\circ$ = reference condition
n = a constant

References

(1) Kirschbaum, E., Distillation and Rectification, Chemical Publishing Co., New York (1948).
(2) Kirschbaum, E., Forsch. Gebiete Ing., **B5,** 245 (1935).
(3) Gautreaux, M. F., and O'Connell, H. E., Chem. Eng. Prog., **51,** 232 (1955).
(4) Anderson, J. E., Sc.D. Thesis, M.I.T., Cambridge (1955).
(5) Brown, J. W., Jr., S.B. Thesis, M.I.T., Cambridge (1954).
(6) Byfield, A., M.S. Thesis, M.I.T., Cambridge (1939).
(7) Mix, T. W., Sc.D. Thesis, M.I.T., Cambridge (1959).
(8) Pollard, R. R., S.B. Thesis, M.I.T., Cambridge (1956).
(9) Stone, H. L., Sc.D. Thesis, M.I.T., Cambridge (1953).
(10) Wharton, L., S. B. Thesis, M.I.T., Cambridge (1955).
(11) Gilbert, T. J., Chem. Eng. Sci., **10,** 243 (1959).
(12) Johnson, A. I., and Marangozis, J., Can. J. Chem. Eng., **36,** 161 (1958).
(13) Oliver, E. D., and Watson, C. C., A.I.Ch.E.J., **2,** 18 (1956).
(14) Warzel, L. A., Ph.D. Thesis, University of Michigan, Ann Arbor (1955).
(15) Foss, A. S., Ph.D. Thesis, University of Delaware, Newark (1956).
(16) Foss, A. S., Gerster, J. A., and Pigford, R. L., A.I.Ch.E.J., **4,** 231 (1958).
(17) Danchwerts, P. V., Chem. Eng. Sci., **2,** 1 (1953).
(18) Schwartz, L. M., Sc.D. Thesis, M.I.T., Cambridge (1959)*.
(19) Hildebrand., F. B., Introduction to Numberical Analysis, McGraw-Hill Book Co., New York (1956).
(20) Mason, S. J., On the Logic of Feedback, Sc.D. Thesis, Dept. of Electrical Engineering, M.I.T., Cambridge (1952).
(21) Mason, S. J., Proceedings, Inst. Radio Engrs., 41, 1144 (1953).

*(The Sc.D. Thesis of L. M. Schwartz has been reproduced as Report 7793-R-4 of the Electronic Systems Laboratory, M.I.T. for limited distribution to sponsoring agencies).

APPENDIX

Generalized Linear Analysis of a Binary, Perfectly Mixed Plate

The objective of the analysis is to specify the dynamic cause-and-effect relationships amongst the variables on the plate. A simultaneous set of algebraic, transcendental, and ordinary differential equations is written which approximates the plate's behavior and implies the cause-and-effect relationships. When the set is written in sufficient detail to include most of the predictable interactions, its complexity is such that exact analytical solutions are generally impossible. Approximate analytical solutions may be obtained, however, if the equations are linearized in time about a steady-state operating condition. Since the linearization is valid only if the system makes small excursions from the steady-state, the approximate solutions are also valid under the same restriction.

The cause-and-effect relationships amongst the system's variables are sought in terms of the transfer functions or complex gains. The method involves the writing of the approximate linearized set of equations from the original set, the Laplace transformation of the linear equations, and finally the rearrangement of the transformed equations in the form of transfer functions between the desired pairs of input-output variables. It is found, however, that when a system involves a fair number of interacting variables, the practical problem of rearranging or manipulating the transformed equations into suitable transfer functions is not easily accomplished if not attacked systematically. In order to facilitate these manipulations, a procedure devised by Professor S. J. Mason[20,21] is employed. The technique, called "signal flow graphs", reduces to a set of rules for the manipulation of transformed, linear equations so that desired transfer functions may be extracted. In the following analysis, the differential equations are written, linearized, and transformed. Then the flow graph technique is explained and finally applied for the solution of the three desired transfer functions.

Rather than proceed by writing the entire set of equations, linearizing the entire set, and then transforming the entire set, these three operations are performed on each individual equation in turn. In the original equations, each variable as a function of time is unmarked with either a bar or a prime. When the equations are linearized, each variable is replaced by the sum of its mean value denoted by a bar and its time-dependent component denoted by a prime. When a nonlinearity occurs which involves the product of dependent vaiables and those variables are replaced by the sum of their mean and time-dependent components, the expansion of the product includes products of time-dependent components. The linearization is effected by neglecting such terms since for small excursions, these are small in comparison to the other terms in the equation. Each equation is then translated to a zero mean by subtracting from it the steady-state form of the original equation. The result is subjected to the Laplace transformation which yields an equation relating the transformed, time-dependent components of the original variables. These transformed variables are functions of the independent complex variable s and are denoted simply by the functional symbol $v(s)$. For the transformation of differential equations, the steady-state operation of the plate about which the linearization is effected represents a convenient set of initial conditions. Physically, this means that at time $\theta = 0$, the sinusoidal disturbance is initially introduced to the plate which has been running quiescently. Mathematically, it specifies a zero initial value for the time-dependent components of each variable.

Overall mass balance: If the vapor holdup is insignificant relative to the liquid holdup, then

$$\frac{dH}{d\theta} = L_i + V_i - L - V$$

Subtraction of the steady-state form leaves

$$\frac{dH'}{d\theta} = L_i' + V_i' - L' - V'$$

which is in terms of time varying components. With the initial value $H'(0^+) = 0$, Laplace transformation yields

$$s\,H(s) = L_i(s) + V_i(s) - L(s) - V(s) \qquad \text{(A - 1)}$$

Component balance: Writing a mass balance for either of the two species present, and assuming perfect mixing of the liquid, results in

$$\frac{d}{d\theta}(xH) = x_iL_i + y_iV_i - xL - yV$$

Substituting for each variable the sum of its mean and deviating components

$$(\bar{H} + H')\frac{dx'}{d\theta} + (\bar{x} + x')\frac{dH'}{d\theta} = (\bar{x}_i + x_i')(\bar{L}_i + L_i') +$$

$$(\bar{y}_i + y_i')(\bar{V}_i + V_i') - (\bar{x} + x')(\bar{L} + L') - (\bar{y} + y')(\bar{V} + V')$$

Neglecting products of primed quantities, the time-dependent variables, and subtracting $\bar{x}_i\bar{L}_i + \bar{y}_i\bar{V}_i - \bar{x}\bar{L} - \bar{y}\bar{V} = 0$, there results

$$\bar{H}\frac{dx'}{d\theta} = x_i'\bar{L}_i + \bar{x}_iL_i' + \bar{y}_iV_i' + y_i'\bar{V}_i - \bar{x}L' - x'\bar{L} - \bar{y}V' - y'\bar{V} - \bar{x}\frac{dH'}{d\theta}$$

Transformation with respect to quiescent initial conditions yields

$$(\bar{H}s + \bar{L})\,x(s) = \bar{L}_ix_i(s) + \bar{x}_iL_i(s) + \bar{V}_iy_i(s) + \bar{y}_iV_i(s) -$$
$$\bar{x}L(s) - \bar{y}V(s) - \bar{V}y(s) - \bar{x}s\,H(s) \qquad \text{(A - 2)}$$

Enthalpy balance: In addition to perfect mixing, the enthalpy balance assumes: (1) adiabatic operation, (2) the plate metal temperature equal to that of the liquid on the plate, and (3) negligible variation of vapor holdup enthalpy in comparison to the total enthalpy flux.

$$\frac{d}{d\theta}(h_LH) = h_{Li}L_i + h_{Vi}V_i - h_LL - h_VV - C_M\frac{dt}{d\theta}$$

Considering C_M a constant and substituting variable components yields

$$(\bar{H} + H')\frac{dh_L'}{d\theta} + (\bar{h}_L + h')\frac{dH'}{d\theta} =$$
$$(\bar{h}_{Li} + h_{Li}')(\bar{L}_i + L_i') + (\bar{h}_{Vi} + h_{Vi}')(\bar{V}_i + V_i') -$$
$$(\bar{h}_L + h_L')(\bar{L} + L') - (\bar{h}_V + h_V')(\bar{V} + V') - C_M\frac{dt'}{d\theta}$$

The linearization is

$$\bar{h}_L\frac{dH'}{d\theta} + \bar{H}\frac{dh_L'}{d\theta} = \bar{h}_{Li}L_i' + h_{Li}'\bar{L}_i + \bar{h}_{Vi}V_i' + h_{Vi}'\bar{V}_i -$$
$$\bar{h}_LL' - h_L'\bar{L} - \bar{h}_VV' - h_V'\bar{V} - C_M\frac{dt'}{d\theta}$$

The transformed relation can be written

$$\bar{h}_L(s)\,H(s) + (\bar{H}s + \bar{L})\,h_L(s) = \bar{L}_i\,h_{Li}(s) + \bar{h}_{Li}L_i(s) + \bar{V}_ih_{Vi}(s) +$$
$$\bar{h}_{Vi}\,V_i(s) - \bar{h}_LL(s) - \bar{h}_VV(s) - \bar{V}h_V(s) - C_Mst(s) \qquad \text{(A - 3)}$$

Molal enthalpy expressions: For each of the two components, zero enthalpy is assigned to the pure liquids at a base temperature t°.

$$h_L = [C_{L1}\,x + C_{L2}(1 - x)]\,(t - t^\circ) + h_{m1}\,x + h_{m2}\,(1 - x)$$

$$h_V = [C_{V1}\,y + C_{V2}(1 - y)]\,(t - t^\circ) + \lambda^\circ_{V1}\,y + \lambda^\circ_{V2}\,(1 - y)$$

Another pair of analogous equations representing h_{Li} and h_{Vi} can be written in which all the variables are subscripted with i. If the heat capacities are assumed independent of temperature, the linearized time-dependent components of the molal enthalpy expressions are given by

$$h_L' = [C_{L1}\,\bar{x} + C_{L2}(1 - \bar{x})]\,t' + (C_{L1} - C_{L2})\,x'(\bar{t} - t^\circ) +$$
$$\bar{x}h_{m1}' + (1 - \bar{x})\,h_{m2}' + (h_{m1} - \bar{h}_{m2})\,x'$$

$$h_V' = [C_{V1}\bar{y} + C_{V2}(1 - \bar{y})]t' + (C_{V1} - C_{V2})y'(\bar{t} - t^\circ) + (\lambda^\circ_{V1} - \lambda^\circ_{V2})y'$$

and two similar expressions for h_{Li}' and h_{Vi}'.

Transformation and definition of new terms (see Nomenclature) yields

$$h_L(s) = C_Lt(s) + (\Delta C_L\Delta t + \Delta h_m)\,x(s) + \bar{x}h_{m1}(s) +$$
$$(1 - \bar{x})h_{m2}(s) \qquad \text{(A - 4)}$$

$$h_V(s) = C_Vt(s) + (\Delta C_V\Delta t + \Delta\lambda_V^\circ)\,y(s) \qquad \text{(A - 5)}$$

$h_{Li}\,(s)$ and $h_{Vi}\,(s)$ are written in the same form as Equations (A-4) and (A-5) but with i subscripts on all relevant symbols.

Vapor-liquid equilibrium: A linear vapor-liquid equilibrium is written:

$$y^* = mx + b$$

Subtracting the mean values and transforming the result yields

$$y^*(s) = mx(s) \qquad \text{(A - 6)}$$

Plate efficiency: The expression relating y to y^* and y_i involves a constant plate efficiency value E

$$(y - y_i) = E(y^* - y_i)$$

Transforming the time-dependent component relation

$$y(s) - y_i(s) = E[y^*(s) - y_i(s)] \qquad \text{(A-7)}$$

Partial molal heats of mixing and activity coefficients: If the solutions are assumed "regular", then there is no excess

partial molal entropy for each component and the heats of mixing are given by

$$h_{m1} = RT \ln \gamma_1 \text{ and } h_{m2} = RT \ln \gamma_2$$

The simplest correlation of activity coefficient with composition and temperature is a Margules-type equation

$$T \ln \gamma_1 = \alpha_1 (1 - x)^2 \text{ and } T \ln \gamma_2 = \alpha_2 x^2$$

where α_1 and α_2 are constants. Eliminating $T \ln \gamma_j$ from the heat of mixing equations, and then linearizing

$$h'_{m1} = -2\alpha_1 R\bar{x}x'; \quad h_{m2} = 2\alpha_2 R\bar{x}x'$$

The transformed heats of mixing are

$$h_{m1}(s) = -2\alpha_1 R\bar{x}x(s) \quad \text{(A-8a)}$$

$$h_{m2}(s) = 2\alpha_2 R\bar{x}x(s) \quad \text{(A-8b)}$$

The transformed activity coefficients must also be expressed explicitly. Substituting mean and time-dependent components into the activity coefficient expressions, there results

$$(\overline{T} + T') \ln (\bar{\gamma}_1 + \gamma'_1) = \alpha_1(1 - \bar{x} - x')^2$$

$$(\overline{T} + T') \ln (\bar{\gamma}_2 + \gamma'_2) = \alpha_2(\bar{x} + x')^2$$

Since pseudo-linear behavior requires each γ' to be much smaller than its $\bar{\gamma}$, the logarithms $\ln (\bar{\gamma} + \gamma')$ are approximately $\ln \bar{\gamma} + \gamma'/\bar{\gamma}$. Making these substitutions and proceeding with the linearization

$$\frac{\overline{T}}{\bar{\gamma}_1}\gamma'_1 + t' \ln \bar{\gamma}_1 = -2\alpha_1 \bar{x}x'$$

$$\frac{\overline{T}}{\bar{\gamma}_2}\gamma'_2 + t' \ln \bar{\gamma}_2 = 2\alpha_2 \bar{x}x'$$

Transforming

$$\frac{\overline{T}}{\bar{\gamma}_1}\gamma_1(s) + \ln \bar{\gamma}_1 t(s) = -2\alpha_1 \bar{x}x(s) \quad \text{(A-9a)}$$

$$\frac{\overline{T}}{\bar{\gamma}_2}\gamma_2(s) + \ln \bar{\gamma}_2 t(s) = 2\alpha_2 \bar{x}x(s) \quad \text{(A-9b)}$$

Pressure-temperature-composition relationship: The total pressure is the sum of the two partial pressures.

$$\pi = \gamma_1 P_1 x + \gamma_2 P_2 (1 - x)$$

$$\pi' = (\bar{\gamma}_1\overline{P}_1 - \bar{\gamma}_2\overline{P}_2)x' + \bar{\gamma}_1\bar{x}P'_1 + \bar{\gamma}_2(1 - \bar{x})P'_2 + \overline{P}_1\bar{x}\gamma' + (1 - \bar{x})\overline{P}_2\gamma'_2$$

The transformed relation is

$$\pi(s) = (\bar{\gamma}_1\overline{P}_1 - \bar{\gamma}_2\overline{P}_2)x(s) + \bar{\gamma}_1\bar{x}P_1(s) + \bar{\gamma}_2(1 - \bar{x})P_2(s) + \overline{P}_1\bar{x}\gamma_1(s) + (1 - \bar{x})\overline{P}_2\gamma_2(s) \quad \text{(A-10)}$$

Vapor pressure: The vapor pressure of each species is assumed to satisfy the Clausius-Clapeyron approximation.

$$\ln P_1 = \alpha_3 - \frac{\lambda_{V1}}{RT}; \quad \ln P_2 = \alpha_4 - \frac{\lambda_{V2}}{RT}$$

Proceeding with the linearization

$$\ln (\overline{P}_j + P_i') = \alpha_{3,4} - \frac{\lambda_{Vj}}{R(\overline{T} + T')}$$

$$\ln \overline{P}_j + \frac{P_j'}{\overline{P}_j} = \alpha_{3,4} - \frac{\lambda_{Vj}}{R}\left(\frac{1}{\overline{T}} - \frac{T'}{\overline{T}^2}\right)$$

$$P_i' = \frac{\overline{P}_j\lambda_{Vj}T'}{\overline{T}^2R}$$

Transforming

$$P_1(s) = \frac{\overline{P}_1\lambda_{V1}}{R\overline{T}^2}T(s) \quad \text{(A-11a)}$$

$$P_2(s) = \frac{\overline{P}_2\lambda_{V2}}{R\overline{T}^2}T(s) \quad \text{(A-11b)}$$

Pressure drop: The pressure drop suffered by the vapor as it passes through the plate is assumed to depend both upon the liquid level on the plate and upon the vapor flow rate.

$$\pi_i - \pi = \alpha_5 + \alpha_6 l + \alpha_7 V_i^2$$

The linearization is

$$\pi_i' - \pi' = \alpha_6 l' + 2\alpha_7 \overline{V}_i V_i'$$

The transform of the linearization is

$$\pi_i(s) - \pi(s) = \alpha_6 l(s) + 2\alpha_7 \overline{V}_i V_i(s) \quad \text{(A-12)}$$

Liquid level: The liquid level is assumed to depend upon the liquid flow rate to some positive power

$$l = \alpha_8 L^n$$

This equation can be approximated linearly by

$$l' = \alpha_8 n(\overline{L})^{n-1} L'$$

which transforms into

$$l(s) = \alpha_8 n(\overline{L})^{n-1} L(s) \quad \text{(A-13)}$$

Liquid holdup: Liquid holdup as related linearly to liquid level

$$H = \alpha_9 + \alpha_{10} l$$

$$H' = \alpha_{10} l'$$

$$H(s) = \alpha_{10} l(s) \quad \text{(A-14)}$$

One additional interaction can be predicted but has not been included. That is the relationship between the pressure under the plate π_i and the incoming vapor flow rate V_i. Clearly, variations in liquid level must introduce variations in pressure drop across the plate and pressure drop fluctuations must be reflected in either the vapor throughput rate or in the under-plate pressure or in both. However, the form of this effect depends almost entirely upon the characteristics of the vapor supply equipment. In all likelihood the interaction will not be sufficiently strong to influence the dynamic behavior of the plate to any great extent but it should be kept in mind when plans are drawn up for an experimental vapor supply system.

The transformed equations governing the linearized behavior of the distillation plate comprise Equations (A-1) through (A-14). At this point, it is convenient to eliminate several of the output variables and thereby reduce the number of equations. $y^*(s)$ may be eliminated from Equations (A-6) and (A-7) so that

$$y(s) - y_i(s) = E[mx(s) - y_i(s)] \quad \text{(A-15)}$$

The heats of mixing are eliminated by substitution of Equations (A-8) into (A-4)

$$h_L(s) = C_L t(s) + (\Delta C_L \Delta t + \Delta h_m)x(s) - 2\alpha_1 R\bar{x}^2 x(s) + 2(1 - \bar{x})\alpha_2 R\bar{x}x(s) \quad \text{(A-16)}$$

Vapor pressures, Equation (A-11) and activity coefficients, Equation (A-9) may be substituted in Equation (A-10)

$$\pi(s) = (\bar{\gamma}_1\overline{P}_1 - \bar{\gamma}_2\overline{P}_2)x(s) + \frac{\bar{\gamma}_1\bar{x}\overline{P}_1\lambda_{V1}}{R\overline{T}^2}T(s) + \frac{\bar{\gamma}_2(1 - \bar{x})\overline{P}_2\lambda_{V2}}{R\overline{T}^2}T(s) + \frac{\overline{P}_1\bar{x}\bar{\gamma}_1}{\overline{T}}[(-\ln \bar{\gamma}_1)t(s) - 2\alpha_1\bar{x}x(s)] + \frac{\overline{P}_2(1 - \bar{x})\bar{\gamma}_2}{\overline{T}}[(-\ln \bar{\gamma}_2)t(s) + 2\alpha_2 \bar{x}x(s)]$$

But since $t(s) = T(s)$

$$\pi(s) = \left[\bar{\gamma}_1\overline{P}_1\left(1 - \frac{2\alpha_1\bar{x}^2}{\overline{T}}\right) - \bar{\gamma}_2\overline{P}_2\left\{1 + \frac{2\alpha_2\bar{x}^2 - 2\alpha_2\bar{x}}{\overline{T}}\right\}\right]x(s) + \left[\frac{\bar{\gamma}_1\bar{x}\overline{P}_1}{\overline{T}}\left(\frac{\lambda_{V1}}{R\overline{T}} - \ln\bar{\gamma}_1\right) + \frac{\bar{\gamma}_2(1-\bar{x})\overline{P}_2}{\overline{T}}\left(\frac{\lambda_{V2}}{R\overline{T}} - \ln\bar{\gamma}_2\right)\right]t(s) \quad \text{(A-17)}$$

The liquid level $L(s)$ is substituted in both Equations (A-12) and (A-14)

$$\pi_i(s) - \pi(s) = \alpha_6\alpha_8 n(\overline{L})^{n-1} L(s) + 2\alpha_7 \overline{V}_i V(s) \quad \text{(A-18)}$$

$$H(s) = \alpha_8\alpha_{10} n(\overline{L})^{n-1} L(s) \quad \text{(A-19)}$$

The remaining transformed variables are now categorized as either input or output. The input variables are, in a sense, independent since they do not depend upon the dynamic behavior of the plate. The output or response variables, on the other hand, must be completely specified by the set of equations.

The input variables are L_i, V_i, x_i, y_i, t_i, h_{Li}, h_{Vi}, and π_i. The output variables are L, V, H, x, y, h_L, h_V, t, and π. These are specified by Equations (A-19), (A-3), (A-1), (A-2), (A-15), (A-16), (A-5), (A-17) and (A-18) respectively.

In this analysis, L_i, x_i, y_i, h_{Li} and h_{Vi} are the only input variables by which disturbances are introduced to the system. The others are held constant and hence their time-deviating components and their transforms are zero. Consequently, $V_i(s)$, $t_i(s)$ and $\pi_i(s)$ are to be ignored.

In the flow graph method for manipulating the equations, the interrelationships amongst the variables are represented by a network of directed branches which connect at nodes. The nodes represent the variables; each branch represents the cause-and-effect relationship or gain with respect to the nodes it connects. One starts the flow graph by establishing a node for each variable in the set of equations, both input and output variety. The system is defined by nine equations, one for each output variable. As an example, Equation (A-1) specifies the variable $H(s)$. It says that each of the variables $L_i(s)$, $L(s)$ and $V(s)$ affects $H(s)$. ($V_i(s)$ is ignored.) Consequently, three directed branches are drawn on the flow graph from $L_i(s)$, $L(s)$ and $V(s)$ to $H(s)$. The gains associated with these branches are given by the equation. For example, the gain of the $L(s)$ to $H(s)$ branch is $(-1/s)$ since this when multiplied by $L(s)$ expresses the $L(s)$ to $H(s)$ relationship in the equation. In the same manner, all the relationships are entered as branches on the flow graph. This is shown for the entire set of equations in Flow Graph A in Figure 5. The branch gains are listed by the format:

$L(s) \xrightarrow{A} H(s) = -1/s$ which specifies a gain of $-1/s$ for the branch from node $L(s)$ to node $H(s)$ on Flow Graph A.

From Equation (A-1) which specifies $H(s)$:

$$L_i(s) \xrightarrow{A} H(s) = 1/s$$

$$L(s) \xrightarrow{A} H(s) = -1/s$$

$$V(s) \xrightarrow{A} H(s) = -1/s$$

From Equation (A-2) which specifies $x(s)$:

$$x_i(s) \xrightarrow{A} x(s) = \bar{L}_i/(\bar{H}s + \bar{L})$$

$$L_i(s) \xrightarrow{A} x(s) = \bar{x}_i/(\bar{H}s + \bar{L})$$

$$y_i(s) \xrightarrow{A} x(s) = \bar{V}_i/(\bar{H}s + \bar{L})$$

$$y(s) \xrightarrow{A} x(s) = -\bar{V}/(\bar{H}s + \bar{L})$$

$$L(s) \xrightarrow{A} x(s) = -x/(\bar{H}s + \bar{L})$$

$$V(s) \xrightarrow{A} x(s) = -\bar{y}/(\bar{H}s + \bar{L})$$

$$H(s) \xrightarrow{A} x(s) = -\bar{x}s/(\bar{H}s + \bar{L})$$

From Equation (A-3) which specifies $V(s)$:

$$H(s) \xrightarrow{A} V(s) = -\bar{h}_L/\bar{h}_V$$

$$h_L(s) \xrightarrow{A} V(s) = -(\bar{H}s + \bar{L})/\bar{h}_V$$

$$L_i(s) \xrightarrow{A} V(s) = \bar{h}_{Li}/\bar{h}_V$$

$$L(s) \xrightarrow{A} V(s) = -\bar{h}_L/\bar{h}_V$$

$$h_V(s) \xrightarrow{A} V(s) = -\bar{V}/\bar{h}_V$$

$$t(s) \xrightarrow{A} V(s) = -sC_M/\bar{h}_V$$

$$h_{Li}(s) \xrightarrow{A} V(s) = \bar{L}_i/\bar{h}_V$$

$$h_{Vi}(s) \xrightarrow{A} V(s) = \bar{V}_i/\bar{h}_V$$

From Equation (A-5) which specifies $h_V(s)$ and $h_{Vi}(s)$:

$$t(s) \xrightarrow{A} h_V(s) = C_V$$

$$y(s) \xrightarrow{A} h_V(s) = \Delta C_V \Delta t + \Delta\lambda_V^\circ$$

$$y_i(s) \xrightarrow{A} h_{Vi}(s) = \Delta C_{Vi} \Delta t_i + \Delta\lambda_V^\circ$$

From Equation (A-15) which specifies $y(s)$:

$$y_i(s) \xrightarrow{A} y(s) = 1 - E$$

$$x(s) \xrightarrow{A} y(s) = Em$$

From Equation (A-16) which specifies $h_L(s)$ and $h_{Li}(s)$:

$$t(s) \xrightarrow{A} h_L(s) = C_L$$

$$x(s) \xrightarrow{A} h_L(s) = \Delta C_L \Delta t + \Delta h_m - 2R\bar{x}[\alpha_1\bar{x} - (1 - \bar{x})\alpha_2]$$

$$x_i(s) \xrightarrow{A} h_{Li}(s) = \Delta C_L \Delta t_i + \Delta h_{mi} - 2R\bar{x}_i[\alpha_1\bar{x}_i - (1 - \bar{x}_i)\alpha_2]$$

From Equation (A-17) which specifies $t(s)$:

$$\pi(s) \xrightarrow{A} t(s) = \frac{\bar{T}}{\bar{\gamma}_1\bar{x}\bar{P}_1\left(\frac{\lambda_{V1}}{R\bar{T}} - ln\,\bar{\gamma}_1\right) + (1 - \bar{x})\,\bar{\gamma}_2\bar{P}_2\left(\frac{\lambda_{V2}}{R\bar{T}} - ln\,\bar{\gamma}_2\right)}$$

$$x(s) \xrightarrow{A} t(s) = \frac{\bar{\gamma}_1\bar{P}_1(\bar{T} - 2\alpha_1\bar{x}^2) - \bar{\gamma}_2\bar{P}_2(\bar{T} + 2\alpha_2\bar{x}^2 - 2\alpha_2\bar{x})}{\bar{\gamma}_1\bar{x}\bar{P}_1\left(\frac{\lambda_{V1}}{R\bar{T}} - ln\,\bar{\gamma}_1\right) + (1 - \bar{x})\,\bar{\gamma}_2\bar{P}_2\left(\frac{\lambda_{V2}}{R\bar{T}} - ln\,\bar{\gamma}_2\right)}$$

From Equation (A-18) which specifies $\pi(s)$:

$$L(s) \xrightarrow{A} \pi(s) = -\alpha_6\alpha_8\, n(\bar{L})^{n-1}$$

From Equation (A-19) which specifies $L(s)$:

$$H(s) \xrightarrow{A} L(s) = \frac{(\bar{L})^{1-n}}{n\alpha_8\,\alpha_{10}}$$

Flow Graph A, in which all the above branches are drawn, topologically represents the set of transformed equations. The first step in the reduction of such a graph is the formation of a new flow graph containing fewer nodes than the first. The nodes which are retained, called residual nodes, are the sources, the sinks, and a minimum set of nodes whose members participate in all the closed loops in the first graph. A source is a node into which no arrows enter, and a sink is one from which no arrows emanate. A closed loop is a series of branches connecting two or more nodes which may be travelled around endlessly, e.g., branches connecting $L(s)$ to $\pi(s)$ to $t(s)$ to $V(s)$ to $H(s)$ to $L(s)$. An examination of Flow Graph A shows that sources are $L_i(s)$, $x_i(s)$ and $y_i(s)$, that $L^*(s)$ is the only sink, and that at least either $H(s)$ or $x(s)$ is part of every closed loop. As a result, all the nodes except $L_i(s)$, $x_i(s)$, $y_i(s)$, $H(s)$ and $x(s)$ can be eliminated. However, the elimination of a node corresponds to elimination of a variable in the equations by a substitution so that the retention of the minimum five nodes just listed means the elimination of $L(s)$. But $L(s)$ constitutes an output variable which must appear in one of the final transfer functions. In order to save $L(s)$, a new variable $L^*(s)$ is introduced which is related to $L(s)$ by $L^*(s) = L(s)$. An $L^*(s)$ node is entered on Flow Graph A and is connected to $(L(s)$ by a branch whose gain is unity.

$$L(s) \xrightarrow{A} L^*(s) = 1$$

Clearly, $L^*(s)$ is a sink and is a residual node.

The residual nodes $L_i(s)$, $x_i(s)$, $y_i(s)$, $H(s)$, $x(s)$ and $L^*(s)$ are entered on Flow Graph B. A branch appears on Flow Graph B connecting two residual nodes if, and only if, Flow Graph A has one or more residual paths connecting the same two nodes. A residual path is defined as a connected series of branches running from a residual node to itself or to another residual node but not passing through any other residual node.

In order to determine the gains of the branches on Flow Graph B only two transformations are needed:

(a) $\boxed{A} \xrightarrow{g_1} \boxed{B} \xrightarrow{g_2} \boxed{C} \equiv \boxed{A} \xrightarrow{g_3} \boxed{C}$ $\quad g_3 = g_1 g_2$

(b) $\boxed{A} \underset{g_2}{\overset{g_1}{\rightrightarrows}} \boxed{B} \equiv \boxed{A} \xrightarrow[g_3]{} \boxed{B}$ $\quad g_3 = g_1 + g_2$

In a cascade transformation (a), the resultant gain is the product of the component gains. In the multipath transformation (b), the resultant gain is the sum of the component gains.

With these transformations, the branches on Flow Graph B can be calculated from Flow Graph A branches. The following

list shows the Flow Graph B branch gains in terms of Flow Graph A gains: The functional notation is suppressed for convenience.

$$H(s)\xrightarrow{B}L^*(s) = (H\xrightarrow{A}L)(L\xrightarrow{A}L^*)$$

$$H(s)\xrightarrow{B}x(s) = (H\xrightarrow{A}x) + (H\xrightarrow{A}V)(V\xrightarrow{A}x) + (H\xrightarrow{A}L)[(L\xrightarrow{A}x) + (L\xrightarrow{A}V)(V\xrightarrow{A}x)] + [(H\xrightarrow{A}L)(L\xrightarrow{A}\pi)(\pi\xrightarrow{A}t)][(t\xrightarrow{A}V) + (t\xrightarrow{A}h_L)(h_L\xrightarrow{A}V) + (t\xrightarrow{A}h_V)(h_V\xrightarrow{A}V)](V\xrightarrow{A}x)$$

$$H(s)\xrightarrow{B}H(s) = (H\xrightarrow{A}V)(V\xrightarrow{A}H) + (H\xrightarrow{A}L)[(L\xrightarrow{A}H) + (L\xrightarrow{A}V)(V\xrightarrow{A}H)] + [(H\xrightarrow{A}L)(L\xrightarrow{A}H)(\pi\xrightarrow{A}t)][(t\xrightarrow{A}V) + (t\xrightarrow{A}h_L)(h_L\xrightarrow{A}V) + (t\xrightarrow{A}h_V)(h_V\xrightarrow{A}V)](V\xrightarrow{A}H)$$

$$x(s)\xrightarrow{B}H(s) = (x\xrightarrow{A}h_L)(h_L\xrightarrow{A}V)(V\xrightarrow{A}H) + (x\xrightarrow{A}y)(y\xrightarrow{A}h_V)(h_V\xrightarrow{A}V)(V\xrightarrow{A}H) + (x\xrightarrow{A}t)[(t\xrightarrow{A}V) + (t\xrightarrow{A}h_L)(h_L\xrightarrow{A}V) + (t\xrightarrow{A}h_V)(h_V\xrightarrow{A}V)](V\xrightarrow{A}H)$$

$$x(s)\xrightarrow{B}x(s) = (x\xrightarrow{A}y)(y\xrightarrow{A}x) + (x\xrightarrow{A}h_L)(h_L\xrightarrow{A}V) + (x\xrightarrow{A}y)(y\xrightarrow{A}h_V)(h_V\xrightarrow{A}V)(V\xrightarrow{A}x) + (x\xrightarrow{A}t)[(t\xrightarrow{A}V) + (t\xrightarrow{A}h_L)(h_L\xrightarrow{A}V) + (t\xrightarrow{A}h_V)(h_V\xrightarrow{A}V)](V\xrightarrow{A}x)$$

$$L_i(s)\xrightarrow{B}H(s) = (L_i\xrightarrow{A}H) + (L_i\xrightarrow{A}V)(V\xrightarrow{A}H)$$

$$L_i(s)\xrightarrow{B}x(s) = (L_i\xrightarrow{A}x) + (L_i\xrightarrow{A}V)(V\xrightarrow{A}x)$$

$$x_i(s)\xrightarrow{B}x(s) = (x_i\xrightarrow{A}x) + (x_i\xrightarrow{A}h_{Li})(h_{Li}\xrightarrow{A}V)(V\xrightarrow{A}x)$$

$$x_i(s)\xrightarrow{B}H(s) = (x_i\xrightarrow{A}h_{Li})(h_{Li}\xrightarrow{A}V)(V\xrightarrow{A}H)$$

$$y_i(s)\xrightarrow{B}H(s) = [(y_i\xrightarrow{A}h_{Vi})(h_{Vi}\xrightarrow{A}V) + (y_i\xrightarrow{A}y)(y\xrightarrow{A}h_V)(h_V\xrightarrow{A}V)](V\xrightarrow{A}H)$$

$$y_i(s)\xrightarrow{B}x(s) = (y_i\xrightarrow{A}x) + (y_i\xrightarrow{A}y)[(y\xrightarrow{A}x) + (y\xrightarrow{A}h_V)(h_V\xrightarrow{A}V)(V\xrightarrow{A}x)] + (y_i\xrightarrow{A}h_{Vi})(h_{Vi}\xrightarrow{A}V)(V\xrightarrow{A}x)$$

$$\frac{x(s)}{x_i(s)} = \frac{\dfrac{(x_i\xrightarrow{B}x)}{1-(x\xrightarrow{B}x)} + \dfrac{(x_i\xrightarrow{B}H)(H\xrightarrow{B}x)}{[1-(x\xrightarrow{B}x)][1-(H\xrightarrow{B}H)]}}{1 - \dfrac{(x\xrightarrow{B}H)(H\xrightarrow{B}x)}{[1-(x\xrightarrow{B}x)][1-(H\xrightarrow{B}H)]}} \quad \text{.....(A-20)}$$

$$\frac{x(s)}{y_i(s)} = \frac{\dfrac{(y_i\xrightarrow{B}x)}{1-(x\xrightarrow{B}x)} + \dfrac{(y_i\xrightarrow{B}H)(H\xrightarrow{B}x)}{[1-(x\xrightarrow{B}x)][1-(H\xrightarrow{B}H)]}}{1 - \dfrac{(x\xrightarrow{B}H)(H\xrightarrow{B}x)}{[1-(x\xrightarrow{B}x)][1-(H\xrightarrow{B}H)]}} \quad \text{.....(A-21)}$$

$$\frac{L(s)}{L_i(s)} = \frac{\dfrac{(L_i\xrightarrow{B}H)(H\xrightarrow{B}L^*)}{1-(H\xrightarrow{B}H)} + \dfrac{(L_i\xrightarrow{B}x)(x\xrightarrow{B}H)(H\xrightarrow{B}L)}{[1-(x\xrightarrow{B}x)][1-(H\xrightarrow{B}H)]}}{1 - \dfrac{(x\xrightarrow{B}H)(H\xrightarrow{B}x)}{[1-(x\xrightarrow{B}x)][1-(H\xrightarrow{B}H)]}} \quad \text{....(A-22)}$$

These transfer functions represent the overall cause-and-effect relationships between the indicated input and output variables. Included as part of each transfer function is that simplified cause-and-effect relationship which forms the basis of the dynamic analysis method. The remainder of each overall transfer function represents dynamic behavior which interferes with the analysis method and, therefore, must be small for the analysis to be successful. For example, Equation (A-20) describes the overall effect on the liquid effluent composition when the incoming liquid composition is disturbed. In its present form, Equation (A-20) is composed of three groups of interactions, the two terms in the numerator and the second term in the denominator. If only the first term in the numerator is expanded in terms of distillation parameters, one sees that the desirable part of the overall transfer function is included in this group.

$$\frac{\dfrac{(x_i\xrightarrow{B}x)}{1-(x\xrightarrow{B}x)} = (x_i\xrightarrow{A}x) + (x_i\xrightarrow{A}h_{Li})(h_{Li}\xrightarrow{A}V)(V\xrightarrow{A}x)}{1-(x\xrightarrow{A}y)(y\xrightarrow{A}x) - [(x\xrightarrow{A}h_L)(h_L\xrightarrow{A}V) + (x\xrightarrow{A}y)(y\xrightarrow{A}h_V)(h_V\xrightarrow{A}V)](V\xrightarrow{A}x) - (x\xrightarrow{A}t)[(t\xrightarrow{A}V) + (t\xrightarrow{A}h_L)(h_L\xrightarrow{A}V) + (t\xrightarrow{A}h_V)(h_V\xrightarrow{A}V)](V\xrightarrow{A}x)}$$

$$\frac{\dfrac{(x_i\xrightarrow{B}x)}{1-(x\xrightarrow{B}x)} = \boxed{\bar{L}_i} + (\bar{H}s + \bar{L})[(x_i\xrightarrow{A}h_{Li})(h_{Li}\xrightarrow{A}V)(V\xrightarrow{A}x)]}{\boxed{\bar{H}s + \bar{L} + mE\bar{V}} - (\bar{H}s + \bar{L})[(x\xrightarrow{A}h_L)(h_L\xrightarrow{A}V) + (x\xrightarrow{A}y)(y\xrightarrow{A}h_V)(h_V\xrightarrow{A}V)](V\xrightarrow{A}x) - (\bar{H}s + \bar{L})(x\xrightarrow{A}t)[(t\xrightarrow{A}V) + (t\xrightarrow{A}h_L)(h_L\xrightarrow{A}V) + (t\xrightarrow{A}h_V)(h_V\xrightarrow{A}V)](V\xrightarrow{A}x)} \quad \text{.....(A-23)}$$

The expression enclosed in dashed lines is that part of the overall transfer which is the basis of the dynamic analysis method (see Equation (9)). Clearly, then, all the remaining parts in Equatio (A-23) plus the two groups of terms

$$\frac{(x_i\xrightarrow{B}H)(H\xrightarrow{B}x)}{[1-(x\xrightarrow{B}x)][1-(H\xrightarrow{B}H)]}$$

and

$$\frac{(x\xrightarrow{B}H)(H\xrightarrow{B}x)}{[1-(x\xrightarrow{B}x)][1-(H\xrightarrow{B}H)]}$$

in Equation (A-20) represent undesirable interactions. Therefore, if the dynamic analysis method is to be unharmed by extraneous effects,

Flow Graph B has a sufficiently simple form that the desired transfer functions may be obtained by inspection. It is necessary first to mention one more transformation:

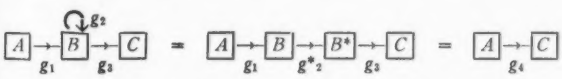

$$g^*_2 = \frac{1}{1-g_2}; \quad g_4 = g_1 g^*_2 g_3 = \frac{g_1 g_3}{1-g_2}$$

A node with self-loop of gain g_2 may be replaced by a cascade branch gain $1/1-g_2$. With this self-loop transformation, the desired transfer functions in terms of Flow Graph B gains are:

$$\frac{x(s)}{x_i(s)} = \frac{\overline{L}_i}{\overline{H}s + \overline{L} + mE\overline{V}}$$

must be a good approximation to Equation (A-20). This will be the case if

$$\overline{L}_i \gg \left| (\overline{H}s + \overline{L})\,(x_i \overset{A}{\rightarrow} h_{Li})\,(h_{Li} \overset{A}{\rightarrow} V)\,(V \overset{A}{\rightarrow} x) \right| \quad \text{.....(A-24)}$$

$$|\overline{H}s + \overline{L} + mE\overline{V}| \gg |(\overline{H}s + \overline{L})\,[(x \overset{A}{\rightarrow} h_L)\,(h_L \overset{A}{\rightarrow} V) + (x \overset{A}{\rightarrow} y)\,(y \overset{A}{\rightarrow} h_V)\,(h_V \overset{A}{\rightarrow} V) + (x \overset{A}{\rightarrow} t)\,\{(t \overset{A}{\rightarrow} V) + (t \overset{A}{\rightarrow} h_L)\,(h_L \overset{A}{\rightarrow} V) + (t \overset{A}{\rightarrow} h_V)\,(h_V \overset{A}{\rightarrow} V)\}]\,(V \overset{A}{\rightarrow} x)| \quad \text{.....(A-25)}$$

$$\left| \frac{\overline{L}_i}{\overline{H}s + \overline{L} + mE\overline{V}} \right| \gg \left| \frac{(x_i \overset{B}{\rightarrow} H)\,(H \overset{B}{\rightarrow} x)}{[1 - (x \overset{B}{\rightarrow} x)]\,[1 - (H \overset{B}{\rightarrow} H)]} \right| \quad \text{...(A-26)}$$

and

$$1 \gg \left| \frac{(x \overset{B}{\rightarrow} H)\,(H \overset{B}{\rightarrow} x)}{[1 - (x \overset{B}{\rightarrow} x)]\,[1 - (H \overset{B}{\rightarrow} H)]} \right| \quad \text{.....(A-27)}$$

If Equation (A-21) is analyzed in this same manner, it is seen that for the desirable part

$$\frac{x(s)}{y_i(s)} = \frac{\overline{V}_i - \overline{V} + E\overline{V}}{\overline{H}s + \overline{L} + mE\overline{V}}$$

to be a good approximation to the overall transfer function, the inequalities (A-25) and (A-27) and also

$$|\overline{V}_i - \overline{V} + E\overline{V}| \gg |(\overline{H}s + \overline{L})\,[(y_i \overset{A}{\rightarrow} y)\,(y \overset{A}{\rightarrow} h_V)\,(h_V \overset{A}{\rightarrow} V)\,(V \overset{A}{\rightarrow} x) + (y \overset{A}{\rightarrow} h_{Vi})\,(h_{Vi} \overset{A}{\rightarrow} V)\,(V \overset{A}{\rightarrow} x)]| \quad \text{.....(A-28)}$$

and

$$\left| \frac{\overline{V}_i - \overline{V} + E\overline{V}}{\overline{H}s + \overline{L} + mE\overline{V}} \right| \gg \left| \frac{(y_i \overset{B}{\rightarrow} H)\,(H \overset{B}{\rightarrow} x)}{[1 - (x \overset{B}{\rightarrow} x)]\,[1 - (H \overset{B}{\rightarrow} H)]} \right| \quad \text{...(A-29)}$$

must be satisfied.

Some comments can be made on the nature of these inequalities: The expressions

$$\frac{(x_i \overset{B}{\rightarrow} H)\,(H \overset{B}{\rightarrow} x)}{[1 - (x \overset{B}{\rightarrow} x)]\,[1 - (H \overset{B}{\rightarrow} H)]},$$

$$\frac{(x \overset{B}{\rightarrow} H)\,(H \overset{B}{\rightarrow} x)}{[1 - (x \overset{B}{\rightarrow} x)]\,[1 - (H \overset{B}{\rightarrow} H)]},$$

and

$$\frac{(y_i \overset{B}{\rightarrow} H)\,(H \overset{B}{\rightarrow} x)}{[1 - (x \overset{B}{\rightarrow} x)]\,[1 - (H \overset{B}{\rightarrow} H)]}$$

in the inequalities (A-26), (A-27) and (A-29), respectively, represent the dynamic behavior which can be pictured crudely as follows: The fluctuation in composition (x_i, x or y_i) causes a fluctuation in the number of mols of holdup on the plate; then the reaction to the holdup fluctuation is a fluctuation in the effluent liquid composition. By intuitive reasoning, neither of these two effects should be strong. The molal holdup on a distillation plate depends primarily on flow rates but also on the relative enthalpies of the feed and effluent streams. The stream enthalpies, of course, depend upon composition, but when the component species are thermodynamically similar, this dependency is weak. It is highly unlikely that reasonable composition fluctuations propagate strongly to the holdup. If this reasoning is correct, then the inequalities (A-26), (A-27) and (A-29) should be easily satisfied.

If inequality (A-24) is written in terms of distillation parameters, it takes the form

$$1 \gg \bar{y}/\bar{h}_V\,[(C_{L1} - C_{L2})(\bar{t}_{Li} - t^\circ) + \Delta h_{Mi} - 2R\bar{x}_i\,\{\alpha_1\bar{x}_i - (1 - \bar{x}_i)\alpha_2\}]$$

This condition should also be satisfied since the right-hand side is made small by the large denominator $\bar{h}_V$. By the same reasoning, inequality (A-28) should be satisfied in most cases. It can be written

$$(\overline{V}_i - \overline{V} + E\overline{V}) \gg \bar{y}/\bar{h}_V\,[(1 - E)\,\overline{V}\,(\Delta C_V \Delta t + \Delta\lambda_V{}^\circ) - \overline{V}_i(\Delta C_{Vi}\Delta t_i + \Delta\lambda_V{}^\circ)]$$

The remaining inequality is (A-25). Since it has been reasoned that all the other inequalities should be easily satisfied, the principal liquid and vapor fluctuation effects must be felt here. If this is, indeed, the case, then a fortunate situation occurs: Equations (A-20) and (A-21) reduce to

$$\frac{x(s)}{x_i(s)} = \frac{\overline{L}_i}{\overline{H}s + \overline{L} + mE\overline{V} + \overline{Q}(s)} \quad \text{.....(A-30)}$$

and

$$\frac{y(s)}{y_i(s)} = \frac{\overline{V}_i - \overline{V} + E\overline{V}}{\overline{H}s + \overline{L} + mE\overline{V} + \overline{Q}(s)} \quad \text{.....(A-31)}$$

where $\overline{Q}(s)$ constitutes all the terms representing the liquid and vapor fluctuation effects and is the right hand side of the inequality (A-25)
The ratio of these equations is

$$\frac{x(s)/y_i(s)}{x(s)/x_i(s)} = \frac{\overline{V}_i - \overline{V} + E\overline{V}}{\overline{L}_i} = \frac{(AR)_{x/y}}{(AR)_{x/x}} \quad \text{.....(A-32)}$$

Equations (A-20), (A-31) and (A-32) with s replaced by $j\omega$ are equations (24), (25) and (26) of the body of this article. $\overline{Q}(j\omega)$ is formally the terms on the right-hand side of the inequality (A-25).

★ ★ ★

The Horizontal Pipeline Flow of Equal Density Oil-Water Mixtures[1]

M. E. CHARLES[2], G. W. GOVIER[3] and G. W. HODGSON[4]

The horizontal flow of equal density oil-water mixtures was investigated in a 1-inch diameter laboratory pipeline. Oils of viscosities 6.29, 16.8 and 65.0 centipoise were used in the experiments. Flow patterns, holdup ratios and pressure gradients were investigated for a range of superficial oil velocity from 0.05 to 3.0 ft./sec. and a range of superficial water velocity from 0.1 to 3.5 ft./sec., with input oil-water ratios ranging from 0.1 to 10.0.

Similar series of flow patterns were observed for each oil and were found to be largely independent of the oil viscosity. At high oil-water ratios oil formed the continuous phase and a water-drops-in-oil regime was noted. As the oil-water ratio was decreased the flow patterns concentric oil-in-water, oil-slugs-in-water, oil-bubbles-in-water and oil-drops-in-water in which water was the continuous phase were observed. The most viscous oil did, however, exhibit anomalous behavior at low superficial water velocities and this is attributed to different interfacial properties.

The pressure drops measured indicated that for a given oil flow rate the pressure gradient was reduced to a minimum by the addition of water provided that the oil was not in turbulent flow. Maximum pressure gradient reduction factors varied from 1.7 for the 6.29 centipoise viscosity oil to 10 for the 65.0 centipoise viscosity oil at input oil-water ratios of 4.5 and 1.0 respectively.

The contact of two immiscible liquids is encountered widely in the chemical and petroleum industries. The design of tubular reactors, liquid-liquid extraction equipment and pipelines for liquid transportation may depend on a knowledge of the flow characteristics of the simultaneous movement of immiscible liquids. Although there is a considerable amount of published information on the flow of liquid-gas and liquid-solid mixtures there is very little on the flow of liquid-liquid mixtures.

A knowledge of the factors affecting the transport of crude oil and water in pipelines is important in the petroleum industry. Water is often produced in large quantities with crude oil and the characteristics of this two-phase flow are of interest both in the well itself, where the flow is vertical in the production tubing, and in horizontal pipelines transporting the crude oil to field treating facilities. The major interest however has been concerned with the beneficial effect, by way of decrease in pressure drop, which results from the introduction of water in controlled amounts into pipelines carrying heavy viscous crude oil. The introduction of water can reduce the pressure gradient along the pipeline[1,2,3,4,5,6] and the power requirement necessary to pump a given quantity of oil.

The flow pattern which appears most attractive from the viewpoint of pressure gradient reduction by the addition of water to a viscous crude oil is that of the concentric flow of oil and water in which the less viscous water forms a uniform annulus in the region of high shear rate next to the pipe wall. Russell and Charles[6] made a theoretical study of the laminar concentric flow of two liquids of equal densities but different viscosities in a smooth circular pipe and also of the laminar stratified flow between wide parallel plates. Concentric flow was also analyzed by Chermikin[3] for the case when the water is in turbulent flow and the oil in laminar flow. Patents by Clark and Shapiro[5] and Chilton and Handley[4] deal with the commercial application of water to reduce oil pipeline pressure gradients. Yuster[7] and Odeh[8] were both concerned with the relative permeability of oil and water in porous media and made theoretical analyses of the flow in idealised capillary systems. Finnigan[9] measured pressure drops and heat transfer for the pipeline flow of oil-water emulsions.

In general, two immiscible liquids of different densities tend to stratify when flowing together in a pipeline. The greater the density difference the more nearly complete is the stratification. In the case of oil and water, the oil usually has a density less than that of the water and forms an upper layer flowing above the water. Stratified flow has been investigated experimentally by Russell, Hodgson and Govier[10] with a light oil in a horizontal pipeline of one-inch diameter and by Charles[1] with a heavy crude oil in 1- and 2½-inch pipelines. Charles and Redberger[2] numerically analysed stratified flow in a circular pipe with the aid of a digital computer.

The relationship between the pressure gradient and flow rate for a single liquid is usually shown as a plot of friction factor against Reynolds number. These quantities incorporate the pressure gradient, the liquid velocity, the pipe diameter, and the density and viscosity of the liquid. The friction factor and the Reynolds number cannot be used in the normal way for the simultaneous flow of two liquids. Also, the interfacial tension of the two liquids, which affects the ease of emulsification, and the contact angle of the liquid-liquid interface on the tubing material, which determines the liquid that preferentially wets the pipe, may be important variables, particularly at low liquid flow rates when the surface forces are no longer negligible

[1]*Manuscript received May 10; accepted September 19, 1960.*
[2]*Junior Research Engineer, Research Council of Alberta, Edmonton, Alta.*
[3]*Professor of Chemical Engineering, Dean of the Faculty of Engineering, University of Alberta, Edmonton, Alta.*
[4]*Head, Petroleum Research, Research Council of Alberta, Edmonton, Alta.*
Contribution from the Research Council of Alberta (No. 125) and the Department of Chemical and Petroleum Engineering, University of Alberta. The work described here was done in partial fulfillment of the requirements for a Master of Science degree at the University of Alberta.

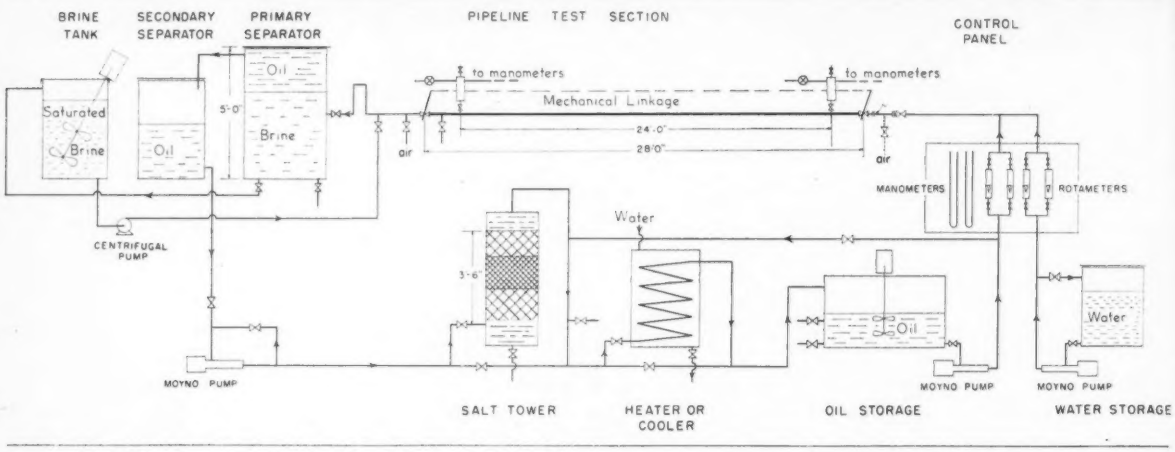

Figure 1—Schematic diagram of the pipeline and accessory equipment used in the study of the simultaneous flow of oil and water of equal densities.

compared with the total kinetic energy. In the present investigation the densities of the liquids were equal and there is no difficulty in representing the density in the two expressions. However, difficulty arises in representing the velocity and viscosity in terms of the composite flowing stream. Russell et al[10] in an investigation of the flow of oil and water with different densities presented their pressure drop data in terms of a friction factor calculated on the basis of the superficial velocity of the water and the density of the water. This technique has correlating advantages but it does not permit a ready visualization of the effect of the introduction of water on the pressure gradient of a flowing oil stream. The more direct relationship of pressure gradient to the ratio of the phases at constant superficial velocity of one of them is useful in demonstrating the practical effect. This method is used in reporting the results of the present investigation.

While the word "superficial" as used to modify the oil and water velocities will be omitted throughout the remainder of this discussion, all liquid velocities referred to will be superficial in the sense that they are calculated from the flow rate and total cross sectional area of the pipe.

Other quantities which are convenient to employ in the treatment of two-phase flow are the input ratio, the in situ ratio and the holdup ratio. The input oil-water ratio, $R_{o/w}$, is defined as the ratio of the oil flow rate to the water flow rate. The in situ ratio is the ratio of the volume of the pipe occupied by oil to the volume occupied by water. In general the input and in situ ratios differ because the liquid in contact with the pipe wall will tend to accumulate in the pipe, and the ratio of the input oil-water ratio to the in situ oil-water ratio is defined as the holdup ratio. Thus, in general, for a given input ratio, if the oil wets the pipe the holdup ratio will tend to be less than unity because the in situ ratio is greater than the input ratio and, if the water wets the pipe the holdup ratio will tend to be greater than unity because the in situ ratio is less than the input ratio. It will also be convenient to consider the input water-oil ratio, $R_{w/o}$, which is the reciprocal of the input oil-water ratio.

Experimental Equipment and Procedure

Test Oils

Three Newtonian oils were used in the investigation and all were obtained by increasing the density of three commercial oils (Marcol GX, Wyrol J, and Teresso 85, marketed by Imperial Oil Ltd.). Sufficient carbon tetrachloride was added to each oil to give the oils the same density as the water (0.998 gm. per cm³. at a temperature of 25°C.). Carbon tetrachloride, with a density of 1.59 gm. per cm.³ was selected on the basis of high density and relatively low cost as the most suitable liquid to increase the density of the oil phase. Precautions were taken to confine the toxic carbon tetrachloride vapor to protect the operating personnel. The properties of the test oils are given in Table 1.

Equipment

A flow diagram of the pipeline and accessory equipment is shown in Figure 1. The test oil and water supplies were contained in storage tanks and the oil was maintained in a uniform condition by means of a double propellor-type mixer. The oil temperature was adjusted by recycling the oil through a heater, until the temperature was indicated to be 25°C. by a bimetallic thermometer situated in the recycle line. The water temperature was controlled by adjusting the relative amounts of hot and cold water flowing into the storage tank. The density of the oil was checked by using a hydrometer in a sample taken from the storage tank and was usually found to be slightly low (for example, 0.995 gm. per cm.³ compared with the required value of 0.998 gm. per cm.³) because of the loss of carbon tetrachloride through evaporation. Sufficient

TABLE 1

TEST OIL PROPERITES

Viscosity, cp. at 25°C.	Density, gm./cm.³ at 25°C.	Color	Approximate carbon tetrachloride content, volume per cent	Commercial oil used as base
6.29	0.998	clear	20.6	Marcol GX
16.8	0.998	clear	18.7	Wyrol J
65.0	0.998	dark green-brown	16.7	Teresso 85

carbon tetrachloride was added to give the oil supply the required density.

The flow of oil and water to the pipeline was established by screw-type positive displacement pumps which delivered the oil and water separately to calibrated rotameters after which the oil and water flows were combined concentrically at the beginning of a ten-foot long section by means of a nozzle in which the oil was introduced inside a water annulus.

The pipeline calming section and twenty-four foot test section were supported in a horizontal position by a wooden trestle. The cellulose acetate-butyrate pipe was smooth and transparent with an internal diameter of 1.04 in. The pipeline was mounted on brass slides and with a flexible coupling between the pipeline and the separation unit so that it was free to expand under the influence of ambient temperature. The test section was supplied with pressure taps for the measurement of the pressure drop and with two quick-action valves joined by a taut steel cable for the measurement of the in situ contents of the pipeline.

The oil was separated from the water for return to storage by establishing a density differential between the immiscible liquids by the addition of saturated brine to the oil and water mixture immediately after it left the test section. The brine increased the density of the aqueous phase which then formed the lower layer in the separator. The upper oil layer was pumped to storage through a salt tower which removed the last traces of water present as small drops.

Observation of flow pattern

The oil and water flow rates were adjusted to the desired values and time was permitted for steady conditions to be established – usually one to five minutes. In general, the slower the flow rates, the longer was the time required to obtain steady conditions. When visual observation indicated steady conditions the flow pattern was noted. Photographs were taken of representative flow patterns.

Pressure drop measurement

The pressure drop measuring system was similar to that used by Russell et al[10] and consisted of two pressure stations, situated 24.0 feet apart on the test section, with copper connecting lines to manometers. The fluid in the connecting lines was air, the pressure of which was adjusted by pressure reduction valves connected to a 40 lb. per in.^{2} gauge air supply. The oil and water mixture was admitted into the splash pot at each pressure station and the liquid levels adjusted to the same elevation by manipulating the air pressure reduction valves until the connecting line pressure balanced the pipeline pressure.

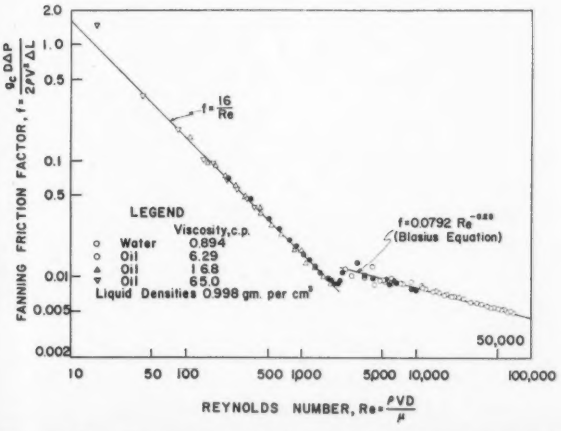

Figure 2 — Comparison of theoretical and experimental friction factors for the flow of water and the 6.29, 16.8 and 65.0 centipoise viscosity oils.

The pressure differential between the pressure taps was indicated on a water or mercury manometer.

Measurement of in situ contents

After closing the pressure taps the quick action valves at the ends of the test section were closed simultaneously and the oil and water pumps stopped. A "pig", which closely fitted the internal surface of the pipeline, was introduced into the pipeline upstream of the test section, and, when forced through the test section by air pressure, ejected the trapped oil and water into volume measuring equipment. The passage of the "pig" provided a fast, efficient method of ejecting the oil and water.

Interfacial tension measurement

The oil-water interfacial tensions were determined using a simple capillary method[11] which involved the measurement of the equilibrium heights of oil and water columns having a joint interface inside a glass capillary of known diameter.

Experimental Results and Discussion

The operation of the pipeline, including the rotameter calibrations and the manometer system for measuring pressure drops, was initially checked by recording pressure drops for the flow of water and the three test oils separately. Fanning friction factors were plotted against Reynolds numbers on logarithmic paper. The good agreement between the experimental data and the accepted curves for the laminar and turbulent regions is evident in Figure 2.

It was desired to observe the flow of the oils with water over as wide ranges of oil and water flow rates as possible and to obtain pressure drop and holdup measurements for the various flow patterns observed. Flow patterns were observed over a range of oil velocity from 0.05 to 3.0 ft./sec. and a range of water velocity from 0.1 to 3.5 ft./sec. Pressure drop and holdup measurements were made at about five oil velocities for each of five water velocities.

Flow patterns

A series of flow patterns was observed for a decrease in the oil flow rate at a constant water flow rate. The flow pattern changed from a dispersion of water in oil, through concentric, oil-slugs-in-water and oil-bubbles-in-water, to oil-drops-in-water. Drawings were prepared from photographs taken for the 16.8 cp. viscosity oil, and are representative for the three oils except for the flow patterns of the most viscous oil at low water flow rates.

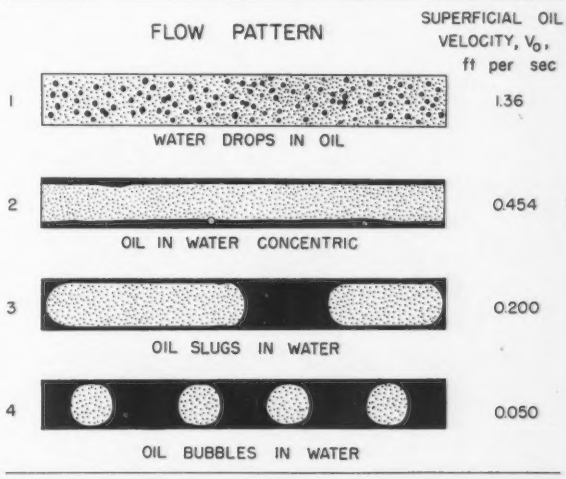

Figure 3 — Drawings prepared from photographs of the 16.8 viscosity oil flowing in the presence of water and showing the variation in flow pattern with oil velocity for a low fixed water velocity of 0.10 ft./sec.

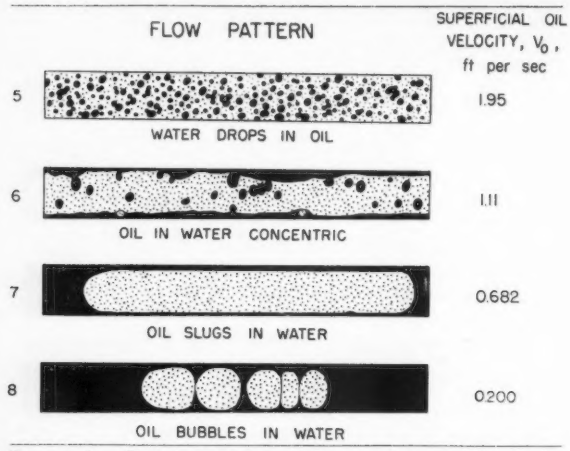

Figure 4 — Drawings prepared from photographs of the 16.8 centipoise viscosity oil flowing in the presence of water and showing the variation in flow pattern with oil velocity for a fixed water velocity of 0.682 ft./sec.

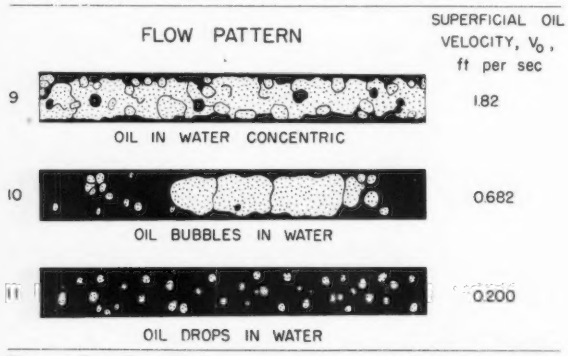

Figure 5 — Drawings prepared from photographs of the 16.8 centipoise viscosity oil flowing in the presence of water and showing the variation in flow pattern with oil velocity for a high fixed water velocity of 2.04 ft./sec.

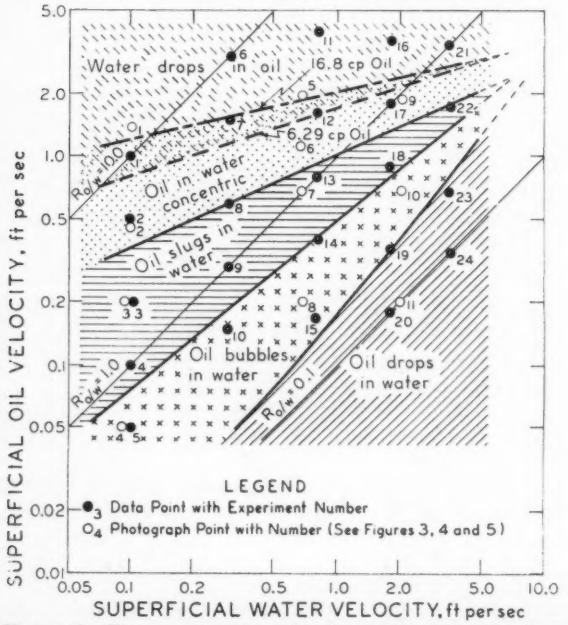

Figure 6—Flow regimes for oils of viscosity 6.29 and 16.8 centipoise and density 0.998 gm./cm.³ flowing in the presence of water with the same density.

The effect on the flow pattern of reducing the oil velocity at the relatively low water velocity of 0.1 ft. per sec. is shown in Figure 3. At high oil velocities the water-drops-in-oil flow pattern was observed as in the example for an oil velocity of 1.36 ft./sec. Reduction in the oil velocity to about 1.2 ft./sec. caused both oil and water to be present as continuous phases. Concentric flow, in which the oil formed a continuous core along the axis of the pipe and the water a uniform layer on the pipe wall, is shown for an oil velocity of 0.454 ft./sec. A further reduction in oil velocity at a water velocity of 0.1 ft./sec. resulted in the oil phase becoming discontinuous. The oil flowed as slugs, and at lower oil velocities, as bubbles. The oil-slugs-in-water flow pattern is shown for an oil velocity of 0.200 ft./sec. and the oil-bubbles-in-water flow pattern is shown for an oil velocity of 0.050 ft./sec.

The effect on the flow pattern of reducing the oil velocity at a higher water velocity is similar, as shown in Figure 4 for a water velocity of 0.682 ft./sec. Again at high oil velocities the water was dispersed as small drops and an example of this flow pattern is given for an oil velocity of 1.95 ft./sec. A reduction in the oil velocity again resulted in concentric oil-in-water flow and an example is shown for an oil velocity of 1.11 ft./sec. The flow was disturbed compared with the concentric flow at a water velocity of 0.10 ft./sec.; the oil-water interface was wavy and some water was entrained in the oil. A further reduction in oil velocity again resulted in oil-slugs-in-water flow and subsequently oil-bubbles-in-water flow. An example of slug flow is shown for an oil velocity of 0.682 ft./sec. and an example of bubble flow for an oil velocity of 0.200 ft./sec.

The effect on the flow pattern of reducing the oil velocity at an even higher water velocity of 2.04 ft./sec. is shown in Figure 5. At high oil velocities the water-drops-in-oil pattern was again encountered. At the lower oil velocity of 1.82 ft./sec. the considerably disturbed form of concentric flow was encountered and further reduction in oil velocity gave the oil-slugs-in-water, the oil-bubbles-in-water and the oil-drops-in-water flow patterns. At this relatively high water velocity it was difficult to differentiate slug, bubble and drop flow patterns because, for a given oil velocity, the oil was often present as slugs, bubbles and drops of various sizes as shown for oil velocities of 0.682 and 0.200 ft./sec. The drawings indicate that for the concentric oil-in-water, oil-slugs-in-water, oil-bubbles-in-water and oil-drops-in-water flow patterns the pipe was always ina water-wet condition.

The flow pattern regimes are summarized for the 6.29 and 16.8 cp. viscosity oils in Figure 6, where the oil and water velocities are represented on logarithmic coordinates and single lines are drawn between the various flow regimes. The change from one regime to another was not well defined and the lines represent gradual transitions. The oil and water velocities for which pressure drop and holdup measurements were made, are plotted along with the corresponding experiment number in Figure 6 – as are also the velocities which are represented by the flow pattern examples in Figures 3, 4 and 5. The flow regimes for these two oils are almost identical. The only difference occurs in the position of the boundary between the water-drops-in-oil and the concentric oil-in-water flow regimes. The boundary is at a somewhat higher oil velocity for the 16.8 cp. oil than for the 6.29 cp. oil. A viscosity differential would appear not to account for this difference since this boundary for the most viscous oil is not displaced further but is in approximately the same position as the boundary for the 6.29 cp. oil as shown in Figure 7.

The flow regimes observed for the 65.0 cp. oil are summarized in Figure 7, and show general agreement with those for the other less viscous oils except at low water velocities where a succession of different flow patterns was obtained with the oil as the continuous phase. The line PQ represents the conditions for which the flow pattern was unstable and represents an inversion between flow patterns in which the oil was

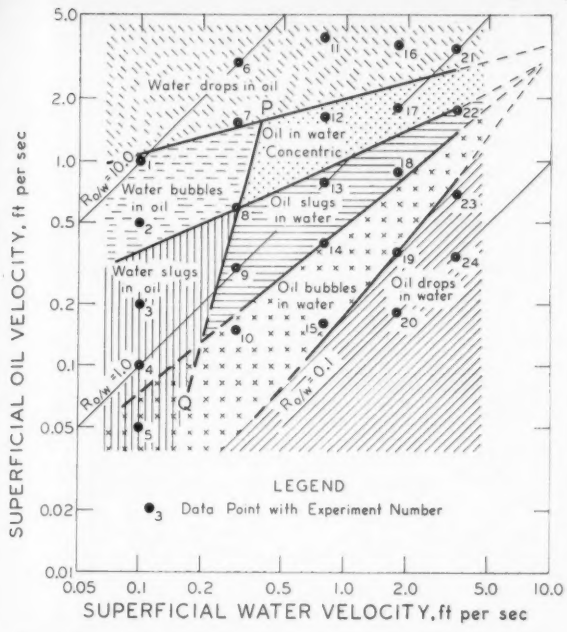

Figure 7—Flow regimes for oil of viscosity 65.0 centipoise and density 0.998 gm./cm.³ flowing in the presence of water with the same density.

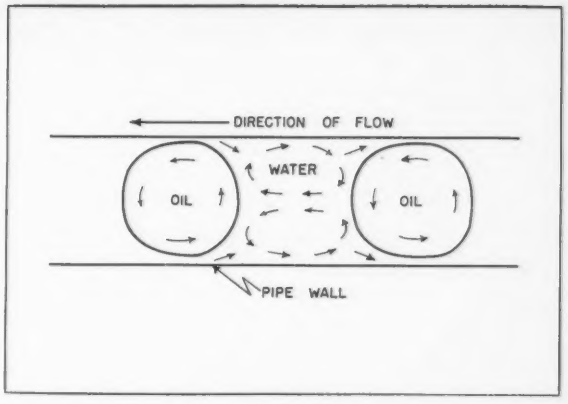

Figure 8 — Liquid movement in the oil-bubbles-in-water flow pattern.

the continuous phase and flow patterns in which water was the continuous phase. For a given oil velocity, a water velocity of less than that indicated at the inversion line gave a flow pattern with oil as the continuous phase, while for a water velocity greater than that indicated at the inversion line, flow patterns with water as the continuous phase were obtained. The boundaries between the regimes in which water was the continuous phase were almost identical with the corresponding boundaries for the less viscous oils. The regime boundaries are represented by broken lines at low oil and water velocities because the flow patterns were less well defined under these conditions.

The flow patterns observed in this study may be related to the flow patterns reported by Russell et al[10] in examining the flow of oil and water of different densities:

(a) bubble flow, in which oil drops and bubbles moved along the top of the pipe.

(b) stratified flow, in which the oil and water flowed in two layers with a quiet interface.

(c) mixed flow, which occurred at high flow rates and was a completely mixed type of flow.

The bubble flow of Russell et al appears to correspond to the oil-drops-in-water and oil-bubbles-in-water and oil-slugs-in-water flow patterns observed in the present study. The stratified flow corresponds to the concentric oil-in-water flow pattern and the mixed flow to the water-drops-in-oil flow pattern.

A circulation of oil within the bubbles and slugs was noted for the oil-slugs-in-water and oil-bubbles-in-water flow patterns. This movement is indicated in Figure 8 for bubble flow. Approximate velocities relative to the average flow velocity are represented by the vector arrows. The direction of rotation of the bubble is probably dependent on the direction of a small density differential between the oil and the water. When the oil is slightly more dense than the water the bubbles would tend to drag more at the lower surface of the pipe and rotate in the direction shown. A circulatory movement was also noticed in the water phase between the bubbles or slugs of oil.

Interfacial properties and their influence on flow pattern

It has been observed in this discussion that the most viscous oil showed behavior different from the less viscous oils at low water velocities. Since under these conditions surface forces may no longer be negligible compared with the total kinetic energy of the flow the dissimilar behavior of the most viscous oil suggested that interfacial properties might be important in the determination of flow pattern. The interfacial oil-water tensions (accurate to within about five per cent) were measured and are reported in Table 2. The similar values for the 6.29 cp. and the 16.8 cp. viscosity oils and the dissimilar value for the 65.0 cp. oil are not surprising, since the 6.29 cp. and the 16.8 cp. viscosity oils were both prepared from white mineral oils while the 65.0 cp. oil was prepared from a lubricating oil containing anti-corrosion compounds. The interfacial contact angles with the pipe surface were observed qualitatively: the pipeline flow was stopped with water as the continuous phase and the most viscous oil was visually observed to make contact with, and spread readily on, the pipe surface, whereas the less viscous oils maintained a definite angle of contact with the pipe surface in the presence of water. The influence of the different interfacial tensions on the flow patterns is not clear since it would be expected that the most viscous oil having a relatively low oil-water interfacial tension would exhibit a greater tendency to form emulsions. However the series of flow patterns in which the most viscous oil formed the continuous phase is probably accounted for by the preferential wetting of the pipe surface by this oil.

Holdup ratio

When two fluids flow together in a pipeline the in situ volumetric ratio is, in general, different from the input volumetric ratio since the liquid in contact with the pipe wall tends to be held back. For highly turbulent flow, however, with both fluids thoroughly mixed together, the in situ volumetric ratio would be approximately equal to the input volumetric ratio. The holdup ratio has been defined as the ratio of the input oil-water ratio to the in situ oil-water ratio. The holdup ratio, then, does in general differ from unity, and will tend to be

TABLE 2

OIL-WATER INTERFACIAL TENSIONS

Oil viscosity cp. at 25°C.	Interfacial oil-water tension dynes/cm. at 25°C.
6.29	44
16.8	45
65.0	30

TABLE 3 (Partial)

EXPERIMENTAL DATA FOR THE FLOW OF THE 16.8 CP. VISCOSITY OIL AND WATER IN A CIRCULAR PIPE

Liquid Temperatures: 25°C. Oil Viscosity: 16.8 cp. Water viscosity: 0.894 cp.

Pipe diameter: 1.04 in. Distance between pressure tappings: 24.0 ft.

Liquid densities: 0.998 gm. per cm.^{3} Volume of pipeline for in situ measurements: 4720 cm^3.

Experiment number	Superficial water velocity ft./sec.	Superficial oil velocity ft./sec.	Input oil-water ratio ft.^{3}/ft.^{3}	Pressure drop over test section in. of water	In situ ratio ft.^{3}/ft.^{3}	Holdup ratio
1	0.100	1.00	10.0	2.50	6.68	1.50
2	0.100	0.500	5.00	1.0–1.2	3.07	1.66
3	0.100	0.200	2.00	0.45	1.56	1.28
4	0.100	0.100	1.00	0.30	0.958	1.05
5	0.100	0.050	0.500	0.30	0.428	1.17
6	0.300	3.00	10.0	17.6	12.1	0.826
7	0.300	1.50	5.00	3.45	3.26	1.53
8	0.300	0.600	2.00	0.70	1.55	1.29
9	0.300	0.300	1.00	0.35	0.775	1.29
10	0.300	0.150	0.500	0.35	0.426	1.17
11	0.800	3.98	4.98	21.0	3.97	1.26
12	0.800	1.60	2.00	7.20	1.48	1.35
13	0.800	0.80	1.00	2.55	0.840	1.19
14	0.800	0.40	0.500	1.60	0.463	1.08
15	0.800	0.159	0.199	1.10	0.178	1.12
16	1.80	3.60	2.00	39.2	1.70	1.18
17	1.80	1.80	1.00	14.2	0.796	1.26
18	1.80	0.900	0.500	8.70	0.440	1.14
19	1.80	0.358	0.199	6.20	0.174	1.15
20	1.80	0.182	0.101	5.20	0.094	1.06
21	3.50	3.50	1.00	40.0	0.953	1.07
22	3.50	1.75	0.500	27.3	0.407	1.23
23	3.50	0.693	0.198	19.6	0.189	1.06
24	3.50	0.350	0.100	17.5	0.094	1.07

greater than unity when water is the component in contact with the pipe wall and to be less than unity when oil is in contact with the pipe wall.

Holdup ratios were measured at various oil-water input ratios and at water velocities of 0.1, 0.3, 0.8, 1.8 and 3.5 ft./sec. for each of the three oils. These water velocities were chosen to give a suitable separation of the data on a logarithmic scale. An example of the experimental data obtained is given in Table 3 where the holdup ratios and pressure drops for the 16.8 cp. viscosity oil are presented*. The experimental holdup ratios are plotted against the input oil-water ratio, with water velocity as parameter, for the 6.29 cp. viscosity oil in Figure 9.

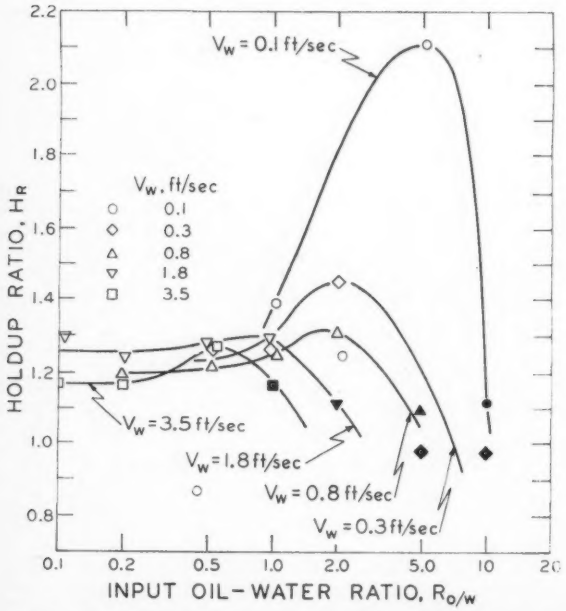

Figure 9 — Holdup ratio as a function of the input oil-water ratio and water velocity for oil of viscosity 6.29 centipoise and density 0.998 gm./cm.^{3}.

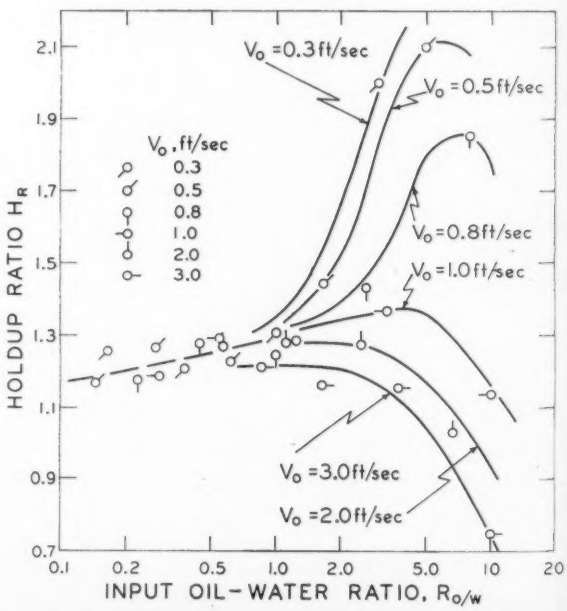

Figure 10—Holdup ratio as a function of the input oil-water ratio and oil velocity for oil of viscosity 6.29 centipoise and density 0.998 gm./cm.^{3}.

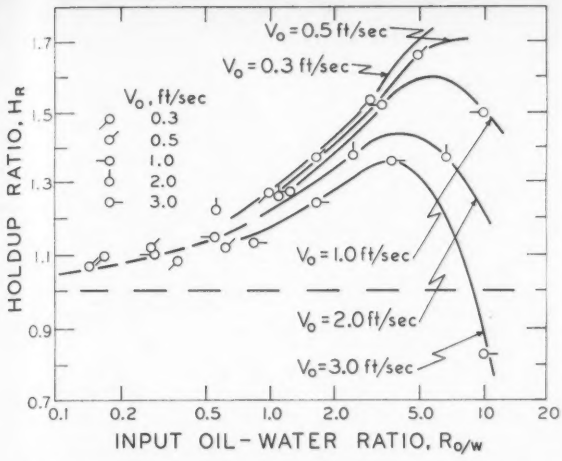

Figure 11—Holdup ratio as a function of the input oil-water ratio and oil velocity for oil of viscosity 16.8 centipoise and density 0.998 gm./cm.³.

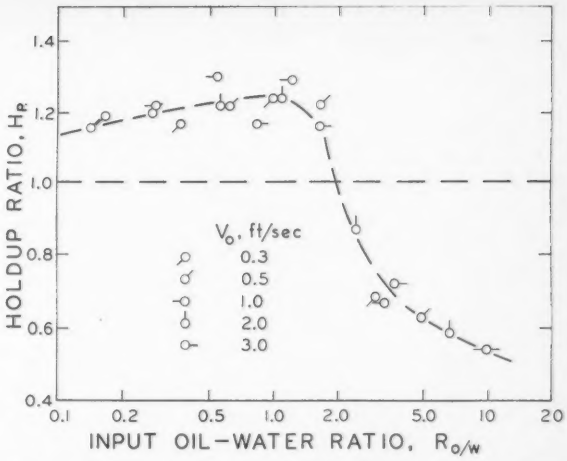

Figure 12—Holdup ratio as a function of the input oil-water ratio and oil velocity for oil of viscosity 65.0 centipoise and density 0.998 gm./cm.³.

(In Figures 9, 13, 15 and 17 the solid data points represent experiments in which the oil wetted the pipe wall and the open points represent experiments in which the water wetted the pipe.) The holdup curves pass through maxima, the locations of which coincide with the concentric oil-in-water and oil-slugs-in-water flow patterns. At high flow velocities the holdup ratios tend to become independent of the flow rate of either oil or water. This is more clearly indicated in Figure 10, where the holdup ratio is plotted against the input oil-water ratio with oil-velocity as parameter. Figure 10 was prepared from the smooth curves drawn for the constant water velocities in Figure 9. The tendency for the holdup ratio to approach unity at low oil-water ratios is well illustrated in Figure 10 for the range of oil velocities investigated.

Figures similar to Figure 10 were prepared from the plots of the experimental data at constant water velocity for the 16.8 and 65.0 cp. viscosity oils. The dependence of the holdup ratio on oil velocity at high oil-water ratios is indicated for the 16.8 cp. oil in Figure 11, with the tendency to approach to a value of unity at low oil-water ratios. The holdup ratio values for the most viscous oil in Figure 12 reflected the different behaviour of this oil at high oil-water ratios. The holdup ratio values were less than unity for the flow regimes in which the oil formed the continuous phase and showed little dependence on

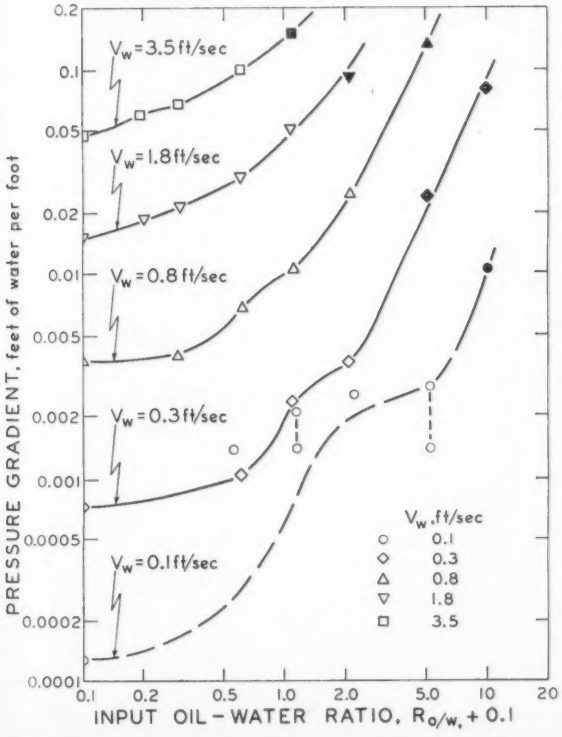

Figure 13—Experimental pressure gradients for the oil of viscosity 6.29 centipoise as a function of the input oil-water ratio and water velocity.

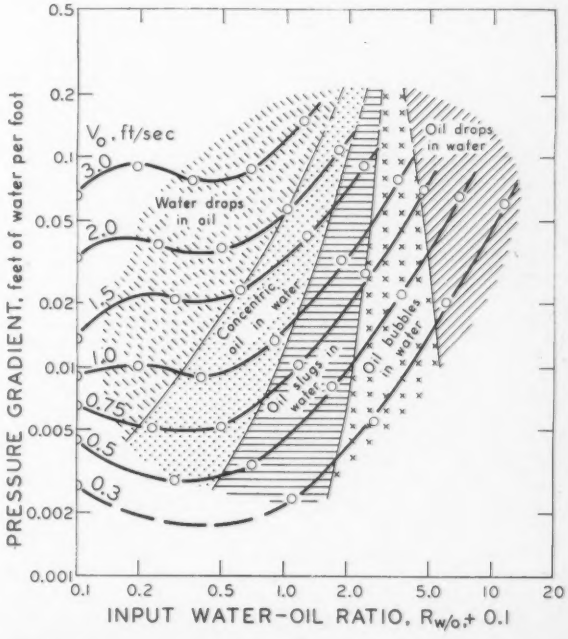

Figure 14—Pressure gradients for the oil of viscosity 6.29 centipoise as a function of the input water-oil ratio and oil velocity. Points are calculated from the curves of Figure 13.

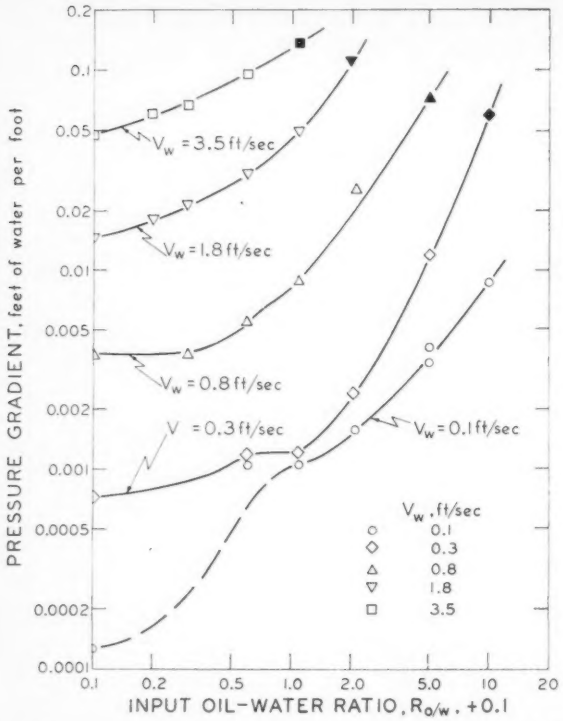

Figure 15—Experimental pressure gradients for the oil of viscosity 16.8 centipoise as a function of the input oil-water ratio and water velocity.

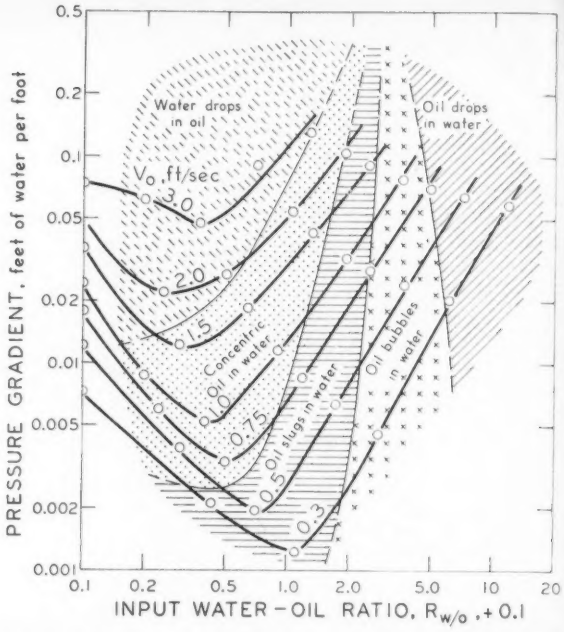

Figure 16—Pressure gradients for the oil of viscosity 16.8 centipoise as a function of the input water-oil ratio and oil velocity. Points are calculated from the curves of Figure 15.

the oil velocity. At low oil-water ratios the holdup ratio values were very similar to the values obtained for the less viscous oils at the same oil-water ratios, and tended to approach unity as the oil-water ratio decreased.

Pressure gradients

Pressure drops were measured at the same oil and water flow rates as those for which holdup ratios were recorded i.e., at various input oil-water ratios for water velocities of 0.1, 0.3, 0.8, 1.8 and 3.5 ft./sec. The pressure drops obtained for the 16.8 cp. viscosity oil are given in Table 3.*

The pressure gradients obtained for the 6.29 cp. viscosity oil are presented in Figure 13 where the pressure gradient is plotted against the input oil-water ratio on logarithmic scales with water velocity as the parameter. The points at zero oil-water ratio represent conditions for which water flows alone and were calculated from the friction factor – Reynolds number curves for the flow of a single liquid in a smooth circular pipe. The experimental data for water velocities of 0.3, 0.8, 1.8 and 3.5 ft./sec. conform to a family of relatively smooth curves. The data for a water velocity of 0.1 ft./sec. are consistent with the data for higher water velocities only at oil-water ratios above about 5; for lower input ratios the pressure gradients observed appear to be three to five times larger than those to be expected from extrapolation of the family of curves from higher water velocities. The pressure gradients at a water velocity of 0.1 ft./sec. were some of the lowest measured but there is no reason to suspect the accuracy of the measurements. It is possible that the apparently high pressure gradients may be accounted for by the tendency, at these low oil and water flow rates, for the oil phase to drag on the pipe wall as a result of a slight density differential between the oil and water phases.

Since primary interest lies in the pressure gradients for a given oil flow rate in the presence of various amounts of water, the results are better plotted, as in Figure 14, as the pressure gradient versus the water-oil input ratio with the oil velocity as the parameter. The curves were constructed from the smooth curves of Figure 13 and the points do not represent direct experimental observations. The points of intersection of the curves with the ordinate were calculated for an oil of viscosity 6.29 cp. from the accepted friction factor – Reynolds number curve.

It is apparent that for oil flow rates below 1 ft./sec. a reduction in pressure gradient is obtained by the addition of water. The factors by which the pressure gradients are reduced are largest at the lowest oil flow rates. The maximum factor by which the pressure gradient was reduced was approximately 1.7 at an oil velocity of 0.5 ft./sec. and an input water-oil ratio of 0.22 (or a water percentage of 18% based on the total liquid flow).

For oil velocities above 1.0 ft./sec. a pressure gradient reduction was not observed and an increase in pressure gradient was indicated immediately upon the addition of water. Maxima occurred in the curves at an input water-oil ratio of 0.1 and are probably accounted for by a transition from laminar to turbulent flow on the addition of the water. This is likely to be so, especially at an oil velocity of 1.5 ft./sec. since, in this case, the Reynolds number for the flow of the oil is nearly 2000. At high water-oil ratios the curves show steady increases in pressure gradient with increase in water-oil ratio and at a ratio of 10 the presence of the oil had little or no effect on the pressure gradient. That is, the pressure drops recorded and the calculated pressure drops assuming the liquid to be all water (rather than 10 parts water and 1 part oil) agree to within a few per cent.

The flow pattern loci from Figure 6 are superimposed in Figure 14 and it is evident that, at the oil flow rates for which the pressure gradient was reduced below that for the oil flowing alone, the pressure gradient was least in the concentric oil-in-water and oil-slugs-in-water patterns.

*Complete experimental data of Table 3 of this paper has been deposited as Document No. 6438 with the ADI Auxiliary Publications Project, Photoduplication Service, Library of Congress, Washington 25, D.C. A copy may be obtained by citing the Document No. and by remitting $1.25 for photoprints, or $1.25 for 35 mm. microfilm. Advance payment is required. Make cheques or money orders payable to: Chief, Photoduplication Servce, Library of Congress.

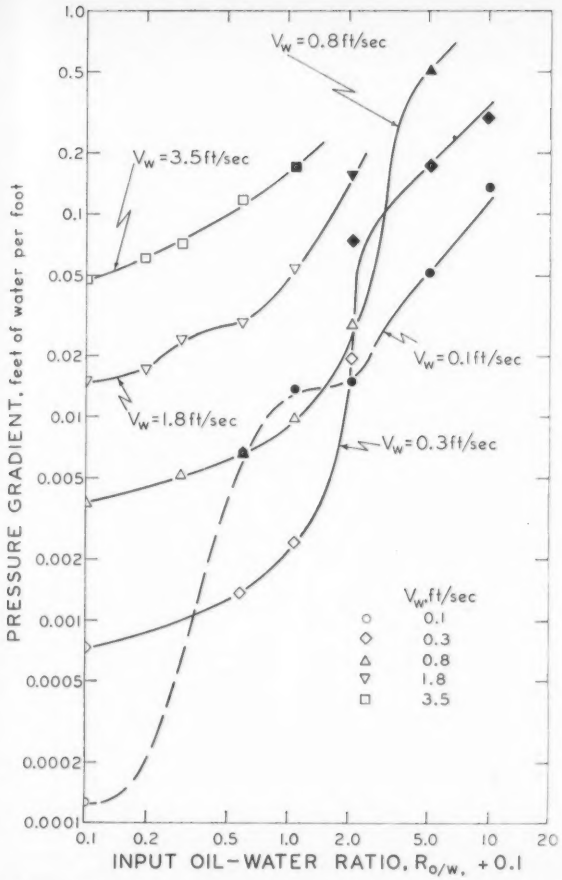

Figure 17—Experimenal pressure gradients for the oil of viscosity 65.0 centipoise as a function of the input oil-water ratio and water velocity.

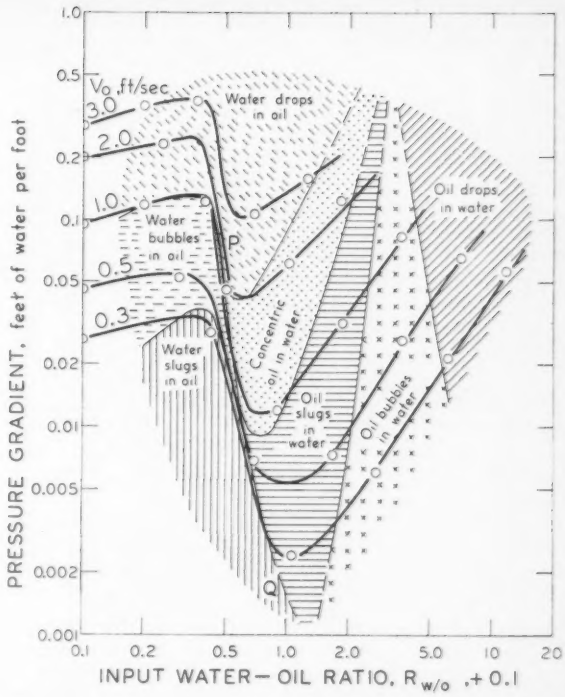

Figure 18—Pressure gradients for the oil of viscosity 65.0 centipoise as a function of the input water-oil ratio and oil velocity. Points are calculated from the curves of Figure 17.

The data for the 16.8 cp. oil are shown in Figure 15, where again the pressure gradient is plotted against input oil-water ratio with water velocity as parameter. The data follow smooth curves except, as for the 6.29 cp. oil, at a water velocity of 0.1 ft./sec. Here again, the pressure gradients were higher than expected and can perhaps be explained in the same way as for the 6.29 cp. oil.

The smooth curves were used to produce Figure 16 in which pressure gradient is plotted against input water-oil ratio with oil velocity as parameter. The flow pattern loci from Figure 6 are superimposed. This figure shows the effect of increasing the water content of the flowing mixture at a constant oil flow rate. With this more viscous oil the pressure gradient reduction obtained by the introduction of water is more pronounced. The maximum pressure gradient reduction factor noted was 6.0 for an oil velocity of 0.5 ft./sec. at an input ratio of 0.65 (or a water percentage of 39.4% based on the total liquid flow). Again at high input water-oil ratios the observed pressure drops were reasonably close to the calculated values assuming that the liquid flowing was all water. The pressure gradient was reduced most markedly in the concentric and oil-slugs-in-water flow pattern regimes. A smaller reduction was evident in the water-drops-in-oil regime and is possibly accounted for by a reduction in the effective viscosity of the water-in-oil emulsion at high water contents below the viscosity of the pure oil.

Figures similar to the figures for the less viscous oils are also presented for the 65.0 cp. oil. Figure 17 is the plot of pressure gradient against input oil-water ratio with water velocity as parameter. Again the data fit smooth curves and with this, the most viscous oil, the high pressure gradients obtained when the oil formed the continuous phase are evident at high input oil-water ratios. For a given water velocity the pressure gradient increased with increasing input oil-water ratio with a rather sharp increase at the point of inversion between the flow patterns with water as the continuous phase and the flow patterns with oil as the continuous phase.

The practical significance of the addition of water to the 65.0 cp. oil is better illustrated in Figure 18 where the pressure gradient is plotted against the input water-oil ratio with oil velocity as parameter. The flow pattern loci from Figure 7 are superimposed. The curves all have the same general shape: a gradual increase in pressure gradient with increase in water content through the flow regimes in which oil is the continuous phase, a pronounced reduction in pressure gradient when the inversion to a flow pattern with water as the continuous phase takes place, and a general increase in pressure gradient with the continued increase in input water-oil ratio.

The maximum pressure gradient reduction factor for the 65.0 cp. oil is approximately 10 and occurs for an oil velocity of 0.3 ft./sec. at an input ratio of 1.0. The superimposed flow pattern regimes indicate that the greatest pressure gradient reduction occurs in the concentric oil-in-water and oil-slugs-in-water regimes. Again the observed pressure gradients at high input water-oil ratios compare very closely with the pressure gradients calculated on the assumption that water alone occupies the pipe.

The maximum pressure gradient reduction factors obtained experimentally, i.e., 1.7 for the 6.29 cp. oil, 6.0 for the 16.8 cp. oil and 10.0 for the 65.0 cp. oil, may be compared with the maximum reduction factors predicted by the theoretical analysis of Russell and Charles[6] for laminar concentric flow in a circular pipe. Russell and Charles predicted the maximum reduction factor to be

$$\frac{\mu_o^2}{(2\mu_o - \mu_w)\mu_w}$$

Substitution of the viscosity values in this expression gives maximum reduction factors of approximately 3.8 for the 6.29 cp. oil, 9.6 for the 16.8 cp. oil and 36.4 for the 65.0 cp. oil. The experimental quantities are, therefore, not so large as the theoretical values. The difference is explained by noting that the flow pattern for which the experimental reduction factors were obtained was closer to slug flow than concentric and, although the flow of the water was probably laminar in the annulus between the oil slugs and the pipe wall, eddies existed in the water phase between the slugs. Nevertheless, the maximum pressure gradient reduction factors determined experimentally are considerable and show a definite increase with oil viscosity.

Conclusions

1. The following flow patterns were noted in the horizontal flow of equal density oil and water mixtures:

   (a) water-drops-in-oil.
   (b) concentric oil-in-water.
   (c) oil-slugs-in-water.
   (d) oil-bubbles-in-water.
   (e) oil-drops-in-water.

The character of the flow patterns and their relationship to the oil and water flow rates were found to be largely independent of the viscosity for oils of viscosities 6.29, 16.8 and 65.0 cp. although the most viscous oil showed dissimilar behaviour at high oil-water input ratios. This was probably due to different oil-water interfacial properties.

2. Holdup ratios were, in general, found to greater than unity when the water was the continuous phase in contact with the pipe wall, less than unity when oil was in contact with the pipe wall and close to unity at high flow velocities.

3. The addition of increasing amounts of water to oil which is originally in laminar flow (Reynolds number of probably not more than 1500) lowers the pressure gradient to a minimum, after which the addition of more water increases the pressure gradient and, with sufficient water, the pressure gradient exceeds the pressure gradient for the oil flowing alone.

Nomenclature

D = diameter of pipeline, ft.
f = Fanning friction factor, dimensionless
g_c = dimensional conversion factor lb_m. ft./lb_f. sec.^{2}
H_R = holdup ratio, the ratio of the input oil-water ratio to the in situ oil-water ratio, dimensionless
ΔL = length of pipeline, ft.
ΔP = pressure drop over length ΔL, lb./ft.^{2}
$R_{o/w}$ = input oil-water volume ratio, ft.^{3}/ft.^{3}
$R_{w/o}$ = input water-oil volume ratio, ft.^{3}/ft.^{3}
Re = Reynolds number, $\rho Vd/\mu$, dimensionless.
V = superficial liquid velocity, ft./sec.
μ = liquid viscosity, lb_m./ft.-sec.
ρ = liquid density, lb_m./ft.^{3}

Subscripts

f = force
m = mass
o = oil
w = water.

References

(1) Charles, M. E., Can. Inst. Min. Met. Bull. **53,** 483 (1960).
(2) Charles, M. E., and Redberger, P. J., "The Reduction of Pressure Gradients in Oil Pipelines by the Addition of Water: Numerical Analysis of Stratified Flow". Paper presented at symposium "Multiphase Flow in the Production and Drilling of Oil Wells", A.I.Ch.E., Tulsa, Oklahoma (Sept. 1960).
(3) Chernikin, V. I., Trudi Mock. Neft in-ta **17,** 101 (1956).
(4) Chilton, E. G., and Handley, L. R., U.S. Patent 2,821,205 (1958).
(5) Clark, A. F., and Shapiro, A., U.S. Patent 2,533,878 (1950).
(6) Russell, T. W. F., and Charles, M. E., Can. J. Chem. Eng. **37,** 18 (1959).
(7) Yuster, S. T., Proc., Third World Petroleum Congress **2,** 437 (1951).
(8) Odeh, A. S., Trans. A.I.M.E. 216, 346 (1959).
(9) Finnigan, J. W., "Liquid-Liquid Dispersions: Pressure Drop and Heat Transfer". Ph.D. Thesis, Oregon State College (1958).
(10) Russell, T. W. F., Hodgson, G. W., and Govier, G. W., Can. J. Chem. Eng. **37,** 9 (1959).
(11) Bartell, F. E., and Miller, F. L., J. Amer. Chem. Soc. **50,** 1961 (1928).

★ ★ ★

Holdup in Liquid-Liquid Extraction Columns[1]

A. I. JOHNSON[2] *and E. A. L. LAVERGNE*[3]

A theoretical study of the countercurrent flow of a dispersed phase in a continuous phase resulted in the following equation relating holdup X to the flow rates of the two phases.

$$A\left(\frac{U_C}{U_D}\right)^{2-n}\left(\frac{X}{1-X}\right)^3 + B = \frac{X^3}{U_D^{2-n}}$$

For packed towers this equation has been used in the following form:

$$\frac{X^3}{U_D^{1.5}} = A'\frac{U_C^{r}}{U_D^{1.5}}\left(\frac{X}{1-X}\right)^3 + B'$$

Values of A', B', and r for three liquid pairs, and two packing types are reported, using new holdup data determined in this research.

Graphical correlations are shown and values of r are reported for some of the data of Gayler and Pratt.

For spray towers the equation suggested a correlation of $\frac{X^3}{U_D^{1.8}}$ against the group $\frac{U_C^{0.2}}{U_D^{1.8}}\left(\frac{X}{1-X}\right)^3$. This has been tested using data previously published by one of the authors.

Holdup in this paper is defined as the fraction of the total liquid flowing in a packed or spray type liquid-liquid extraction column occupied by the dispersed phase.

The importance of holdup is related to the mass transfer coefficient Ka which is the product of the transfer rate coefficient and the interfacial area per unit of volume. For a given drop size the latter is proportional to the holdup. Alternately, it would be impossible to obtain values of the transfer rate coefficient K without a knowledge of the holdup and drop characteristics.

Previous Work

Holdup data in the literature can be classified into two categories depending on the manner in which it was obtained. In the drainage method, measurements were made by closing off flows to the column, draining the column and measuring each phase[1,2]. By the displacement method, all streams to and from the column are closed off, and then continuous phase added until the interface has been restored to its initial position[2,3,4,5].

Holdup has also been estimated by observing the velocity of individual droplets and calculating the number of drops held up in a particular tower[6].

Gayler and Pratt[2], in an extensive study, observed that the holdup measured by the displacement method, which they termed the *normal holdup*, was less than the holdup measured by drainage. The difference, which has been called *permanent holdup*, was presumably caused by droplets trapped in the packing. Gayler, Roberts, and Pratt[7] have proposed the following equation relating holdup and superficial velocities below flooding

$$U_D + \frac{X}{1-X}U_C = Fv_o\,X(1-X) \quad \ldots\ldots\ldots\ldots (1)$$

Wicks and Beckmann[8] investigated the holdup of toluene in water using a rather wide range of column diameters and packing sizes. It is interesting to note that they found that the reproducibility of holdup results was improved greatly by blowing the column with air after dumping the packing. This has been found in the present research also. These authors proposed an empirical equation of the type

$$X = A_1\,U_D^{r} + B_1\,(U_D)\,(U_C)^{s} \quad \ldots\ldots\ldots\ldots (2)$$

Here X is the total holdup, the sum of the normal and permanent holdup defined above. In this equation the first term on the right side predominates and accordingly there is some difficulty in establishing values of B_1 and s[8].

Correlating Equation Proposed in This Work

Equation (19) of the paper by Sakiadis and Johnson[9] relating the holdup of the dispersed phase to the physical properties of the system and the flow rates of both phases will be used as a starting point for the derivation of the holdup correlation. A similar starting equation is presented by Dell and Pratt[10]. This equation was derived by applying Bernoulli's Theorem to each phase separately and may be written as follows:

$$\frac{C_C\rho_C^{1-n}\,U_C^{2-n}\,\mu_C^{n}\,\rho_C^{1+n}}{(1-X)^3} + \frac{C_D\rho_D^{1-n}\,U_D^{2-n}\,\mu_D^{n}\,\rho_D^{1+n}}{X^3} = 2g\Delta\rho \quad \ldots (3)$$

Sakiadis found the value of n to be of the order of 0.2 for flooding conditions. However, at conditions other than flooding it is difficult to determine the value of n theoretically. Consequently it was decided to rearrange Equation (3) to the following form:

$$\frac{C_C\rho_C^{1-n}\,U_C^{2-n}\,\mu_C^{n}\,\rho_C^{1+n}}{2g\,(1-X)^3\,\Delta\rho} + \frac{C_D\rho_D^{1-n}\,U_D^{2-n}\,\mu_D^{n}\,\rho_D^{1+n}}{2g\,X^3\,\Delta\rho} = 1 \quad \ldots\ldots (4)$$

[1]*Manuscript received June 22, 1959; accepted November 4, 1960.*
[2]*Associate Professor, Department of Chemical Engineering, University of Toronto, Toronto, Ont.*
[3]*Union Carbide Chemicals Company, South Charleston, W. Virginia, U.S.A.*
Contribution from the Department of Chemical Engineering, University of Toronto, Toronto, Ont.

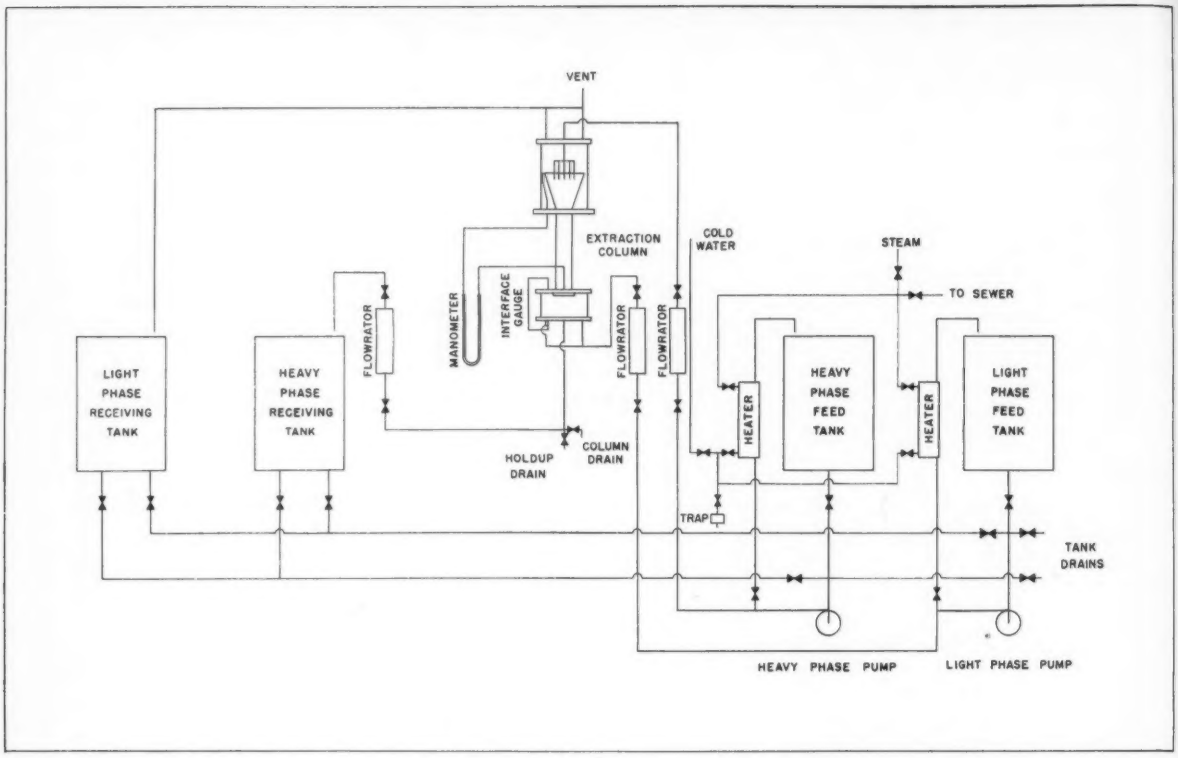

Figure 1—Flowsheet of liquid-liquid extraction apparatus. Heavy phase dispersed.

Dividing through by U_D^{2-n}/X^3 gives

$$\frac{C_C \rho_C^{1-n} p_C^{1+n} \mu_C^n}{2g\ \Delta\rho}\left(\frac{U_C}{U_D}\right)^{2-n}\left(\frac{X}{1-X}\right)^3 + \frac{C_D \rho_D^{1-n} p_D^{1+n} \mu_D^n}{2g\ \Delta\rho} = \frac{X^3}{U_D^{2-n}} \quad \ldots\ldots(5)$$

The groups containing the physical properties of the phases were considered constant for any one system and type of packing. Equation (5) may then be written more simply as

$$A\left(\frac{U_C}{U_D}\right)^{2-}\left(\frac{X}{1-X}\right)^3 + B = \frac{X^3}{U_D^{2-n}} \quad \ldots\ldots(6)$$

This equation has three constants for any system and packing: A, B and n. To obtain these, the equation suggests that values of n be assumed until a correlating line is obtained when X^3/U_D^{2-n} is plotted against $\left(\frac{U_C}{U_D}\right)^{2-n}\left(\frac{X}{1-X}\right)^3$.

In this paper this equation will be examined using spray tower data previously reported[10], packed tower data obtained in this study[11], and packed tower data of Gayler and Pratt.

Apparatus and its Operation

A flow diagram of the apparatus used for holdup measurements in packed towers is shown in Figure 1. The arrangement is essentially the same as that used in the spray tower studies whose results are also used in this paper. The major difference is the replacement of the swinging loop by a needle valve and flowrator for more precise control of the dispersed phase flow leaving the column.

Figure 2 shows details of the tower. The column proper consisted of a 2-ft. length of Pyrex pipe 4-in. i.d. The spray nozzle was made up of a cluster of eight ¼-in. tubes arranged on a circle 4.5-in. in diameter. The packing support was constructed of ½-in. wide strips of type 302 stainless steel sheet mounted on two ¼-in. rods and separated by ⅜-in. porcelain Raschig rings as spacers.

The packings used were ½-in. unglazed porcelain Raschig rings and Intalox saddles supplied by the United States Stoneware Company, Akron, Ohio.

For the packed tower runs, holdup was measured using a combination of the displacement and drainage methods as follows:

The two phases were brought to the operating temperature of 25°C. by the use of the heat exchangers shown in Figure 1, and each liquid was saturated with the other before a run was started. The column was filled with the continuous phase and after a few minutes of circulation the dispersed phase was introduced at the top of the column. The column was allowed to reach a steady state and to operate at this condition for 30 min., the dispersed phase being removed at the bottom at a rate maintaining a constant interface level in the settling chamber.

All flows to and from the column were shut off simultaneously. The dispersed phase in the packing was allowed to settle and was then drained and measured in a graduated cylinder while an equivalent volume of continuous phase was added to the column. This measured the *normal* or *freely falling* holdup.

The column was then drained and washed several times with continuous phase to remove any of the *permanent* holdup trapped in the packing interstices.

The sum of the free falling and permanent holdups yield the total holdup.

Presentation of Holdup Data

(a) Packed tower data

The packed tower holdup data reported here were measured during the course of studies of transient behavior of liquid-liquid

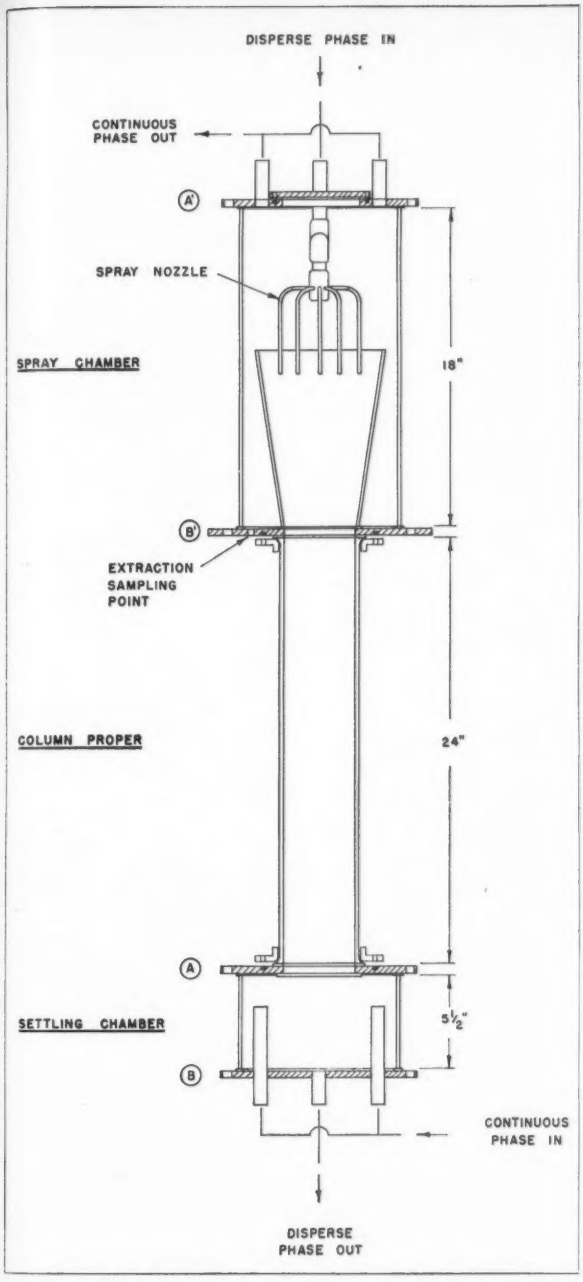

Figure 2—Extraction column. Heavy phase dispersed.

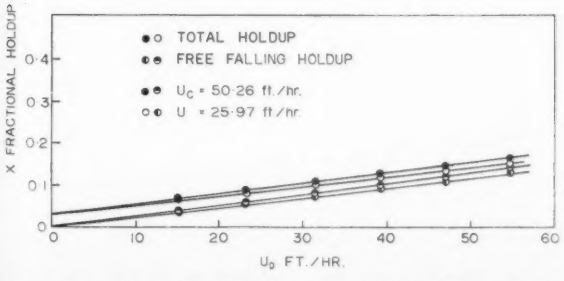

Figure 3 — Typical holdup data. System: CCl_4 — water; Packing: ½-in. Tutalox saddles $\epsilon = 0.756$.

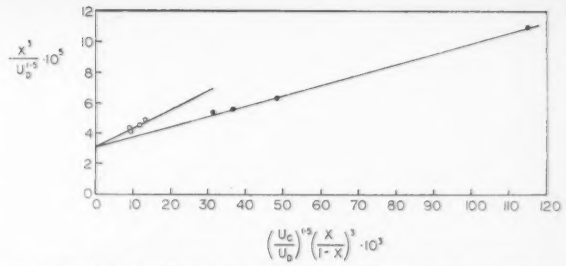

Figure 4 — Holdup correlation. System: CCl_4 — water; Packing: ½-in. Raschig rings $\epsilon = 0.587$.

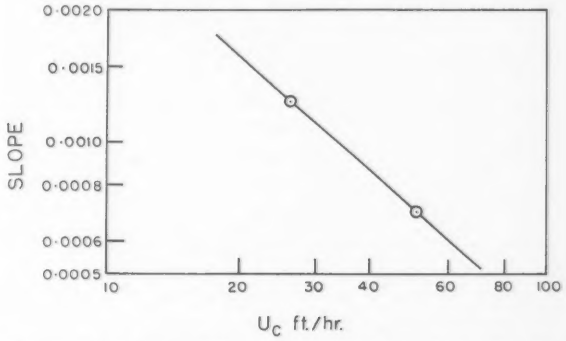

Figure 5—System: CCl_4 — water; Packing: ½-in. Raschig rings.

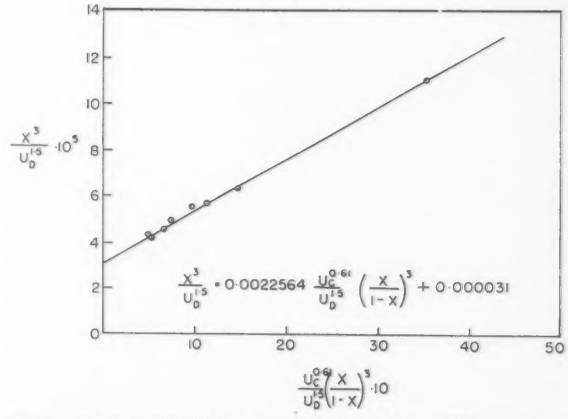

Figure 6—Final holdup correlation. System: CCl_4—water; Packing: ½-in. Raschig rings $\epsilon = 0.587$.

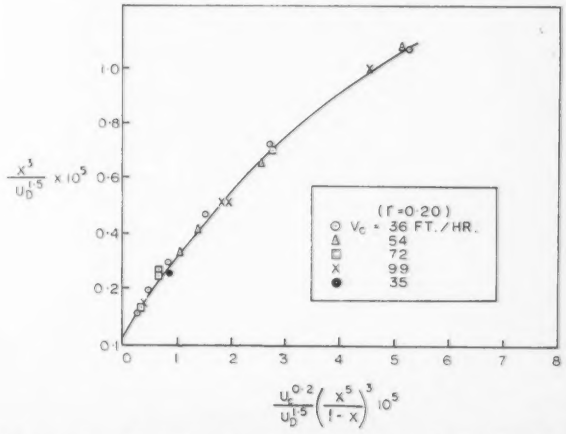

Figure 7 — Methyl isobutyl ketone-water; ½-in. Raschig rings. (Data of Gayler and Pratt).

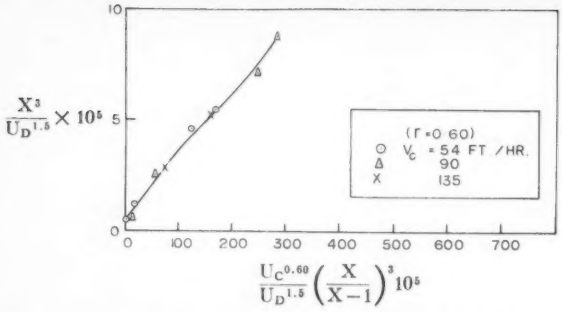

Figure 8 — Butyl acetate-water. Packing: ½-in. Raschig rings. (Data of Gayler and Pratt).

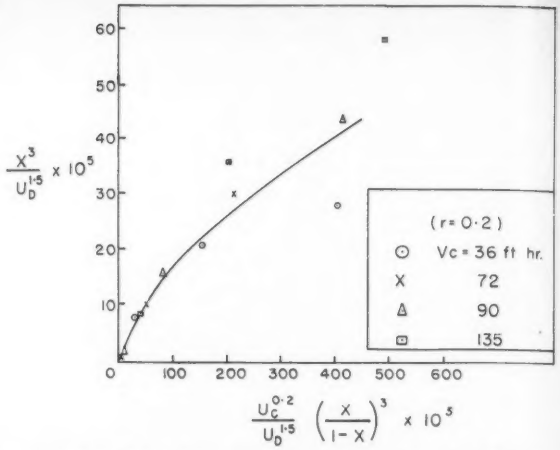

Figure 9 — Dibutyl carbitol-water. Packing: ½-in. Raschig rings. (Data of Gayler and Pratt).

extraction in packed towers. Accordingly the intention was to obtain precise data over a rather small range of flows.

Previous authors found that the method of packing a column had an appreciable effect on the reproduceability of holdup data; in general, data deviated as much as 20% after repacking. Wicks and Beckmann[8] settled the packing by passing air through a randomly packed column full of water at a rate sufficient to cause the packing to surge. In this study this method of repacking resulted in columns that were reproduceable to 13%.

Typical holdup data for carbon tetrachloride dispersed in water are shown in Figure 3. The free falling and total holdup both appear to be linear functions of the disperse phase rate at a given continuous phase rate up to the loading point. This is in agreement with the findings of previous investigators[2,3,5,8].

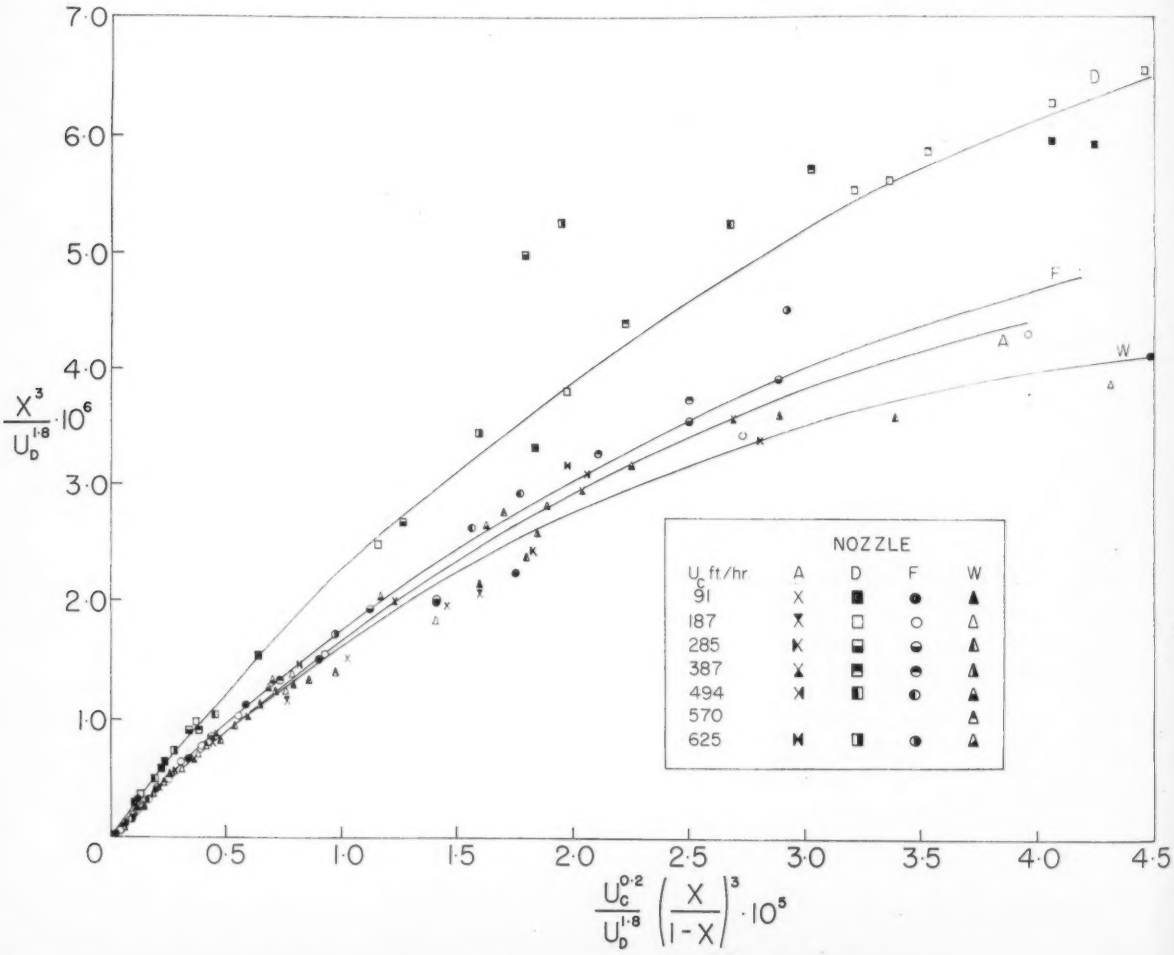

Figure 10—4-in. i.d. spray tower data. System: Ethylene dichloride-water.

The permanent holdup data, which is the difference between the holdups shown on this graph, increases with increasing dispersed phase rate as well as with increasing continuous phase rate.

The holdup in the Intalox saddle packing was found to be less than that in the Raschig ring packing. This is in agreement with other investigators[2,13] who found that holdup decreased with an increase in the fraction void or packing size.

The total holdup data below flooding for three systems and two packing shapes were correlated as suggested by Equation (6). As indicated on Figure 4, when n of Equation (6) was taken as 0.5, straight lines of differing slope but with a common intercept could be drawn. Assuming that the slope would vary exponentially as the continuous phase rate, Figure 5 was drawn. This led to the following modified form of Equation (6).

$$\frac{X^3}{U_D^{1.5}} = A' \frac{U_C'}{U_D^{1.5}} \left(\frac{X}{1-X}\right)^3 + B' \quad \ldots\ldots\ldots\ldots (7)$$

Based on this equation the total holdup correlation for carbon tetrachloride water is shown on Figure 6.

Table 1 shows values of A', B' and r of Equation (7). It would appear the r may be a function of the type of packing. It would be expected that A' and B' are functions of the physical properties of the systems but there is insufficient data in this study to find the relationship, if any.

(b) Packed tower data of Gayler and Pratt (2)

For comparison purposes and to test the generality of the correlating equations proposed in this paper the data for ½-in. Raschig rings of Gayler and Pratt[2] were examined. Plots such as those shown in Figures 4 and 5 of this paper were first prepared, and the final correlating graphs shown as Figures 7, 8, and 9 were produced.

It is seen that compared with Figure 6 considerable curvature was obtained, perhaps due to use of data covering a higher range of holdup values and also that a less satisfactory correlation of the data for dibutyl carbitol-water than for the other two systems was obtained.

(c) Spray tower data

Holdup data for the system ethylene dichloride-water, determined in a 4-in. i.d. spray column of the Elgin design[10] have been correlated by the method proposed in this investigation. In this case n was taken to have the value of 0.2 proposed by Sakiadis[9].

As indicated on Figure 10, four different curves were obtained, rather than straight lines. The reason for the curvature may lie in the wider range of flow conditions covered, these data extending to the *rejection* definition of flooding[10]. The four curves represent four different nozzles, producing different drop sizes and distributions.

It should be remarked that on Figures 4, 6, 7, 8, 9 and 10 the value of the ordinate x^3/U_D^{2-n} appears in the abscissa and one might have expected a greater tendency for the data to yield a graph of slope unity. The fact that such a slope was not obtained indicates that the plotting technique is not a false one and that the A^1 and B^1 values of Equation (7) are significant. However, this fact, along with the high powers of x and $1-x$ that appear in the correlations, will limit the usefulness of the correlating technique.

Conclusion

In this paper a theoretical approach to holdup below flooding has been proposed, resulting in Equation (6). In practice this equation has been modified as Equation (7) which must be regarded as empirical.

Some new data for packed towers has been presented by the proposed correlation. Previously reported spray tower data have been handled by the method also.

TABLE 1

CONSTANTS OF HOLDUP CORRELATION

$$\frac{x^3}{U_D^{1.5}} = A \frac{U_C'}{U_D^{1.5}} \left(\frac{x}{1-x}\right)^3 + B$$

1/2 in. Raschig ring packing

System	A'	B'	r
Carbon tetrachloride—water	0.023	0.000031	0.61
Ethylene dichloride —water	0.0093	0.000152	0.64
Carbon tetrachloride naphtha—water	0.0114	0.000030	0.65

1/2 in. Intalox saddle packing

System	A'	B'	r
Carbon tetrachloride—water	0.343	0.0000026	0.12
Ethylene dichloride —water	0.248	0.0000123	0.12
Carbon tetrachloride naphtha—water	0.244	0.0000073	0.12

Nomenclature

Roman

a	=	Interfacial area	ft.²/ft.³
F	=	Fractional voidage of packing	
g	=	Gravitational constant	ft./hr.²
K	=	Transfer coefficient	ft./hr.
$p_{C,D}$	=	Periphery terms for the continuous or dispersed phases, as defined by Sakiadis	ft.$^{-1}$
U_D	=	Superficial velocity of disperse phase	ft./hr.
U_C	=	Superficial velocity of continuous phase	ft./hr.
v_s	=	A characteristic velocity	ft./hr.
X	=	Fractional holdup	

Greek

μ_D	=	Viscosity of disperse phase	lb$_M$./hr. ft.
μ_C	=	Viscosity of continuous phase	lb$_M$./hr. ft.
ρ_D	=	Density of disperse phase	lb$_M$./ft.³
ρ_C	=	Density of continuous phase	lb$_M$./ft.³
$\Delta\rho$	=	Density difference	lb$_M$./ft.³

Coefficients

A, B, A_1, B_1, A', B', C

Exponents

n, r, s

References

(1) Meissner, H. P., Stokes, C. A., Hunter, C. M., and Morrow, G. M., Ind. Eng. Chem. **36,** 917 (1944).

(2) Gayler, R., and Pratt, H. R. C., Trans. Inst. Chem. Engrs. (London) **29,** 110 (1951).

(3) Appel, F. J., and Elgin, J. C., Ind. Eng. Chem. **29,** 451 (1950).

(4) Row, S. B., Koffolt, J. H., and Withrow, J. R., Trans. Am. Inst. Chem. Engrs. **37,** 559 (1941).

(5) Gier, T. E., and Hougen, J. O., Ind. Eng. Chem. **45,** 1362 (1953).

(6) Johnson, H. F., and Bliss, H., Trans. Am. Inst. Chem. Engrs. **42,** 331 (1946).

(7) Gayler, R., Roberts, N. W., and Pratt, H. R. C., Trans. Inst. Chem. Engrs. (London) **31,** 57 (1953).

(8) Wicks, C. E., and Beckmann, R. B., J. Am. Inst. Chem. Engrs. **1,** 426 (1955).

(9) Sakiadis, B. C., and Johnson, A. I., Ind. Eng. Chem. **46,** 1229 (1954).

(10) Minard, G. W., and Johnson, A. I., Chem. Eng. Prog. **48,** 62 (1952).

(11) Lavergne, E. A. L., Ph.D. Thesis, University of Toronto (1956).

(12) Allerton, J., Strom, B. O., and Treybal, R. E., Trans. Am. Inst. Chem. Engrs. **39,** 361 (1943).

(13) Leibson, I., D.Sc. Thesis, Carnegie Institute of Technology (1952).

★ ★ ★

Approximate Solutions of Conduction of Heat through Non-Homogeneous Medium[1]

CHI TIEN[2]

By comparing the respective difference equations of heat conduction through a homogeneous and non-homogeneous media, an approximate analogy is established. This analogy enables the finding of the solution of conduction through a non-homogeneous medium in terms of the known solution for homogeneous cases. An illustrative example is given to demonstrate the working details.

The study of the mathematical solutions of heat conduction has been a subject of interest for many years. Numerous solutions corresponding to various boundary conditions are available and these have been summarized in the excellent work of Carslaw and Jaeger[(1)]. However, most of these solutions apply only to cases where the conduction takes place through a homogeneous medium. In the case of non-homogeneous medium — where the physical properties are functions of location — although there is no difficulty in obtaining the solution in the strict mathematical sense, the solutions are often expressed in terms of infinite integral. The evaluation of these integrals often requires elaborate and tedious computation. This has been proved impractical in some of the engineering applications.

The object of this investigation is to propose a simple method which can be used to obtain approximate solutions for such a problem. This method is based on the analogy between conduction in a homogeneous medium and that in a non-homogeneous one, which is established by considering the respective difference equations.

Mathematical Development

For the case of one-dimensional conduction in a non-homogeneous medium where the physical properties are functions of location, the conduction equation in Cartesian coordinates can be written as:

$$\frac{\partial}{\partial x}\left[k(x)\frac{\partial T}{\partial x}\right] = \rho(x)\, C_p(x)\frac{\partial T}{\partial t} \qquad \ldots\ldots(1)$$

The corresponding difference equation can be given as:

$$\frac{k_{m+1/2}\dfrac{T^j_{m+1}-T^j_m}{\Delta x_{m+1}} - k_{m-1/2}\dfrac{T^j_m - T^j_{m-1}}{\Delta x_m}}{[\Delta x_{m+1}+\Delta x_m]/2} = \rho C_p \frac{T_m^{j+1}-T_m^j}{\Delta t} \qquad \ldots\ldots(2)$$

Where Δx and Δt denote the magnitude of the position and time increments respectively; the subscript m indicates the value at the mth position increment while the superscript j designates the value at the jth time increment. It should be noted that although the time increment is being kept constant, the magnitude of the succeeding position increment is not the same but varies with a given relationship to be given later. Equation (2) can be written as:

$$\frac{2}{\Delta x_m\,\Delta x_{m+1}(\Delta x_m+\Delta x_{m+1})}[k_{m+1/2}\,\Delta x_m\,T^j_{m+1}+k_{m-1/2}\,\Delta x_{m+1}\,T^j_{m-1} - (k_{m+1/2}\,\Delta x_m + k_{m-1/2}\,\Delta x_{m+1})T_m^j] = \frac{T_m^{j+1}-T_m^j}{\Delta t}(C_p\,.\,\rho)_m \qquad \ldots\ldots(3)$$

For sufficiently small increments, the following approximation is believed to be applicable:

$$k_{m+1/2}\,\Delta x_m \simeq k_{m-1/2}\,\Delta x_{m+1} \simeq 1/2k_m(\Delta x_m + \Delta x_{m+1}) \qquad \ldots\ldots(4)$$

Substituting Equations (4) into (3), results:

$$\frac{k_m}{\Delta x_m\,\Delta x_{m+1}}[T^j_{m+1} + T^j_{m-1} - 2T_m] = (C_p\,.\,\rho)_m\frac{T_m^{j+1}-T_m^j}{\Delta t} \qquad \ldots(5)$$

Furthermore, Equation (5) would be simplified to the following form:

$$T_m^{j+1} = \tfrac{1}{2}[T^j_{m+1} + T^j_{m-1}] \qquad \ldots\ldots(6)$$

if the following condition is satisfied

$$\frac{\alpha_m\,\Delta t}{\Delta x_{m+1}\,\Delta x_m} = \tfrac{1}{2} \qquad \ldots\ldots(7)$$

where

$$\alpha_m = \left(\frac{k}{C_p\,.\,\rho}\right)_m \qquad \ldots\ldots(8)$$

For the case of homogeneous medium, the corresponding difference equation is known as:

$$T_m^{j+1} = \tfrac{1}{2}[T^j_{m+1} + T^j_{m-1}] \qquad \ldots\ldots(9)$$

and

$$\frac{\alpha\Delta t}{(\Delta x)^2} = \tfrac{1}{2} \qquad \ldots\ldots(10)$$

Equations (6) and (10) are identical in form except that in the latter case (homogeneous), the magnitude of Δx is constant while in the non-homogeneous case Δx varies depending on the particular location and the recurrent formula is given by Equation (7). This identity of functional forms leads to the conclusion that with a proper choice of position increments, the temperature history at one point in the homogeneous medium and that of another in the non-homogeneous medium are the same provided there exists a similar initial and boundary condition in these two cases. By similar initial condition, it does not necessarily mean that the two initial conditions are identical; it implies rather that the temperature at the corresponding points are the same. This conclusion can also be stated as follows: With

[1]*Manuscript received September 2; accepted October 17 1960.*
[2]*Department of Chemical Engineering, Essex College, Assumption University of Windsor, Windsor, Ont.*

similar initial and boundary conditions, the temperature history at $x = K.(\Delta x)_k$ for a homogeneous medium, where K is any arbitrary integer and $(\Delta x)_k$ designates the convenient space increment, and that at $x = \sum_{i=1}^{K} \Delta x_i$ for non-homogeneous medium, where Δx_i and Δx_{i+1} are related by Equation (7) and $\Delta x_o = \Delta x_1 = \sqrt{a_o/a_k}\ (\Delta x_k)$ with a_k as the thermal diffusivity of the homogeneous medium and a_o as the thermal diffusivity at the surface of the non-homogeneous medium, will be the same. With this conclusion, it becomes possible to estimate the solution of heat conduction through a non-homogeneous medium provided the similar solution for the case of homogeneous medium is available. Furthermore, although this conclusion is based on the special case of unidirectional and with Cartesian coordinates, similar results may be obtained for other cases too. The application of this method then becomes fairly simple. In order to obtain the temperature distribution throughout a non-homogeneous medium with its physical properties given as a function of position, the corresponding solution for the homogeneous case should be obtained first. This information is usually available in the literature. With the information, one can obtain the temperature history at several selected points of the non-homogeneous medium with the use of the method stated before. By cross-plotting this temperature history, the temperature distribution at any time can be obtained. It is obvious that the choice of the initial position increment, Δx_o, can be very critical since the validity of the approximation given by Equation (4) is totally dependent on the magnitude of the increment. In this regard, it is suggested that results should be obtained by using at least two different values for the initial increment and the limiting value obtained through χ^2 — extrapolation should be taken as the actual value.

Various attempts have been made to express this relationship in a more explicit form. Unfortunately this has not been successful. However, for the special case where thermal diffusivity is a linear function of the depth of the medium, a more direct relationship can be obtained. This will be shown as follows:

Assume that the thermal diffusivity of this particular medium has the following form:

$$a = a_o(1 + ax) \qquad (11)$$

The corresponding locations in the homogeneous and non-homogeneous media, where the temperature histories are similar, are:

$$x_k = N(\Delta x)_k \qquad (12)$$

$$(\Delta x)_k = \sqrt{2a_k \cdot \Delta t} \qquad (13)$$

$$x_{n\cdot k\cdot} = \sum_{i=1}^{N} \Delta xi \qquad (14)$$

$$\Delta x_o = \Delta x_1 = \sqrt{2a_o\ \Delta t} \qquad (15)$$

$$\Delta x_{m+1} = (2a_m\ \Delta t)/\Delta x_m \qquad (16)$$

Substituting Equation (11) into (16) for $m = 1$, we have:

$$\Delta x_2 = \frac{2a_1 \cdot \Delta t}{\Delta x_1} = \frac{2a_o[1 + a\Delta x_1]}{\Delta x_1} \cdot \Delta t =$$

$$\frac{2a_o\Delta t}{\Delta x_1} + 2a_o \cdot a \cdot \Delta t = \sqrt{2a_o \cdot \Delta t} + 2a_o \cdot a \cdot \Delta t \qquad (17)$$

Similarly, for $m = 2$, we have:

$$\Delta x_3 = 2\frac{a_2\ \Delta t}{\Delta x_2} = 2\frac{a[1 + a(\Delta x_1 + \Delta x_2)]}{\Delta x_2} \cdot \Delta t =$$

$$2\frac{a_o[(1 + a\ \Delta x_1) + a\ \Delta x_2]}{\Delta x_2} \cdot \Delta t =$$

$$2\frac{a_o(1 + a\ \Delta x_1)}{\Delta x_2} \cdot \Delta t + 2a_o \cdot a \cdot \Delta t =$$

$$2\frac{a_1}{\Delta x_2} \cdot \Delta t + 2a_o\ a\ \Delta t = \Delta x_1 + 2a_o\ a\ \Delta t =$$

$$\sqrt{2a_o\ \Delta t} + 2a_o \cdot a \cdot \Delta t \qquad (18)$$

In general, one obtains:

$$\Delta x_{2m} = \sqrt{2a_o\ \Delta t} + 2_{ma}\ a_o \cdot \Delta t \qquad (19a)$$

$$\Delta x_{2m-1} = \sqrt{2a_o\ \Delta t} + 2(m-1)_a\ a_o \cdot \Delta t \qquad (19b)$$

Substituting Equations (19a) and (19b) into (14), we obtain:

$$X_{n\cdot k} = \sum_{i=1}^{N} \Delta x_i = N\sqrt{2a_o(\Delta t)} + 2\sum_{i=1}^{\frac{N-2}{2}} (2a_o\ a\ \Delta t)_i +$$

$$N(2a_o\ a\ \Delta t) \qquad \text{for } N = \text{even}$$

$$= N\sqrt{2a_o(\Delta t)} + 2\sum_{i=1}^{\frac{N-1}{2}} (2a_o\ a\ \Delta t)_i \qquad \text{for } N = \text{odd}$$

$$= N\sqrt{2a_o\Delta t} + N^2/2\ a_o\ a\ \Delta t \qquad \text{for } N = \text{even}$$

$$= N\sqrt{2a_o\ \Delta t} + N^2{-}1/2\ a_o\ a\ \Delta t \qquad \text{for } N = \text{odd} \qquad (20)$$

We now seek the limit of the ratio, $X_{n\cdot k}/X_k$ for a given value of X_k as $\Delta x \to 0$. This in turn implies that $N = \infty$ and $\Delta t = 0$ since $N\ (\Delta x)_k$ = constant, and $(\Delta x)_k = \sqrt{2a_k\Delta t}$

$$\lim_{\substack{\Delta t \to 0 \\ N \to \infty \\ N\sqrt{\Delta t} = \text{constant}}} \frac{X_{N\cdot k}}{Xh} = \lim_{\substack{\Delta t \to 0 \\ N \to 0 \\ N\sqrt{\Delta t} = \text{constant}}} \frac{\sum_{i=1}^{N} \Delta x_i}{N\sqrt{2a_k\ \Delta t}}$$

$$= \lim_{\substack{\Delta t \to 0 \\ N \to \infty \\ N\sqrt{\Delta t} = \text{constant}}} \left[\frac{N\sqrt{2a_o\ \Delta t}}{N\sqrt{2a_k \cdot \Delta t}} + \frac{N^2}{2}\frac{a_o\ a\ \Delta t}{N\sqrt{2a_k\ \Delta t}}\right] \qquad \text{for } N = \text{even number}$$

$$= \lim_{\substack{\Delta t = 0 \\ N = \infty \\ N\sqrt{\Delta t} = \text{constant}}} \left[\frac{N\sqrt{2a_o\Delta t}}{N\sqrt{2a_k\Delta t}} + \frac{N^2-1}{2}\frac{a_o\ a\ \Delta t}{N\sqrt{2a_k\ \Delta t}}\right] \qquad \text{for } N = \text{odd number}$$

$$= \sqrt{\frac{a_o}{a_k}} \lim_{\substack{\Delta t \to 0 \\ N \to \infty \\ N(\Delta x_k) = N\sqrt{2a_k\ \Delta t} = X_k}} \left[\frac{a}{4}\frac{(N\sqrt{2a_k\ \Delta t})^2}{N\sqrt{2a_k\ \Delta t}}\frac{a_o}{a_k}\right]$$

$$= \sqrt{\frac{a_o}{a_k}} + \frac{a}{4}\frac{a_o}{a_k}X_k$$

or

$$\frac{X_{N\cdot k}}{X_k} = \sqrt{\frac{a_o}{a_k}} + \frac{a}{4}\frac{a_o}{a_k}X_k \qquad (21)$$

$$= 1 + \frac{a}{4}X_k \qquad \text{if } a_o = a_k \qquad (21a)$$

Solving the quadratic equation of Equation (21a), we have:

$$X_k = \frac{2}{a}[-1 + \sqrt{1 + a\ X_{n\cdot k}}] \qquad (22)$$

With this relationship established, one can obtain the temperature distribution in a non-homogeneous medium where $a = a_o(1+ax)$ by simply substituting $2/a(-1+\sqrt{1+ax})$ for x into the solution for the case where $a = a_o$. An illustrative example will be given in the following section.

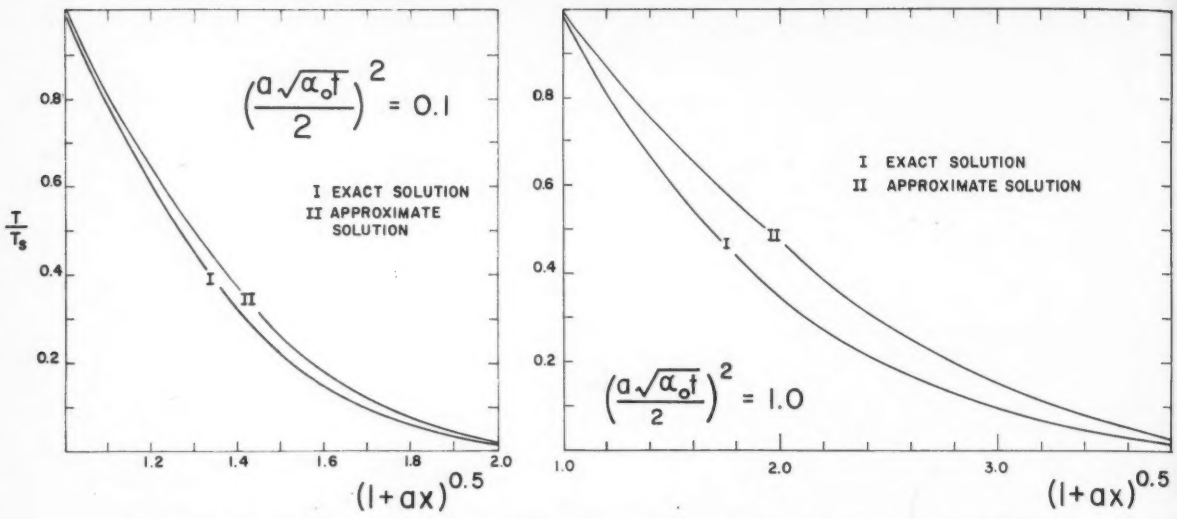

Figure 1—Comparisons between the exact and approximate solutions for two sets of conditions.

Illustrative Example

For illustration, consider the following problem: A semi-infinite solid where $\alpha = \alpha_o(1+ax)$ is initially at zero temperature and at $t \geq 0$, a constant temperature T (other than zero) is imposed at the surface. The exact solution for the temperature distribution as given by Carslaw and Jaeger[1] is:

$$\frac{T}{T_s} = 1 + \frac{2}{\pi}\int_o^\infty e^{-\alpha_o u^2 \frac{a^2 t}{4}} \frac{J_o[u(1+ax)^{1/2}]Y_o(a) - Y_o[u(1+ax)^{1/2}]J_o(a)}{J_o^2(a) + Y_o^2(a)} \cdot \frac{da}{u} \quad \ldots\ldots(23)$$

Numerical values of T/Ts are available in Reference (2)

If the approximate method is applied, first for a similar problem in a homogeneous medium where $\alpha = \alpha_o$ the temperature distribution is given by:

$$\frac{T}{T_s} = 1 - erf\left(\frac{x}{2\sqrt{\alpha_o t}}\right) \quad \ldots\ldots(24)$$

Substituting Equation (22) for the x in Equation (24), one obtains the approximate solution as:

$$\frac{T}{T_s} = 1 - erf\left[\frac{-1+\sqrt{1+ax}}{a\sqrt{\alpha_o t}}\right] \quad \ldots\ldots(25)$$

Comparison between Equation (23) and (25) is shown in Figure 1. For both cases the approximate solution gives a higher numerical value. It is conceded that the degree of accuracy is not as good as expected (about 10% for T/Ts in the range of .01/−0.9), the time saved in computation is quite significant.

For some preliminary engineering calculations, the use of this method may be more advantageous.

Nomenclature

- a = Constant
- C_p = Heat capacity
- j = Superscript designating the value at the jth time increment.
- k = Thermal conductivity
- m = Subscript indicating the value at the mth position increment.
- N = Positive integer
- T = Temperature
- t = Time
- x = Distance
- α = Thermal diffusivity
- Δt = Time increment
- Δx = Position increment
- ρ = Density

References

(1) Carslaw, H. S., and Jaeger, J. C., Conduction of Heat in Solid, 2nd Edition Oxford Press (1959).

(2) Jaeger, J. C., J. Math. Phys. **34**, 316-21 (1956).

★ ★ ★

NOTE TO THE EDITOR

The Extension of Couette Flow Solution to Non-Newtonian Fluid

CHI TIEN

Essex College, Assumption University of Windsor, Windsor, Ont.

The purpose of this note is to show that the solution of a Couette flow problem in laminar heat transfer for Newtonian fluid can also be applied to the case of non-Newtonian system, provided that the relevant parameters are properly defined.

By Couette flow, we refer to the case of flow between two parallel plates, of which one is stationary, while the other is moving at constant velocity U. A prescribed thermal condition is imposed on these two plates and the question is to obtain the temperature distribution. For the treatment of this problem with Newtonian fluid, one can refer to a standard heat transfer textbook, i.e., Schlichting[1].

The two-dimensional energy equation of an incompressible, constant property fluid is given as:

$$C_p\rho\left[u\frac{\partial T}{\partial x}+v\frac{\partial T}{\partial y}\right]=k\left(\frac{\partial^2 T}{\partial x^2}+\frac{\partial^2 T}{\partial y^2}\right)-(\tau:\nabla V)\qquad(1)$$

For Couette flow, when pressure drop along x-direction is insignificant, $u = y/h$. U and $v = 0$ where h is the width between these two plates.

The last term represent the heat dissipation due to friction. For a case like this, it is given by:

$$\tau:\nabla V=\tau_{yx}\frac{\partial u}{\partial y}\qquad(2)$$

Although there are no general postulates relating the stress and strain tensors for non-Newtonian fluid, for a large class of material, a power model relationship can be used, i.e.,

$$\tau_{yx}=-K\left(\frac{\partial u}{\partial y}\right)^n\qquad(3)$$

Substituting (2) and (3) into (1) together with the velocity distribution, we obtain:

$$k\frac{\partial^2 T}{\partial y^2}=-K\left(\frac{\partial u}{\partial y}\right)^{1+n}=-K\left(\frac{U}{h}\right)^{1+n}\qquad(4)$$

If the two plates are maintained at constant temperatures such as:

$$T=T_o \quad \text{at } y=o$$
$$T=T \quad \text{at } y=h$$

Integrating Equation (4) twice, the temperature distribution is given as:

$$\frac{T-T_o}{T_1-T_o}=\left(\frac{y}{h}\right)+\left(\frac{1}{2}\right)\frac{KU^{n+1}}{k(T_1-T_o)h^{n-1}}\left(\frac{y}{h}\right)\left(1-\frac{y}{h}\right)\qquad(5)$$

Rewrite the dimensionless coefficient of the second term as:

$$\frac{KU^{n+1}}{k(T_1-T_o)h^{n-1}}=\left(\frac{kU^{n-1}C_p}{kh^{n-1}}\right)\left(\frac{U^2}{C_p\,\Delta T}\right)\qquad(6)$$

The second group on the right is known as Eckert number. The first group can be written as:

$$\frac{C_pKU^{n-1}}{kh^{n-1}}=\frac{C_pU\rho h}{k}\,\frac{K}{\rho h^nU^{2-n}}=\frac{N_{Pe}}{N_{Re}}\qquad(7)$$

Since

$$N_{Re}=\frac{\rho h^nU^{2-n}}{K}$$

for non-Newtonian fluid.

If one assumes that the same reationship exists between the various dimensionless groups for non-Newtonian fluid as that of Newtonian fluid, such as $N_{Pr} = N_{Pe}/N_{Re}$ Equation (5) can be put in the following form:

$$\frac{T-T_o}{T_1-T_o}=\left(\frac{y}{h}\right)+\left(\frac{1}{2}\right)N_{Pr}\cdot N_{Ec}\left(\frac{y}{h}\right)\left(1-\frac{y}{h}\right)\qquad(8)$$

This expression is identical to that of the Newtonian fluid.

Another case worthwhile to be considered is the one in which one plate is insulated while the other is maintained at constant temperature such as:

$$\frac{\partial T}{dy}=0,\ y=0 \qquad T=T_o,\ y=h$$

The temperature corresponding to this condition can be shown as:

$$T-T_o=\frac{KU^{1+n}}{2kh^{n-1}}\left[1-\left(\frac{y}{h}\right)^2\right]\qquad(9)$$

The temperature difference between the bottom and top plate, as a result of adiabatic heating is given as:

$$T(o)-T_o=T_a-T_o=\frac{KU^{1+n}}{2kh^{n-1}}=\frac{C_pV^{n-1}K}{kh^{n-1}}\,\frac{U^2}{2C_p}=N_{Pr}\frac{U^2}{2C_p}\qquad(10)$$

or the recovery factor defined as:

$$\text{Recovery factor}=\frac{T_a-T_o}{V^2/_2\,C_p}=N_{Pr}\qquad(11)$$

These two expressions are again identical in form with those of Newtonian fluid.

Nomenclature

C_p = Heat capacity B.t.u./lb.−°F.
h = Width between plated ft.
k = Thermal conductivity B.t.u./hr.-sq. ft.−1F./ft.
K = Parameter in the Power Law model for non-Newtonian fluid
n = Exponent in the Power Law model for non-Newtonian fluid, dimensionless
N_{Ec} = Echert number defined as $U^2/C_p\Delta T$
N_{Pe} = Peclet number defined as $C_pU\rho h/k$
N_{Pr} = Prandtl number defined as N_{Pe}/N_{Re}
N_{Re} = Reynold number defined as $\dfrac{\rho h^nU^{2-n}}{k}$
T = Temperature °F.
u = Velocity along x-direction ft./hr.
U = Velocity of the lower plate ft./hr.
v = Velocity along y-direction ft./hr.
V = Velocity vector
ρ = Density lb./ft.^{3}
τ = Stress tensor

Reference

(1) Schlichting, H., "Boundary Layer Theory", Pergamon Press (1955).

★ ★ ★

The Explosive Limits and Flammability of Xanthate Dusts in Air[1]

J. M. ROXBURGH[2]

The minimum concentrations of xanthate dusts in air which will form explosive mixtures have been determined. Comparison with other dusts considered to be hazardous industrially indicates that xanthates of the lower alcohols should be classified as readily explosive. The explosive limit increases rapidly with particle size; dusts coarser than 150 mesh are relatively safe. Xanthate dusts are easily ignited and have very low ignition temperatures. Under conditions such that fine wood flour ignites at 540°C. the xanthates will ignite between 230°C. and 290°C.

Xanthic acids are the O-esters of dithiocarbonic acids. The sodium and potassium salts of xanthic acids derived from the lower aliphatic alcohols are water soluble and stable and find extensive use in froth flotation. They are usually manufactured by reacting sodium or potassium hydroxide with an exess of the appropriate alcohol and carbon disulphide. Purity of the commercial product may range from 75% up with dithiocarbonates and thiosulphates the main impurities. The free xanthic acids are unstable but their alkali metal salts may be handled relatively safely in either pellet or powder form. It is generally accepted[(1)] that they should be kept cool and dry to prevent excessive decomposition, and cases of spontaneous combustion have been reported.

No reference to the flammability or explosive tendencies of xanthates is reported in the literature, but since their decomposition by both heat and moisture is known to regenerate much of the carbon disulphide and alcohol it might be expected that they will burn and their dusts explode fairly readily.

The hazard of fire from flammable dusts is usually less significant than the explosion hazard and occurs only when layers are allowed to accumulate. The temperature required to ignite such layers establishes the degree of hazard and in some cases is low enough so that low temperature sources of ignition such as overheated bearings and motors, light bulbs and steam lines must be considered

The hazard of dust explosions in a given manufacturing operation depends on many factors. The minimum explosive concentration of dust in air depends primarily on the material constituting the cloud and the particle size distribution in it. In addition, the type of ignition source and its temperature will affect this minimum concentration, as will such factors as the relative humidity and moisture content and the presence or absence of air currents. Generally speaking, industrial interest is centered on that minimum concentration which will explode under optimum conditions of all other factors. For this reason it is most practical to test dusts under conditions of low moisture content and relative humidity in still air using a high energy source of ignition. Finer and finer fractions of the dust should be tested until little or no further effect from decreasing particle size is observed.

Under certain conditions the assessment of hazard and design of prevention techniques may require a knowledge of characteristics of the dust which are of purely academic interest in other cases. The minimum spark energy necessary to ignite dust clouds under various conditions and the pressures developed by the explosion are known for many dusts[(2)]. Where inert atmospheres are to be maintained in process equipment the minimum oxygen content in which a dust explosion can be induced will be important.

Certain broad limits can be set on the conditions under which a dust cloud is likely to be hazardous. Most flammable substances which are not pyrophoric or true explosives are not hazardous if the particles are all or nearly all coarser than will pass a 200 mesh screen. Large particles settle quickly in still air and are difficult to ignite in suspension. The lowest concentration of fine dust which will explode is usually in the range 20 to 100 mg. per liter of air, but some resins will explode in concentrations as low as 15 mg. per liter. Very few substances will explode in atmospheres containing less than 10% oxygen.

In establishing the potential hazard from dust explosion and ignition of settled dust for a specific compound the method of testing must be carefully selected. Ideally, an infinitely large cloud of uniform composition in still air is required to establish a lower explosive limit for dusts. Practically, a small chamber of about one liter is used and the dust dispersed by a sudden puff of air. By comparison with other substances of known explosive tendencies a value can be obtained in such equipment that will be close to the true lower explosive limit, but care must be taken to ensure good dispersion of the dust and adequate energy and temperature in the igniting source. The detection of explosions near the explosive limit is sometimes doubtful and somewhat subjective.

Ignition temperatures of layers of dust may be subject to similar experimental variations. The rate of heating and the length of time that the sample is held at the test temperature are important. Air currents and the materials in contact with the dust will also affect the temperature at which ignition occurs. Again, comparison with materials of generally known hazard tested under the same conditions seems advisable.

[1]*Manuscript received June 14; accepted August 8, 1960.*
[2]*Prairie Regional Laboratory, National Research Council, Saskatoon, Sask.*
Based on a paper presented to the C.I.C. Annual Conference, Ottawa, June 13-15, 1960.

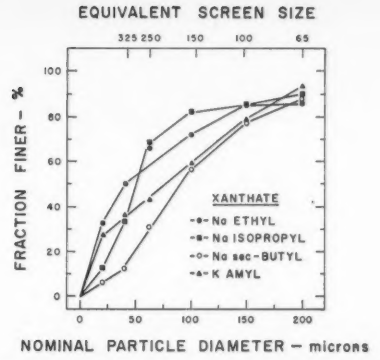

Figure 1—Particle size distribution in commercial samples of "crystal" xanthates.

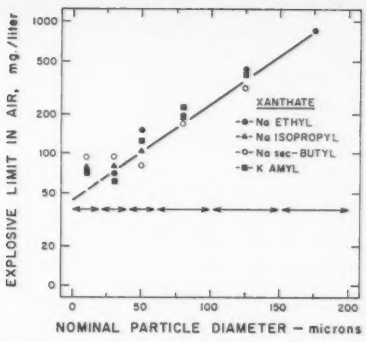

Figure 2—The effect of particle size on the minimum explosive limit of xanthate dusts in air.

Experimental and Results

The explosion chamber used for these tests was described in an earlier paper[3]. A weighed sample of the dust to be tested was dispersed by a metered puff of compressed air in a one liter transparent plastic chamber. A 5000 volt a.c. spark was used to induce explosions. A positive test was recorded if the paper covering the top of the chamber was ignited or burst. Ignition temperatures were determined by placing 50 mg. of the sample on a stainless steel plate (1 in. × 8 in.) in the immediate vicinity of a thermocouple silver soldered to the plate. A burner was placed under the other end of the plate and regulated so that the temperature rise at the thermocouple was 80°C. per minute. The output from the thermocouple was recorded. The ignition was readily observed on the chart as a sharp rise in temperature.

Samples of dust were equilibrated at various relative humidities to determine moisture content and its effect on explosive limits. Relative humidities were kept constant by saturated solutions of suitable salts in the humidity chambers.

Separation of the samples into fractions of known particle size was carried out in a Roller Particle size Analyzer* modified for higher air flows.

Samples of four xanthates of commercial grade were separated into six fractions. The particle size distribution in all four samples was similar (Figure 1). It is to be noted that from 50 to 70% of each of the samples tested was in the size range which could be expected to cause a dust explosion. The samples as received were essentially anhydrous and lost 2% or less of their weight on prolonged vacuum drying at room temperature.

As a preliminary test, the minimum explosive concentration in air of the fraction passing a 250 mesh screen was determined for three of these xanthates. Results were somewhat variable because the dusts failed to disperse well in the test chamber but values in the range from 40 mg. per liter for sodium ethyl xanthate to 70 mg. per liter for sodium isopropyl xanthate were recorded. These tests were conducted at a time when the ambient relative humidity was very low (less than 10%) and later could only be duplicated on samples dried under vacuum.

Potassium amyl xanthate agglomerated to such an extent that it could not be screened successfully, and the other xanthates were nearly as bad, so further fractions were obtained by air separation.

Figure 2 shows the effect of particle size on the explosive limit of vacuum dried fractions. Even the fraction finer than 20 microns did not have an explosive limit lower than the nominally much coarser 250 mesh screened sample previously tested, possibly indicating some degradation of these compounds in the course of air separation. As expected, the explosive limit rises sharply for coarser particles, and beyond the 100 micron (150 mesh) level the hazard represented is small.

The xanthates take up considerable moisture but quite slowly. Potassium amyl xanthate does not absorb appreciable moisture at relative humidities less than 50% but the other three absorb from relative humidities of 12% up (Figure 3). Sodium isopropyl xanthate comes to the same moisture content at all levels of humidity tested whether the sample originally had more or less than the equilibrium amount, but sodium ethyl xanthate and sodium sec-butyl xanthate exhibit hysteresis at the lowest levels of relative humidity tested (Figure 3). It is possible that this results from the formation of a hydrate at the higher humidities which, once formed, is stable at the lower humidity. A projection of the descending moisture content relative humidity relation shown in Figure 3 for the three sodium aryl xanthates gives an intercept in each case very close to the theoretical for the moisture content of the monohydrate.

Moisture absorption at the highest relative humidity tested (77%) continues very slowly after the 48 hours used to determine "equilibrium" moisture contents in these tests, and after some weeks sodium ethyl xanthate will dissolve in the water absorbed. This slow absorption is accompanied by decomposition of the compound, probably through hydrolysis to carbonate and trithiocarbonate. Potassium amyl xanthate absorbs moisture very slowly and after one month at 77% relative humidity contains less than 15% moisture.

Because of the moisture absorbed, the explosive limits of these three xanthates are very much higher after equilibration at even low relative humidities (from higher moisture contents) than the limits given for the anhydrous compounds (Table 1). Since the effect of moisture is typical and maximum hazards are of most concern a single example is shown. Equilibration is slow (Figure 4) and even in thin layers is not complete for many hours at room temperature so that the sample may exhibit explosive properties characteristic of the anhydrous compound for some time after exposure to ambient conditions, particularly at relative humidities in the range where hysteresis may occur.

TABLE 1

TYPICAL EFFECT OF MOISTURE ON THE MINIMUM EXPLOSIVE LIMIT OF XANTHATE DUSTS IN AIR.
SODIUM ISOPROPYL XANTHATE, 40 TO 60 MICRON FRACTION

Moisture Content %	Explosive Limit mg/liter
0	110
5	170–180
15.5	240

*American Instrument Company, Silver Springs, Md., U.S.A.

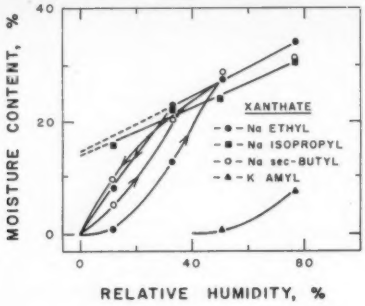

Figure 3—Moisture content of xanthates after exposure to atmospheres of various relative humidities for 48 hours.

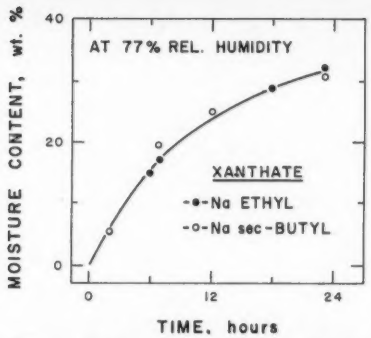

Figure 4—The rate of uptake of moisture by two xanthates exposed to an atmosphere with a relative humidity of 77%.

TABLE 2

IGNITION TEMPERATURES OF XANTHATES AND OTHER SUBSTANCES

Compound	Ignition Temperature
	°C.
Na Ethyl Xanthate	245
Na Isopropyl Xanthate	270
Na sec-Butyl Xanthate	260
K Amyl Xanthate	280
Sulphur	250
Wood Flour	550
Starch	>800

The ignition temperatures of the four xanthates tested are given in Table 2 along with ignition temperatures for fine wood flour and sulphur, determined in the same way. Starch was also tested but failed to ignite up to 800°C. Since wood flour and sulphur have ignition temperatures among the lowest recorded for industrial dusts, the xanthates can be said to have very low ignition temperatures. The ignition temperature found by this method for wood flour is higher than reported in the literature[2] which may be a result of moisture content or the variety of wood used, but the ignition temperature for sulphur agrees with reported values. Moisture content did not affect the ignition temperature of the xanthates to any large extent.

Summary

Commercial samples of four xanthates contained 50 to 70% of material fine enough to constitute a potential dust explosion hazard. Materials as received were anhydrous but three appeared to form rather unstable monohydrates when exposed to atmospheres with a relative humidity above 50%. Two of the xanthates exhibited hysteresis in the lower regions of relative humidity but sodium isopropyl xanthate had the same equilibrium moisture content at 12% relative humidity whether equilibrium was approached from higher or lower moisture levels.

Explosive limits for the finest fractions of the anhydrous xanthates dispersed in air were in the range 40 to 80 mg. per liter. The samples containing moisture equivalent to the monohydrate had explosive limits about 100% higher and were more difficult to disperse in the test chamber.

The ignition temperatures for these four xanthates were in the range 245°C. to 280°C., comparable with such hazardous materials as sulphur. The method used to determine ignition temperatures would not ignite starch up to 800°C. and would barely ignite fine wood flour (550°C.)

In the anhydrous state these xanthates represent a distinct hazard with respect to dust explosions, particularly since they contain large amounts of fine material and absorb appreciable amounts of moisture only very slowly. Their ignition temperatures are low enough to rank xanthates as one of the more flammable commercial chemicals.

Bibliography

(1) Harris, G. H., in "Encyclopedia of Chemical Technology", ed. R. E. Kirk and D. F. Othmer, The Interscience Encyclopedia Inc., New York, N.Y. 1956.
(2) Hartmann, I., in "Industrial Hygiene and Toxicology", Vol. I, ed. F. A. Patty, Interscience Publishers Inc., New York, N.Y. 1948.
(3) Roxburgh, J. M., Can. J. of Tech. **34**: 260, 1956.

★ ★ ★

A Method of Measuring the Surface Area of Granular Material[1]

C. P. HEDLIN[2] and S. H. COLLINS[3]

A method is described which permits measurement of the exterior surface areas of objects down to about 0.1 sq. in. in area. In this method, the object is coated with an adhesive and a single layer of small metal particles. The change in weight gives a measure of the external area of the object.

Systematic variations in the density of the metal particle coating are discussed, and appropriate correction factors are given.

This method is intended for use in research that involves objects whose exterior surface areas have an effect on the process being investigated. Examples are the drying of agricultural grains and foodstuffs, the comminution of ores and chemicals, and the hydraulic and pneumatic transport of materials.

The precision of the method is adequate, the root-mean-square error being about 1%.

The measurement of the surface areas of irregular objects has occupied the attentions of a number of investigators. Many of the methods have been reviewed by Dalla Valle(1), Scheidegger(2), and Orr and Dalla Valle(3).

The term "surface area" requires careful definition and its numerical value may depend upon the method of measurement. For example, it is necessary to distinguish between an exterior surface area and one associated with pores and fissures within the body; the technique of measurement would depend upon which "surface area" was required.

The method that is the subject of this paper consists of attaching a single randomly-packed layer of metal particles to the surface of the object of which the area is to be determined, (Figure 1) and measuring the attendant change in weight. There is no obvious upper limit on the size of object, and the method is applicable for surface areas down to about 0.1 sq. in. Such objects may be tested singly or in groups.

The metal particles adhere to the exterior, visible surface of the object, and it is the area of this surface that is measured. This type of surface, in the above mentioned range of surface areas, is not readily measured by other techniques, such as adsorption or permeability. The adsorption technique is applicable to much smaller particles and, larger total areas, and includes the areas of pores and fissures. The permeability method is indirect and depends upon the packing and porosity of a bulk material.

[1]*Manuscript received January 6; accepted October 21, 1960.*
[2]*Division of Building Research, Prairie Regional Laboratory, National Research Council, Saskatoon, Sask.*
[3]*Associate Professor, Department of Engineering Science, Ontario Agricultural College, Guelph, Ont.*
Contribution from the Department of Engineering Science, Ontario Agricultural College, Guelph, Ont.

When formulating an expression to describe the behavior of particles in an engineering process, it is frequently necessary to include characterizing physical dimensions in the formula. The technique discussed here may be useful in investigations of processes in which the exterior surface area plays a part. This area may enter the formula directly, or may be used to derive a shape factor to characterize the particles. Examples are: the motion of particles in gases and liquids, the rates of drying of granular materials, the rates of chemical reaction at particle surfaces, and the crushing and grinding of ores and chemical substances.

Method of Coating

In the selection of the powder, several factors were considered. The particle size must be small compared with the object to be measured, and indeed should be small compared to the smallest radii of curvature that commonly occur on the object. The particles should have a high density to provide an easily measured change in weight and, finally, they should not stick together. The powder actually selected met these requirements satisfactorily. It was pure nickel powder, with particles of fairly regular form. A quantity was procured* and sieved to obtain particles in the sieve size range −270 +325 (U.S. Standard Sieve) (2.1 to 1.7 mils diameter).

The critical problem in this method is that of attaching the particles in a single layer of uniform and reproducible density. Success depends primarily on the selection and proper application of a suitable adhesive. Experience showed that the thickness of the adhesive layer had to be considerably smaller than the diameter of the powder particle in order to prevent multiple layering. The best results were obtained by using a slow-drying varnish*.

A uniform layer of adhesive about 0.0002 in. thick was placed on the object by first dipping it in the varnish, then shaking it vigorously in about 500 gm. of −4 to +8 mesh sand until the sand did not adhere to it. (10 to 15 seconds usually sufficed). Since dry sand removed too much of the varnish, it was necessary to prepare it in advance by thoroughly mixing 10 gm. of varnish with 500 gm. of sand, and spreading the coated sand out to dry in air for about 20 min. at room temperature.

The adhesive-coated objects were removed from the sand and were allowed to dry in air on a fine screen for 2-3 min. They were then placed in a vessel containing nickel powder and were shaken with it for a predetermined length of time. The vessel was emptied onto a wire screen over a beaker to recover the objects which were then rolled on the screen or tapped lightly to remove unattached powder. The coatings

*The pure nickel powder was kindly supplied by Mr. Galley of Sherritt-Gordon Mines Ltd., Toronto.
*Berry Bros. Lionoil floor varnish was used in most of the tests.

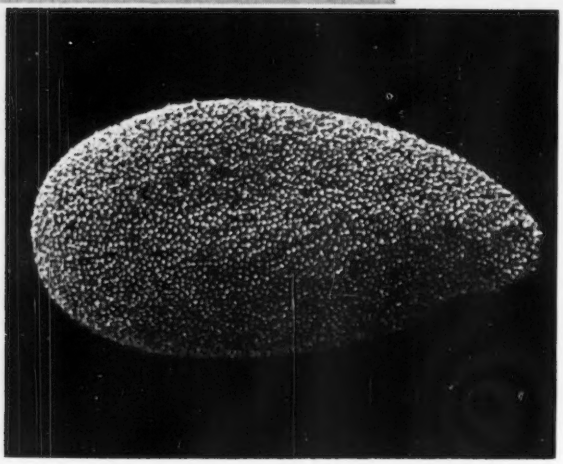

Figure 1—Nickel powder coating on a flax seed.

proved to be quite securely attached and could be handled with tweezers without damage. The objects were weighed on an analytical balance before coating with adhesive and after coating with nickel powder.

Factors Affecting the Deposition of Metal Powder

During the development of the method it became apparent that a number of variables systematically influenced the weight of powder attached per unit area. An investigation was carried out to isolate and study the most important effects arising from the two principal sources: (1) the properties of the object being coated and (2) the experimental technique itself. For this purpose, a variety of regular objects was made of materials such as steel, glass, aluminum, Bakelite and Plexiglas, in a variety of shapes and sizes. In each case, the area and density of the object was determined by measurement. While many other objects were tried, the ones most used were among the following:—

(a) Spheres, in diameters from 0.1 in. to 0.8 in.

(b) Cylindrical rods and wires, in diameters from 0.003 in. to 0.25 in. and lengths from 0.25 in. to 2 in.

(c) Square and rectangular bars with cross-sectional dimensions from 0.016 in. to 0.2 in. and lengths from 0.9 in. to 2 in.

(d) Flat plates, in thicknesses from 0.02 in. to 0.1 in. and in other dimensions from 0.25 in. to 1 in.

The various effects are discussed below.

Time of Shaking in the Nickel Powder

In the coating process the surface density of the powder increased rapidly in the initial stages, and the rate of increase dropped sharply as available spaces were occupied by the particles. A shaking time of 4 or 5 min. proved to be satisfactory.

Envelope Effect

For any surface with a radius of curvature much larger than the powder particle diameter d, this method estimates the actual surface area. It may be assumed that the particles occupy an envelope area that stands at a distance s, equal to one-half the particle diameter, from the object surface. If such is the case, the areas of curved surfaces will be overestimated in the ratio $(D+d)/D$ for rods and wires or $[(D+d)/D]^2$ for spheres. This assumption may be tested by deducing the envelope thickness s from experimental results and comparing it with the particle radius $d/2$.

If we let

ρ_o = weight gain/unit of actual surface area

ρ_e = weight gain/unit of envelope area

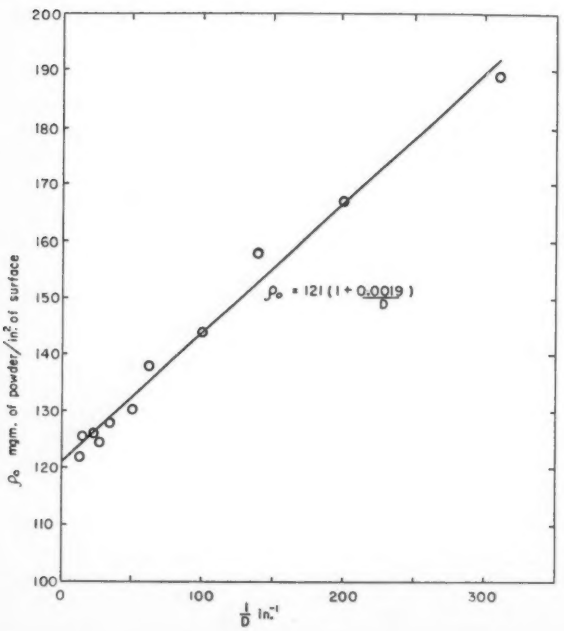

Figure 2—The envelope density of powder vs. reciprocal wire diameter.

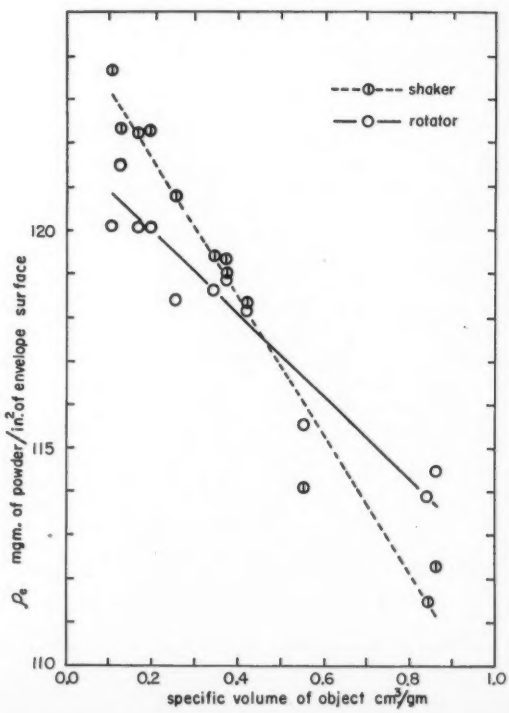

Figure 3—The envelope density of powder vs. object specific volume for two methods of coating.

then $\frac{\rho_o}{\rho_e} = \frac{D+2s}{D}$ for rods and wires

and $\rho_o = \rho_e(1 + 2s/D)$

A series of experiments was performed using rods and wires ranging in diameter from 0.071 in. to 0.0032 in. For these sizes the ratio $(D+d)/D$ ranges from about 1.03 to 1.60, based on a powder particle diameter of 0.0019 in.

Figure 2 shows the graph of ρ_o vs. $1/D$. The straight line was fitted by the method of least squares, giving the results:

$$s = 0.0095 \text{ in.}$$
$$\rho_e = 121 \text{ mgm./in.}^2$$

A second series of experiments performed with different wires gave:

$$s = 0.0011 \text{ in.}$$
$$\rho_e = 123.8 \text{ mgm./in.}^2$$

The agreement between the experimental values of s and the value of $d/2$ is sufficiently close to support the use of this concept as the basis for a practical correction factor.

Density Effect

The density of the object being coated had a small but significant effect upon the surface density of the coating. To investigate the influence of object density in the absence of any shape or size variation, identical steel cylinders were drilled axially with holes of various sizes and filled with lead or plastic. The result was a series of cylinders which, other than the density variation, had only a slight variation in the surface condition at the ends.

These objects, togenther with geometrically identical objects of Plexiglas, Bakelite and aluminum, showed clearly that surface density of coating increases with object density.

Effect of Method of Coating

The magnitude of the density effect was influenced by a fourth variable, the method of coating. Three methods of applying the nickel powder were tried. In each the object was placed in a vessel with an amount of the powder and was shaken. In the first method, a 100 ml. test-tube with 25 cm.^{3} of nickel powder was shaken vigorously by hand. In the second, a 2000 ml. beaker containing 200-300 gm. of powder was shaken on a bottle shaker that carried the beaker at 180 r.p.m. on a horizontal circle of 1¾ in. diameter. In the third, a 1000 ml. bottle containing about 300 gm. of powder was rotated end over end at 20 r.p.m.

Figure 3 shows the results of three runs on each of the variable-density objects by the second and by the third coating methods. Both methods show the density effect, the shaker more strongly.

When the shaker was used, the buoyancy effect of the nickel powder kept the low density objects partly above the powder, and therefore less exposed to packing influences.

The variation of density effect with coating method at present precludes the application of a simple correction factor and can best be accounted for by including a standard object having about the same density as that of the unknown object.

Figure 3 shows that, apart from the influence on density effect, the results of the two methods are very similar.

Precision of the Method

To find the precision of the method, a series of six runs was made on 12 objects of four different shapes (sphere, rod, bar, plate) and three different densities (steel, glass or aluminum, plastic). (Figure 4). The third (rotator) coating method was used, and the results in mg./sq. in. are given in Table 1. An analysis of variance shows that, while the density effect is highly significant, the variations between shapes and between runs are not significant (their mean squares being quite close to the error mean square). The analysis gave a root-mean-square error of 1.0%, or 1.2 mg./sq. in.

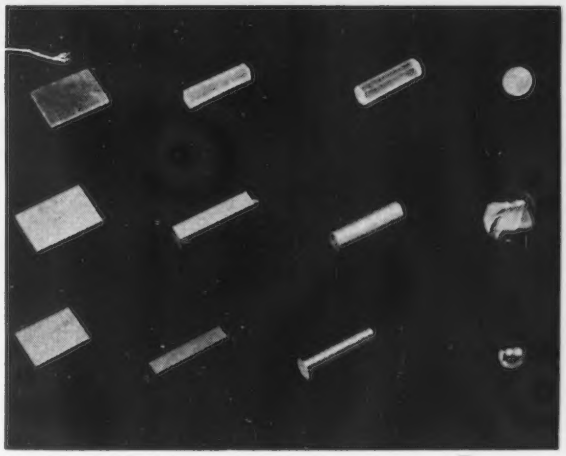

Figure 4—Objects used to obtain the results illustrated in Figure 3 (the rods and bars are about 1-in. long).

TABLE 1

RANGES OF POWDER COATING DENSITY FROM 12 OBJECT EXPERIMENT
mg./in.^{2}

Object	Object material and density (gm./cm.^{3})		
	7.76 Steel	2.48 to 2.70 (Glass, Aluminum)	1.16 Plexiglas
Plate	120—121.5	117 —122	117 —118.5
Bar	121—123.5	119 —120	115.5—119
Rod	122—124.5	118 —120.5	117.5—118.5
Sphere	123	117.5—119.5	117.5—119.5

Summary

A method has been devised for estimating the external surface area for objects in a particular size range. This method was developed for research on cereal grains but has applications to research on any particles of similar size. For example, it might be used to measure the surface area of granular materials entering a chemical process.

In this method the critical problem is that of placing a suitable layer of adhesive on the object. The technique described here was satisfactory for the objects used in this experiment. For other shapes, particularly those with negative curvatures, it is not entirely satisfactory and some other technique might prove to be better.

Certain simple precautions may be taken to ensure the validity of the measurements. Examination of the coatings with a stereoscopic microscope provides control of the coating technique. The systematic variations due to the nature of the object are small, and can be handled by a comparison method. That is, standard objects of known area, roughly similar in size, shape, and density to the unknown objects, may be included with them in the coating and weighing techniques. As experience is gained, the amount of control applied may be reduced.

References

(1) Dalla Valle, J. M., Micromeritics, 2nd Ed. (Pitman). 1948.
(2) Scheidegger, A. E., The Physics of Flow Through Porous Media (University of Toronto Press). 1957.
(3) Orr, Jr., C., Dalla Valle, J. M., Fine Particles Measurement (MacMillan). 1959.

★ ★ ★